Ubiquitylation in Canonical Wnt Signaling

By

Victoria Hoylon Ng

Dissertation

Submitted to the Faculty of the

Graduate School of Vanderbilt University

in partial fulfillment of the requirements

for the degree of

DOCTOR OF PHILOSOPHY

in

Cancer Biology

May 14, 2021

Nashville, TN

Albert B. Reynolds, Ph.D. (Chair)

Ambra Pozzi, Ph.D.

Andrea Page-McCaw, Ph.D.

William P. Tansey, Ph.D.

Ethan Lee, M.D., Ph.D. (Advisor)

ACKNOWLEDGMENTS

I would like to thank Dr. Ethan Lee for giving me free rein to try any experiment, buy any reagent (within a reasonable price tag, of course), and take up an inordinate amount of bench space to do research. He is incredibly passionate about his work and is always excited to discuss data or new ideas. These discussions and the support that he has given me has made me a better scientist. I would also like to thank my committee members, Dr. Al Reynolds, Dr. Bill Tansey, Dr. Ambra Pozzi, Dr. Andrea Page-McCaw, and Dr. Steve Hann who have given me guidance throughout my graduate career.

I am thankful to have had the chance to work with Lee lab members past and present. To Aja Hyde and Rubin Baskir, I absolutely enjoyed the time we spent talking about everything from science to life. The laughs we shared really made stressful days feel a lot less hectic. To Brian Hang, I am glad that we had a chance to work on a project together and I always enjoyed hearing about your hilarious experiences as a teacher. To Amanda Hansen, I am thankful for the early work that you did on our project and the time we spent bouncing ideas around. To Leah Sawyer, I am grateful for your efforts in keeping the lab stocked and running. Even when I would always try to slip in one more reagent to the orders at the last minute, you manage to squeeze in most of my last-minute requests. To Kenyi Saito-Diaz, thank you for always listening to my random science musings and sharing your bench space with me during your final years in the lab. To Jamal Bryant, Sara Kassel, and Christin Anthony, I have had such a great

time with you guys, and I am excited to see what this new generation of the lab will produce.

Though I always longed for the days that I would be back on a coast, I have met and become friends with some really amazing people who have made my time in Nashville much more enjoyable, and we have shared some wonderful memories. I look forward to making more memories with these people as we take the next steps in our careers and in life. I am also thankful for my friends back on the east coast who have dragged me away from being a workaholic with visits/trips and cheered me on through graduate school.

Out of everyone that I have met at Vanderbilt, I have to thank Greg, my partner in everything and the person who keeps me most grounded when things get difficult. You have been so supportive of me and having you by my side has given me so much joy. Lastly, I must thank my parents for supporting me all these years. They have helped me navigate some of the most challenging times and worked hard to provide me with the opportunity to do things that they never had the chance to do. I would not be who I am today without their love and support.

TABLE OF CONTENTS

Page

LIST OF TABLES

Table **Page**

LIST OF FIGURES

Figure **Page**

LIST OF ABBREVIATIONS

AP2, Adaptor Protein 2

APC, Adenomatous Polyposis Coli

BCL9, B-cell Lymphoma 9

BIR, Baculovirus Inhibitor of Apoptosis Protein Repeat

c-CBL, Casitas B-lineage Lymphoma

CBP, CREB Binding Protein

CK1, Casein Kinase 1

CSN, COP9 signalosome

CRD, Cysteine Rich Domain

CRL, Cullin RING Ligases

CYLD, Cylindromatosis

DKK, Dickkopf

DVL, Dishevelled

DUB, Deubiquitylase

E1, E1 activating enzyme

E2, E2 conjugating enzyme

E3, E3 ligase

EGF, Epidermal Growth Factor

ER, Endoplasmic Reticulum

ESCRT, Endosomal Sorting Complexes Required for Transport

FAP, Familial Adenomatous Polyposis

FZD, Frizzled

GSK3, Glycogen Synthase Kinase 3

Gro, Groucho

HDAC, Histone Deacetylase

HECT, Homologous to the E6-AP Carboxyl Terminus

HMG, High Mobility Group

IQGAP1, IQ motif containing GTPase Activating Protein 1

JAMM, JAB1/MPN/MOV34

LDLR, Low Density Lipoprotein Receptor

LEF, Lymphoid Enhancer Factor

LGR, Leucine rich repeat containing G protein-coupled Receptor

LRP5/6, Low-Density Lipoprotein Receptor-Related Protein 5/6

MBP, Maltose Binding Protein

MMTV, Mouse Mammary Tumor Virus

MO, Morpholino

NDLB, Non-Denaturing Lysis Buffer

OTU, Ovarian Tumor Proteases

PIP2, Phosphatidylinositol (4,5)-biphosphate

PORCN, Porcupine

RBR, RING-in-between-RING

RING, Really Interesting New Gene

RNF43, Ring Finger 43

RNF138, Ring Finger 138

RNF146, Ring Finger 146

RNF220, Ring Finger 220

RSPO, R-spondin

SCF, Skp1-Cullin-F-box

sFRP, secreted Frizzled-Related Protein

SOST, Sclerostin

TCF, T-cell Factor

TLE, Transducin-Like Enhancer of Split

TNKS, Tankyrases

TRIM33, Tripartite Motif-containing 33

UAF1, USP1-Associated Factor 1

UCH, Ubiquitin C-terminal Hydrolases

USP, Ubiquitin Specific Protease

WDR20, WD-repeat containing 20

Wg, Wingless

WIF, Wnt Inhibitory Factor

Wls, Wntless

WRE, Wnt Responsive Element

WT, Wild Type

XIAP, X-linked Inhibitor of Apoptosis Protein

ZNRF3, Zinc and Ring Finger 3

Chapter 1

INTRODUCTION

Wnt Signaling

The developmental origins of the Wnt pathway

For a multicellular organism (metazoan) with varying tissue types and organs to develop from a single cell, a dizzying array of coordinated communication needs to occur between cells (Gerhart, 1999). Through a process called signal transduction, cells receive signals from their environments and transduce them intracellularly, leading to various events such as cell death, motility, and changes in gene expression (Gomperts et al., 2009). Metazoans are quite diverse with wide ranges in morphologies, tissues, and cells. However, it has been proposed that there are only 17 signal transduction pathways used to account for this diversity and most of these pathways are evolutionarily conserved (Gerhart, 1999). It is important to note that in humans, mutations in these signaling pathways often result in developmental disorders and disease. As there are only a few signaling pathways that process all of the biological activity across metazoans, there is great interest in characterizing the mechanisms in these pathways to better understand development and disease.

The Wnt signaling pathway is conserved throughout metazoa and has critical roles in development and disease (Clevers and Nusse, 2012; Klaus and Birchmeier, 2008; Logan and Nusse, 2004). Early studies of the Wnt pathway came in the form of

observations in *Drosophila* and mice. Sharma and Chopra identified a *Drosophila melanogaster* mutant that lacked wings and named the mutation *wingless* (Sharma and Chopra, 1976). Shortly thereafter, Christiane Nusslein-Volhard and Eric Wieschaus identified multiple segmental patterning genes – one of which was *wingless* – in their Nobel prize-winning saturation mutagenesis screen in *Drosophila*. They showed that *wingless* (Wg) is a segment polarity gene required for proper segmentation in early *Drosophila* development (Nusslein-Volhard and Wieschaus, 1980). A few years later, Roel Nusse and Harold Varmus demonstrated that the mouse mammary tumor virus (MMTV) led to oncogenesis in mice by inserting within a locus they named *Int1*, thereby driving increased expression of an adjacent secreted glycoprotein. At the time, *Int1* was the first novel proto-oncogene identified by a proviral insertion (Nusse and Varmus, 1982). A connection was formed amongst these observations in mice and *Drosophila* when cloning and chromosome mapping showed that *wingless* is the *Drosophila* homolog of mouse *Int1* (Baker, 1987; Cabrera et al., 1987; Rijsewijk et al., 1987). This led to the genesis of the term “Wnt,” born out of the combination of *wingless* and *Int1* (Nusse et al., 1991).

Around the same time that Drosophila Wg and mouse Int1 were found to be homologs, Andy McMahon and Randy Moon injected *Int1* mRNA into the ventral blastomeres of *Xenopus laevis* embryos and found that this led to axis duplications (McMahon and Moon, 1989). This sensational observation provided a molecular explanation for early embryogenesis work performed by Hilde Spemann and Hans Mangold in 1924, where they showed that transplantation of tissue from the dorsal region of *Xenopus laevis* embryos to the ventral region of the embryo resulted in

twinned axes a few days later (Spemann and Mangold, 2001). Following McMahon and Moon's experiments in *Xenopus* embryos, many components of the Wnt pathway have since been validated using the *Xenopus* axis duplication assay. Collectively, these findings indicate that Wnts are highly conserved and play key roles in development.

Canonical Wnt signaling

Broadly, Wnt signaling has been divided into canonical (β-catenin dependent) and non-canonical (β-catenin independent) signaling. I will only be discussing canonical Wnt signaling as the work presented here exclusively focuses on effects in the canonical pathway. Most of the early studies that identified components of the canonical pathway used *Drosophila* and *Xenopus* as these two systems allowed for easy manipulation and, generally, clear phenotypes such as patterning and axiation defects in *Drosophila* and *Xenopus*, respectively.

Following the groundbreaking *Drosophila* screen by Nusslein-Volhard and Wieschaus that identified *wingless* in 1980, numerous *Drosophila* mutants with early embryonic segment polarity patterning defects were reported. Many of these mutants identified key components of the Wnt signaling pathway through biochemical and epistasis studies. These major players of the Wnt pathway include *armadillo* (*Drosophila* ortholog of β-catenin that was previously established as a key component of adherens junctions) (Riggleman et al., 1990; Riggleman et al., 1989; Wieschaus and Riggleman, 1987), *dishevelled* (Klingensmith et al., 1994; Noordermeer et al., 1994; Perrimon and Mahowald, 1987), *shaggy* (*Drosophila* ortholog of glycogen synthase kinase 3 (GSK3)) (Blair, 1994; Siegfried et al., 1992), *frizzled* (Bhanot et al., 1996), and *dTCF* and

groucho (Cavallo et al., 1998). Many of these early studies form the basis of our current understanding of the mechanism of action of the Wnt signal transduction pathway.

Wnt ligands

Wnt ligands are a class of secreted, lipid-modified glycoproteins that are involved in cell communication, long-range signaling and have been considered morphogens for their roles in tissue patterning (Martinez Arias, 2003; Mikels and Nusse, 2006; Port and Basler, 2010; Willert and Nusse, 2012). There are 19 different Wnt ligands encoded in the mammalian genome. Wnts have a hydrophobic N-terminal signal sequence that directs them to the endoplasmic reticulum (ER) for processing prior to the final secretion of an active Wnt protein (Coudreuse and Korswagen, 2007). In the ER, Wnts are first N-glycosylated (Komekado et al., 2007), and then palmitoylated by the membrane-bound *O*-acyltransferase Porcupine (PORCN) (Kadowaki et al., 1996; Zhai et al., 2004) at specific conserved cysteine and serine sites (Takada et al., 2006; Willert et al., 2003). Efficient secretion of the now glycosylated and palmitoylated Wnt typically requires transmembrane protein, Wntless (Wls) (Banziger et al., 2006; Bartscherer et al., 2006). Multiple modes of trafficking have been proposed for Wnts in long-range signaling including transfer by heparan sulfate proteoglycans, liposomes, and exosomes (Port and Basler, 2010; Routledge and Scholpp, 2019). Wnts can also be sequestered and blocked from binding their receptors. Secreted Frizzled-related proteins (sFRPs) and Wnt inhibitory factor 1 (WIF1) are secreted Wnt antagonists that bind Wnt ligands and prevent them from binding Frizzled receptors (Bovolenta et al., 2008; Kawano and Kypta, 2003; Nathan and Tzahor, 2009). Wnt ligands can also be blocked from binding

the LRP5/6 co-receptors by Dickkopf (DKK) family members (Bafico et al., 2001; Bao et al., 2012; Mao et al., 2001a; Semenov et al., 2001) and Sclerostin (SOST) (Li et al., 2005; Semenov et al., 2005), which compete with Wnt ligands to bind LRP5/6.

Wnt receptor activation and formation of Wnt signalosomes

Wnt ligands bind FZD and LRP5/6 co-receptors to activate the pathway, and binding of both receptors is required for activation of the canonical pathway. The mammalian FZD family of seven-pass transmembrane receptors belongs to the G-protein coupled receptor superfamily and contains 10 different members (Schulte and Wright, 2018). Wnt ligands bind FZD in their extracellular cysteine-rich domain (CRD) (Hirai et al., 2019; Janda et al., 2012). While Wnt ligands typically bind the CRD of FZD, different Wnt ligands have varying preferential binding sites on LRP5/6. LRP5 and LRP6 are single-pass transmembrane receptors that are functionally redundant and essential for Wnt signaling due to their roles as co-receptors for Wnt ligands (He et al., 2004; Pinson et al., 2000; Wehrli et al., 2000). They have four tandem β-propeller/epidermal growth factor (EGF) repeats followed by three low density lipoprotein receptor (LDLR) type A repeats (MacDonald and He, 2012). Wnt ligands, DKK, and SOST bind various regions within the four tandem β-propeller/epidermal growth factor (EGF) repeats (Bourhis et al., 2010; Chen et al., 2011; Kim et al., 2020; Mao et al., 2001a). The function of the LDLR type A repeats is not clear, but recently, it has been proposed to be involved in regulating endocytosis of LRP5/6 (Vijayakumar et al., 2017).

The binding of Wnt ligand to FZD and LRP6 forms a trimeric complex (Bourhis et al., 2010; Cong et al., 2004; He et al., 2004; Tamai et al., 2000). It has been proposed

that the formation of this complex initiates the production of phosphatidylinositol (4,5)-biphosphate (PIP2), which leads to LRP6 aggregation, LRP6 phosphorylation, and Axin translocation to the membrane (Pan et al., 2008). PIP2 has also been shown to recruit clathrin and adaptor protein 2 (AP2), which are components of endocytic vesicles, to LRP6 aggregates (Kim et al., 2013). These phosphorylated LRP6 aggregates can be visualized at the plasma membrane and contain components of the Wnt pathway such as DVL, GSK3, and Axin. These macromolecular complexes have been coined the term "Wnt signalosomes" (Bilic et al., 2007). Along with the formation of trimeric complexes and signalosomes, binding of Wnt ligand results in recruitment of the cytoplasmic effector DVL to FZD and LRP6 activation. DVL oligomerization and binding to the C-terminus of FZD is necessary for activation of the pathway (Ma et al., 2020; Tauriello et al., 2012). Phosphorylation of DVL following Wnt ligand binding LRP6 and FZD is proposed to promote its oligomerization (Ma et al., 2020; Yanagawa et al., 1995). While some components of these signalosomes have been identified, many details regarding the mechanism and additional components in these signalosomes still remain to be determined.

The formation of signalosomes is associated with LRP6 receptor activation. LRP6 is activated by phosphorylation of each of its conserved intracellular PPPSPxS motifs and mutational analysis of these motifs have shown that they act cooperatively (MacDonald et al., 2008). LRP5/6 undergoes sequential phosphorylation with GSK3 serving as the priming kinase that phosphorylates the serine in PPPSP motifs, followed by phosphorylation of xS by CK1 (Davidson et al., 2005; Zeng et al., 2005). While it is well-established that GSK3 and CK1 are the main kinases involved in activating LRP6,

there are, of course, other possible phosphorylation sites on LRP6 that might be phosphorylated by GSK3, CK1, or even other unidentified kinases. Following initial phosphorylation of LRP6, cytoplasmic Axin-GSK3 complexes are recruited to LRP6, further driving GSK3 phosphorylation of LRP6 and thus, amplify the signal initiated by binding of Wnt ligand (Baig-Lewis et al., 2007; Mao et al., 2001b; Zeng et al., 2008).

How receptor activation leads to inhibition of the destruction complex is not clear as many different mechanisms have been proposed. Recruitment of Axin-GSK3 complexes to activated receptors provides a simple dissolution mechanism (Liu et al., 2005) to explain increased levels of β-catenin during active Wnt signaling and this would agree with the observation that Axin is the limiting component of the destruction complex (Lee et al., 2003). However, it is still unclear whether the destruction complex actually dissociates, as many have demonstrated that multiple members of the destruction complex, or even the whole destruction complex including β-catenin, can localize to the plasma membrane following Wnt stimulation (Bilic et al., 2007; Hendriksen et al., 2008; Li et al., 2012). Another model suggests that the phosphorylated intracellular domain of LRP6 can directly inhibit GSK3 activity towards β-catenin (Cselenyi et al., 2008; Piao et al., 2008; Wu et al., 2009). Thus, the steps between receptor activation and β-catenin stabilization still require further investigation.

Activation of a Wnt transcriptional program

Following receptor activation, β-catenin accumulates in the cytoplasm as it is no longer phosphorylated by GSK3. In the absence of GSK3 phosphorylation, β-catenin is no longer targeted for ubiquitylation and degradation by β-TRCP. This increase in

cytoplasmic β-catenin leads to eventual translocation into the nucleus through a poorly understood mechanism (albeit multiple distinct mechanisms have been proposed). β-catenin does not have a nuclear localization signal or a nuclear export signal, but clearly, it can shuttle between the cytoplasm and nucleus without the use of the importin/exportin system to activate the Wnt transcriptional program (Anthony et al., 2020; Wiechens and Fagotto, 2001; Yokoya et al., 1999). Some studies have indicated that APC, Axin, and the GTPase Rac1 assist in the retention of β-catenin in the nucleus (Cong and Varmus, 2004; Henderson and Fagotto, 2002; Krieghoff et al., 2006; Wu et al., 2008). Recently, it has been proposed that the rap guanine nucleotide exchange factor 5 (RAPGEF5) controls the nuclear translocation of β-catenin by activating nuclear Rap GTPases (Griffin et al., 2018). It is possible that there are multiple mechanisms that connect β-catenin shuttling between the cytoplasm and nucleus.

In the nucleus, β-catenin binds the transcription factors, TCF/LEF to activate the Wnt transcriptional program (Behrens et al., 1996; Graham et al., 2000). In mammals, there are four members in the TCF/LEF family which include TCF1, TCF3, TCF4, and LEF1. TCF/LEF binds to Wnt responsive elements (WRE) through their high mobility group (HMG) box (van de Wetering and Clevers, 1992). TCF/LEF cannot activate transcription on its own and requires binding of β-catenin to activate transcription of Wnt target genes. Some other transcriptional co-activators such as CREB binding protein (CBP)/p300, B-cell lymphoma 9 (BCL9), and Pygopus have also been implicated in this process and have been shown to form large multimeric complexes with TCF/LEF and β-catenin to form “enhanceosomes” (Kramps et al., 2002; Mosimann et al., 2009; Thompson et al., 2002; Wolf et al., 2002). In the absence of pathway activation and β-

catenin binding, TCF/LEF represses transcription of Wnt target genes (Cadigan and Waterman, 2012). The most well-characterized family of transcriptional co-repressors is the Groucho/transducin-like enhancer of split (Gro/TLE) family. All members within this family interact with members in the TCF/LEF family (Brantjes et al., 2001). It has been shown that Gro/TLE interacts with histone deacetylases (HDACs), which typically maintain chromatin in a transcriptionally inactive form (Brantjes et al., 2001; Narlikar et al., 2002). β-catenin directly displaces Gro/TLE on TCF/LEF through competition for overlapping binding sites (Daniels and Weis, 2005). Studies from our laboratory have shown that the E3 X-linked inhibitor of apoptosis (XIAP) ubiquitylates Gro/TLE to promote dissociation of Gro/TLE and TCF/LEF. Dissociation of Gro/TLE allows β-catenin to bind TCF/LEF and form transcriptionally active complexes, which initiates a Wnt transcriptional program (Hanson et al., 2012).

Summary of canonical Wnt signaling

In the current model of the canonical pathway, cytoplasmic β-catenin levels are tightly regulated by its synthesis and degradation. When the pathway is inactive, β-catenin is normally maintained at low levels in the cytoplasm. β-catenin degradation occurs in a multiprotein complex called the destruction complex. The destruction complex is comprised of the scaffolding proteins APC and Axin, and the kinases glycogen synthase kinase 3 (GSK3) and casein kinase 1 (CK1) (Kimelman and Xu, 2006). CK1 phosphorylates β-catenin at serine 45, which primes it for phosphorylation by GSK3 at serine 33, serine 37, and threonine 41 (Amit et al., 2002; Liu et al., 2002). A complex containing Skp1, Cul1, and the F-box containing ubiquitin ligase, β-transducin

repeat-containing protein (β-TRCP) form the $SCF^{\beta\text{-}TRCP}$ complex which ubiquitylates phosphorylated β-catenin (Latres et al., 1999; Liu et al., 1999). The ubiquitylation of β-catenin leads to its subsequent degradation by the 26S proteasome (Aberle et al., 1997) (Figure 1-1A). Upon binding of Wnt ligand to the co-receptors low-density lipoprotein receptor-related protein 5/6 (LRP5/6) and Frizzled (FZD), the pathway is activated and Dishevelled (DVL) is recruited to bind FZD. Axin-bound CK1 and GSK3 phosphorylate LRP5/6, and, in a poorly defined mechanism, β-catenin phosphorylation is inhibited. Subsequently, β-catenin levels begin to rise in the cytoplasm. Accumulated cytoplasmic β-catenin translocates into the nucleus to bind the transcription factors, T-cell factor/lymphoid enhancer factor (TCF/LEF), and other nuclear factors to activate the Wnt transcriptional program (Anthony et al., 2020; MacDonald et al., 2009; Saito-Diaz et al., 2013) (Figure 1-1B).

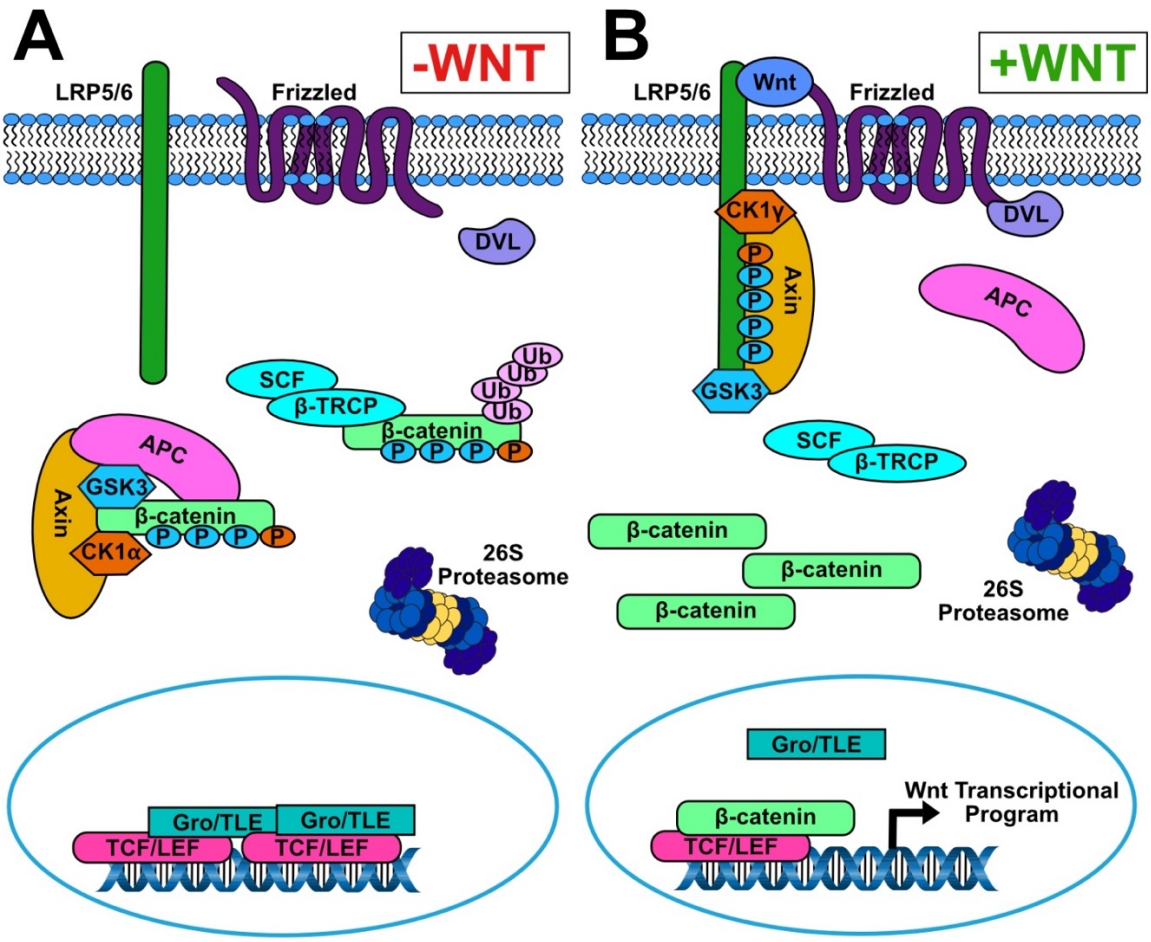

Figure 1-1. Schematic of canonical Wnt signaling
(A) In the absence of Wnt ligand, low, steady-state levels of β-catenin are regulated by the destruction complex, which is comprised of the scaffolding proteins, APC and Axin, and the kinases, CK1 and GSK3. CK1 and GSK3 phosphorylate β-catenin which targets β-catenin for ubiquitylation by β-TRCP. Subsequently, β-catenin is degraded by the 26S proteasome. **(B)** When Wnt ligand binds FZD and LRP6 co-receptors, DVL is recruited to FZD and LRP6 is phosphorylated by CK1 and GSK3. Because β-catenin is no longer phosphorylated, β-catenin begins to rapidly increase in the cytoplasm, leading to its eventual translocation into the nucleus. Gro/TLE is released and β-catenin binds TCF/LEF to activate the Wnt transcriptional program.

Wnt signaling in disease

Given that Wnt signaling plays a major role in development, it is no surprise that the Wnt pathway has been implicated in a multitude of diseases ranging from cancer to osteoarthritis. Most notably, over 90% of colorectal cancer cases have mutations in Wnt signaling that leads to overactivation of the pathway (Cancer Genome Atlas, 2012). Adenomatous polyposis coli (APC) is a key member of the Wnt pathway and well-established gatekeeper gene due to its role in the hereditary precancerous syndrome familial adenomatous polyposis (FAP) that leads to the development of hundreds to thousands of polyps in the colon and rectum (Kinzler and Vogelstein, 1996). Invariably, these polyps progress to cancer with an average age of 39 years. In 1991, it was determined that mutations in APC were a key factor in FAP (Kinzler et al., 1991; Nishisho et al., 1991). Soon after, it was shown that APC associated with catenins, including β-catenin (Su et al., 1993). β-catenin is the mammalian ortholog of *Drosophila armadillo*, which was identified as a segment polarity gene that is regulated by *wingless* in *Drosophila* (Riggleman et al., 1990; Riggleman et al., 1989; Wieschaus and Riggleman, 1987). These observations provided early indicators of the connection between Wnt signaling and colorectal cancer. Although colorectal cancer is the most striking example of misregulated Wnt signaling, aberrant Wnt signaling has also been found in cancers such as leukemia, breast cancer, and melanoma (Klaus and Birchmeier, 2008; Zhan et al., 2017). In addition to its roles in cancer, Wnt signaling has also been implicated in cardiovascular disease (Foulquier et al., 2018), diabetes (Welters and Kulkarni, 2008), and neurological disorders (De Ferrari and Moon, 2006).

A deeper understanding of the mechanisms of Wnt signaling, would contribute greatly to uncovering treatments for diseases in which Wnt signaling is misregulated.

Wnt signaling and stem cells

Wnt signaling is a key developmental pathway, and it has been shown that the Wnt pathway has critical roles in the maintenance of stem cell niches. With their ability to self-renew and differentiate into multiple cell types, stem cells are important for tissue homeostasis and regeneration in the adult organism (Chacon-Martinez et al., 2018). Epithelial tissues such as the skin and intestine routinely turn over, and it has been shown that Wnt signaling is integral in this process and in maintaining the stem cell niche necessary to support tissue homeostasis and regeneration (Clevers et al., 2014; Lim and Nusse, 2013; Schepers and Clevers, 2012; Wend et al., 2010). The pioneering study that provided evidence for this idea was in the T-cell factor 4 (TCF-4) (*Tcf7L2*) knockout mice, which, at birth, lacked proliferative stem cells in the crypt regions located between intestinal villi (Korinek et al., 1998). Subsequently, it was shown that genetic deletion of β-catenin resulted in a complete loss of intestinal crypts in the adult mouse (Fevr et al., 2007). These studies, among others, have demonstrated a critical role for Wnt signaling in the intestinal stem cell niche. Another prominent example of Wnt signaling in maintaining the stem cell niche is in hematopoiesis where Wnt signaling is not only critical in maintaining stemness, but also in coordinating differentiation (Lento et al., 2013; Luis et al., 2012). For example, germline deletion of one of the 19 different Wnt ligands, *Wnt3a,* results in a significant decrease in the amount of hematopoietic and progenitor stem cells in the fetal livers of mice (Luis et al., 2009). Another example

is in mice lacking TCF1, where loss of TCF1 leads to impaired thymocyte development (Schilham et al., 1998). It is clear that the Wnt pathway has multifaceted roles in maintaining stem cell niches, tissue homeostasis, and regeneration.

The Ubiquitin System

The Ubiquitylation Machinery

Ubiquitylation is the ATP-dependent process whereby ubiquitin, a small 8.5 kDa protein, is covalently attached to target proteins through a series of enzymatic reactions. The first enzymatic reaction involves the ubiquitin-activating enzyme E1, where the cysteine in its catalytic site forms a covalent thioester bond with the C-terminal glycine of ubiquitin to activate ubiquitin (Ciechanover et al., 1982; Haas et al., 1982; Handley et al., 1991). Now, the activated ubiquitin is transferred to the cysteine in the catalytic site of an ubiquitin-conjugating enzyme E2 (van Wijk and Timmers, 2010). Lastly, an ubiquitin-protein ligase E3 binds the target protein to catalyze the attachment of ubiquitin to a specific lysine residue of the target protein (Talis et al., 1998) (Figure 1-2). In this system, there are two E1 enzymes, about forty E2 enzymes, and hundreds of E3 enzymes. Across this stepwise process, selectivity increases at each step with the E3 conferring the most selectivity for the substrate. E3s are generally separated into two major classes: Homologous to the E6-AP Carboxyl Terminus (HECT) and Really Interesting New Gene (RING) (Metzger et al., 2012). In the last couple of years, other subclasses of E3s have emerged and they are the RING-in-between-RING (RBR), U-box, and Cullin RING ligases (CRL) (Deshaies and Joazeiro, 2009; Patterson, 2002; Petroski and Deshaies, 2005; Smit and Sixma, 2014). Because the majority of E3s contain RING domains, it is not surprising that these subclasses all contain RING domains.

Along with selectivity, there are layers of complexity added to the process with how much ubiquitin is attached to the substrate and the kinds of ubiquitin chains that are made after the addition of the first ubiquitin. Polyubiquitylated proteins are usually targeted for degradation via the 26S proteasome. Monoubiquitylated proteins are typically not targeted for degradation but are involved in many different processes that range from endocytosis to histone regulation. While monoubiquitylated proteins are typically not targeted for degradation by the 26S proteasome, they are degraded by lysosomes (Hicke, 2001). Ubiquitin itself contains seven lysines (Lys6, Lys11, Lys27, Lys29, Lys33, Lys48, and Lys63), each of which can be ubiquitylated and this is key to forming ubiquitin chains on a substrate. The methionine (Met1) on ubiquitin can also form a chain when it is linked to the N-terminus of another ubiquitin protein. The different chains regulate the activity of the protein substrate whether it be degradation or some other control of that protein (Swatek and Komander, 2016).

Although this covalent attachment of ubiquitins can successfully target a protein for a diverse array of activity, it is also reversible through the action of deubiquitylases (DUB). In humans, there are about 90 known DUBs and as such, this would suggest that there are multiple substrates for each one. DUBs cleave the peptide or isopeptide bonds between a protein substrate and ubiquitin. Beyond removing ubiquitin from protein substrates, DUBs also process ubiquitin before it is recruited in ubiquitylation, recycle ubiquitins, and trim ubiquitin linkages. There are five classes of DUBs with ubiquitin-specific proteases (USP), ubiquitin C-terminal hydrolases (UCH), ovarian tumor proteases (OTU), and Josephins being cysteine proteases and JAB1/MPN/MOV34 (JAMM) being zinc metalloproteases (Komander et al., 2009).

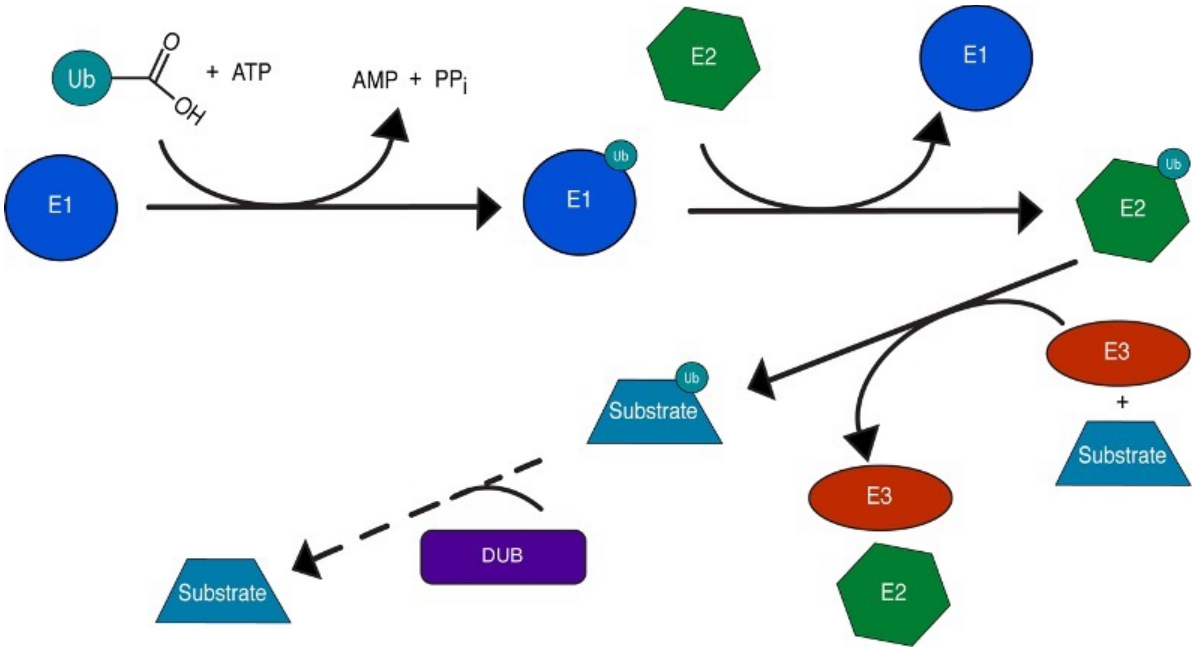

Figure 1-2. The process of ubiquitylation and deubiquitylation.
E1 activates ubiquitin. The activated ubiquitin is transferred to the E2. The E2 and E3 then work together to transfer ubiquitin to the substrate. Deubiquitylases (DUB) remove ubiquitin from substrates by cleaving ubiquitin.

Beyond protein degradation: emerging roles of ubiquitylation

Over the past quarter century, our understanding of the ubiquitylation and deubiquitylation processes have evolved past proteasomal degradation and expanded into multifaceted nodes of regulation with a simple ubiquitin modification. Ubiquitin modifications or removal of ubiquitin modifications on their substrates can have a profound effect of the substrate's biological activities in processes such as signaling and transcription (Finley and Chau, 1991; Oh et al., 2018). At the membrane level, ubiquitylation has key roles in regulating lysosomal degradation where it not only directly marks proteins in the plasma membrane for degradation, but it also allows for recognition by endosomal sorting complexes required for transport (ESCRT) machinery (Raiborg and Stenmark, 2009). Another example is ubiquitylation of histones in transcription, where ubiquitylation of histones has roles in gene activation and inactivation, higher order chromatin folding, and recruitment of other histone modifications such as acetylation and methylation (Muratani and Tansey, 2003a; Zhang, 2003). In signaling, ubiquitin modifications can affect protein-protein interactions and even coordination of signaling events within a pathway (Oh et al., 2018). One such example is in DNA repair where ubiquitylation of Ku by the E3 ring finger protein 138 (RNF138) following DNA damage, dictates DNA repair pathway choice (Ismail et al., 2015).

Histone ubiquitylation and recruitment of histone acetylation and methylation is one example of crosstalk amongst posttranslational modifications. Another example of posttranslational modification crosstalk are the connections formed between ubiquitylation and phosphorylation which can be seen in Wnt signaling with β-catenin

phosphorylation by GSK3 and CK1, and subsequent ubiquitylation by β-TRCP. Crosstalk between posttranslational modifications adds yet another layer to the complexity in the roles of ubiquitylation and how protein substrates can be controlled and directed for specific biological activities (Hunter, 2007).

Regulation of Wnt Signaling by the Ubiquitin System

Ubiquitylation has important roles in controlling signaling events ranging from regulating protein-protein interactions to marking proteins for degradation. In the Wnt pathway, multiple E3s and DUBs have been identified for their roles in regulating various components in the pathway. A prime example is the tightly regulated levels of β-catenin that are controlled by the destruction complex whereby, phosphorylation and subsequent ubiquitylation of β-catenin maintains low levels of β-catenin in the absence of Wnt ligand. Within Wnt signaling, there are multiple levels where ubiquitin modifications play major regulatory roles, and this extends from the receptor level all the way to the nuclear level.

Ubiquitylation at the membrane: modulating the receptors and signal transducer

Recently, the homologous E3s, zinc and ring finger 3/ring finger 43 (ZNRF3/RNF43) have come to forefront as components of a novel mechanism by which Wnt receptors can be targeted for degradation. ZNRF3/RNF43 are transmembrane RING E3 ligases. Mutations in *RNF43* promote Wnt signaling in multiple tumor types including pancreatic tumors (Jiang et al., 2013). Deletion of both *ZNRF3* and *RNF43* in

mice results in formation of adenomas in the intestinal epithelium (Koo et al., 2012). *ZNRF3* and *RNF43* are β-catenin target genes, suggesting that they may be involved in a negative feedback loop that regulates Wnt signaling. Accordingly, ZNRF3/RNF43 associate with the Wnt receptors to ubiquitylate Frizzled and promote receptor turnover (Hao et al., 2012). Interaction between ZNRF3/RNF43 and the receptors are facilitated by interaction between ZNRF3/RNF43 and DVL (Jiang et al., 2015). DVL itself is also subjected to ubiquitylation by ITCH and NEDD4L. These HECT-domain ligases are suggested to ubiquitylate DVL and negatively regulate Wnt signaling by targeting DVL for degradation (Ding et al., 2013; Wei et al., 2012).

Ubiquitylation of the transcriptional activator, β-catenin, in Wnt signaling

The most well-known E3 ligase in Wnt signaling is β-TRCP. β-TRCPs are a subfamily of E3 ligases that are within a larger family of F-box proteins, Fbw. F-box proteins are the substrate recognition component of Skp1-Cul1-F-box (SCF) protein complexes. The two major motifs of β-TRCPs are its F-box motif and C-terminal WD40-repeat domain. In Wnt signaling, β-TRCP is important in recognizing and targeting phosphorylated β-catenin for degradation by the 26S proteasome (Hart et al., 1999; Liu et al., 1999). As mentioned previously, when the pathway is off, CK1 phosphorylates β-catenin at Ser45 and this primes β-catenin to be sequentially phosphorylated at Thr41, Ser37, and Ser33 by GSK3 (Amit et al., 2002; Liu et al., 2002). β-TRCP, as part of the SCF complex, recognizes the GSK3 phosphorylated β-catenin through its WD40 domain. The F-box motif binds Skp1 to ultimately ubiquitylate the β-catenin that is bound simultaneously (Liu et al., 1999).

Besides β-TRCP, multiple E3 ligases have been characterized for their roles in ubiquitylating β-catenin in Wnt signaling. Ring Finger 220 (RNF220) stabilizes β-catenin in a complex that is then deubiquitylated to promote Wnt signaling. Here RNF220 is acting outside of its ligase activity but is instead an adaptor for β-catenin deubiquitylation. However, its ligase domain is necessary for binding the DUB that deubiquitylates β-catenin (Ma et al., 2014). Casitas B-lineage lymphoma (c-Cbl) is a RING E3 that can ubiquitylate β-catenin irrespective of Wnt activity, but it can ubiquitylate nuclear β-catenin when the pathway is on. When Wnt signaling is active, c-Cbl is phosphorylated at Tyr731, which promotes c-Cbl dimerization and binding to β-catenin (Shivanna et al., 2015). Ubiquitylating nuclear β-catenin poses a novel event in degrading active β-catenin that typically activates the Wnt transcriptional program. Like c-Cbl, tripartite motif-containing protein 33 (TRIM33) ubiquitylates nuclear β-catenin. TRIMM33 activity is independent of destruction complex activity. Phosphorylation of β-catenin at Ser715 by PKCγ is required for TRIM33 to interact with and ubiquitylate β-catenin (Xue et al., 2015). Regulation by the E3s, Jade-1 and SIAH1 suggest a connection between Wnt signaling and the von Hippel-Lindau protein (pVHL) and the tumor suppressor p53 respectively. pVHL stablilzes Jade-1 and regulates β-catenin to inhibit Wnt signaling. Jade-1 facilitates this inhibition by ubiquitylating phosphorylated and non-phosphorylated β-catenin and can regulate active Wnt signaling in this manner (Chitalia et al., 2008). Similarly, SIAH1 ubiquitylates β-catenin independent of GSK3 phosphorylation to inhibit Wnt signaling in a manner that is dependent on SIAH1 binding the C-terminus of APC. *Siah1* is a p53-inducible gene and was also found to be involved in mediating p53-induced β-catenin ubiquitylation (Liu et al., 2001).

Ubiquitylation of the destruction complex and nuclear components

Regulation of components that affect β-catenin stability and its ability to activate transcription are also key events in Wnt signaling. Axin is suggested to be the rate limiting factor in the destruction complex and its turnover has mechanistic implications in Wnt signaling (Lee et al., 2003). Ring Finger 146 (RNF146) regulates Axin degradation in a tankyrase-dependent manner to promote Wnt signaling (Zhang et al., 2011). RNF146 ubiquitylates and degrades Axin through PARylation-dependent ubiquitylation (Callow et al., 2011; DaRosa et al., 2015; Huang et al., 2009a). Segments of tankyrases (TNKS) bind Axin at critical glycine selection gates and directly parsylates Axin. RNF146 interacts with TNKS to promote Axin degradation and without this interaction, Axin turnover is disrupted (DaRosa et al., 2015). RNF146 represents a class of E3s that recognize PARsylation on substrates as the signal to ubiquitylate those substrates. Another E3 that regulates Axin is SIAH1, which has been proposed to regulate Wnt-induced Axin degradation by binding and ubiquitylating the GSK3 binding domain on Axin. SIAH1 can also compete with GSK3 to bind Axin. A short Wnt3a time course shows that Axin is ubiquitylated in the presence of Wnt3a within 3 hours. Depletion of SIAH1 results in a loss of this Wnt-induced Axin ubiquitylation. Thus, SIAH1 is a positive regulator of Wnt signaling by promoting Wnt-induced ubiquitylation of Axin, leading to proteasomal degradation of Axin (Ji et al., 2017). In contrast, an interaction between APC and Axin mediated by HectD1 polyubiquitylation of APC negatively regulates Wnt signaling (Tran et al., 2013).

At the nuclear level, XIAP monoubiquitylates the transcriptional co-repressor, Gro/TLE. When Wnt is on, XIAP monoubiquitylates the Gro/TLE that is bound to TCF/LEF and this ubiquitylation reduces binding of Gro/TLE to TCF/LEF. β-catenin can now bind TCF/LEF and initiate the Wnt transcriptional program (Hanson et al., 2012).

Deubiquitylation at the membrane: maintaining cell surface receptor levels and DVL interaction

At the receptor level, DUBs can regulate the stability of receptors and their ability to facilitate Wnt signaling. USP8/UBPY deubiquitylates FZD4 independent of Wnt activation and promotes endocytosis of the receptor. Ubiquitylation of FZD4 results in FZD4 degradation most likely through lysosomal degradation. Expression of a constitutively active USP8/UBPY mutant increased the cell surface levels of FZD (Mukai et al., 2010). USP6 also modulates cell surface availability of FZD receptors by deubiquitylating FZD (Madan et al., 2016). Ubiquitylation and deubiquitylation of FZD receptors maintain a fine balance of receptors available to respond to Wnt ligands.

DVL deubiquitylation is also important in modulating Wnt activity. Originally identified for its role in promoting NFκB signaling, cylindromatosis (CYLD) inhibits Wnt signaling by deubiquitylating DVL. Loss of CYLD promotes Wnt signaling because a Lys63 polyubiquitylation on the DIX domain of DVL is preserved. Mutations in CYLD that are associated with cylindromatosis disease results in overactive Wnt signaling which drives cylindroma tumor formation (Tauriello et al., 2010). In contrast, USP14 deubiquitylates the Lys63 polyubiquitylation in the C-terminus region of DVL to promote Wnt signaling (Jung et al., 2013). This shows how DUBs with the same target, but

different ubiquitin modifications on the targets can affect Wnt signaling negatively or positively.

Deubiquitylation in the cytoplasm and nucleus: regulating β-catenin, destruction complex, and transcriptional activity

Fine-tuning the destruction complex and its regulation of β-catenin includes many different DUB activities. TRABID (ZRANB1) deubiquitylates APC to promote Wnt signaling. Knockdown of TRABID results in hyperubiquitylation of APC (Tran et al., 2008). TRABID is a prime example of how a DUB can remove ubiquitin chains in a chain-dependent manner. TRABID has shown specificity for Lys29, Lys33, and Lys63 ubiquitin chains (Licchesi et al., 2012). USP15 also acts on APC via complexing with the COP9 signalosome (CSN) to stabilize APC and promote β-catenin degradation (Huang et al., 2009b). As mentioned previously, RNF220 complexes with USP7 to promote deubiquitylation of β-catenin and ultimately, promote Wnt signaling. USP47, which shares some similarity with USP7, also deubiquitylates β-catenin to promote Wnt signaling (Shi et al., 2015).

Unlike DUBs for APC, USP34 deubiquitylates Axin and promotes β-catenin transcriptional activity downstream of the destruction complex. Axin deubiquitylation promotes Axin stability and localization of Axin in the nucleus was shown to positively regulate β-catenin mediated transcription by an unknown mechanism (Lui et al., 2011). USP4 has also been implicated in playing a role in regulating Wnt at the nuclear level by deubiquitylating TCF4 to promote Wnt signaling (Zhao et al., 2009).

Two projects that bridge ubiquitylation and Wnt signaling

Our understanding of ubiquitylation in Wnt signaling is still expanding and as we identify more E3s and DUBs involved in Wnt signaling, we are finding that ubiquitylation regulates many aspects ranging from receptor availability to transcriptional activation. With over hundreds of E3s and about 90 DUBs, there is a vast amount of regulation and signaling control that still remains to be characterized. Some even suggest that the sheer number of these components and their diverse activities allows for even more complexity than phosphorylation (Komander, 2009). Besides the components themselves, there are also factors such as monoubiquitylation, polyubiquitylation, and different lysine linkages that influence how the ubiquitin modification will dictate its protein substrate's activity. What we already know with the few E3s and DUBs identified to play roles in Wnt signaling shows that these modifications are critical in modulating the activities of key Wnt signaling components such as β-catenin, Wnt receptors, and DVL.

Previously, the Lee Lab identified XIAP as the E3 for Gro/TLE, and ubiquitylation of Gro/TLE decreases its affinity for TCF/LEF (Hanson et al., 2012), thereby allowing β-catenin to bind TCF/LEF. However, the mechanism of XIAP recruitment to Gro/TLE remains unknown. One study showed that XIAP interacts with GSK3 (Sun et al., 2009) A simple *in vitro* kinase experiment was performed to determine if GSK3 phosphorylates XIAP, and if so, we wanted to identify the sites that were modified. Following mass spectrometry analysis, multiple phosphorylation sites were identified, of which we found that the threonine 180 site on XIAP is important for XIAP activity in Wnt signaling. We hypothesized that phosphorylation of XIAP by GSK3 is necessary for the activity of

XIAP in Wnt signaling (Figure 1-3). The results from testing this hypothesis will be discussed in Chapter 3 and future directions will be discussed in Chapter 5.

As discussed previously, the E3s, RNF43 and ZNRF3, ubiquitylate the Wnt receptors and promote their turnover. Various DUBs, specifically USP8 and USP6, have been shown to regulate Wnt receptor levels. However, the activity of these DUBs does not seem to be regulated by Wnt signaling, and their activities have mainly been characterized for FZDs. In a gene-trap retrovirus screen using haploid cells stably expressing an EGFP Wnt reporter, WDR20, a member of the USP46 complex was identified as a positive regulator of Wnt signaling (Lebensohn et al., 2016). The members of the USP46 complex are the deubiquitylase ubiquitin specific protease 46 (USP46), WD repeat-containing 20 (WDR20), and USP1-associated factor 1 (UAF1)/WD repeat-containing 48 (WDR48). USP46 exhibits minimal catalytic activity in the absence of WDR20 and UAF1 (Kee et al., 2010; Li et al., 2016a; Yin et al., 2015; Zhu et al., 2019). Thus, we sought to uncover the function of the USP46 complex in Wnt signaling. We found that overexpressing the USP46 complex in HEK293 cells increased steady-state levels of LRP6, and conversely, knockdown of USP46 reduced steady-state levels of LRP6. We hypothesized that the USP46 complex deubiquitylates LRP6 in the presence of Wnt ligand to increase cell-surface levels of LRP6 that can bind Wnt ligands and activate the Wnt pathway (Figure 1-4). The results from testing this hypothesis will be discussed in Chapter 4 and future directions will be discussed in Chapter 5.

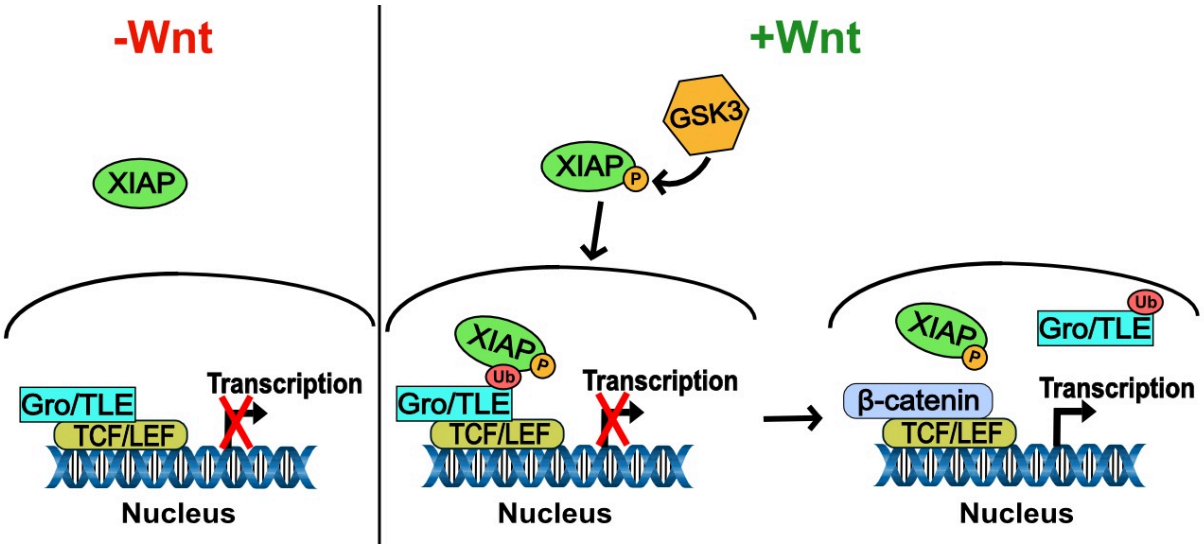

Figure 1-3. Schematic of the hypothesized mechanism of regulation of XIAP activity in Wnt signaling.
The hypothesis is that XIAP is phosphorylated by GSK3 to promote XIAP activity in Wnt signaling. Two specific aims are explored: (A) Determine whether GSK3 phosphorylates XIAP (B) Determine whether the XIAP phosphomutant results in loss of XIAP activity in Wnt signaling.

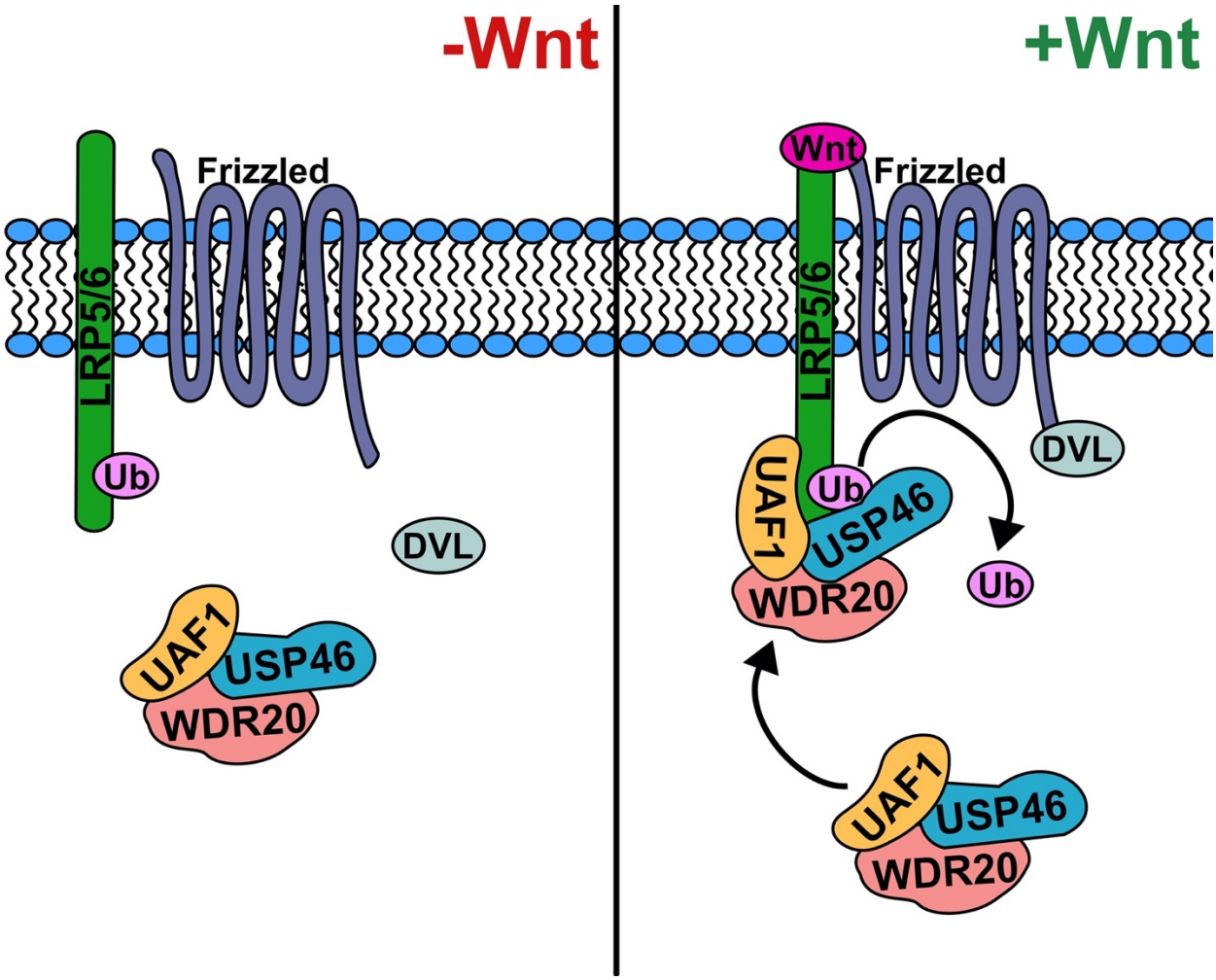

Figure 1-4. Schematic of the hypothesized mechanism of the USP46 complex in Wnt signaling.
The hypothesis is that the USP46 complex deubiquitylates LRP6 to promote Wnt signaling by blocking LRP6 turnover. Two specific aims are explored: (A) Determine the mechanism by which the USP46 complex regulates LRP6 levels. (B) Determine whether the USP46 complex assembly and association with LRP6 is dependent on active Wnt signaling

Chapter 2

MATERIALS & METHODS

Cell lines

The colorectal cancer cell line, SW480, the cervical cancer cell line, HeLa, and the human embryonic kidney cell line, HEK293, were purchased from ATCC (CCL-228, CCL-2, CRL-1573). The HEK293 cell line containing a stably integrated Super TOPFlash (STF) reporter for Wnt signaling, HEK293STF, was obtained from the Vanderbilt Antibody Protein Resource. The colorectal cancer cell line, HCT116, was a gift from the laboratory of Bert Vogelstein. Glioblastoma cell lines, A172 and U87, were generous gifts from William Weiss (University of California, San Francisco). All lines were maintained in DMEM supplemented with 8% FBS.

Generation of the LRP6-FLAG (LF203) cell line

The LRP6-FLAG Clone #203 (LF203) cell line was created using CRISPR-mediated editing to knock-in a FLAG tag on the C-terminus of LRP6 in HEK293 cells. The gRNA sequence (5'-TGTACAGACTCCTCCTGAGG-3') used for targeting the C-terminus of LRP6 was identified using the CHOPCHOP resource. Briefly, the LRP6 gRNA was cloned into the pCas-Guide-EF1a-GFP vector (Origene) following the manufacturer's protocol. HEK293 cells were transfected with the LRP6 gRNA plasmid and a gene block (IDT) with homology arms flanking a FLAG tag (5'-

AGAGGAGAACTATGAAAGCTGCCCACCTTCTCCATACACAGAGAGGAGCTATTCTC
ATCACCTCTACCCACCGCCACCCTCTCCCTGTACAGACTCCTCCGGTGGAGGTGG
AGGTGGAGACTACAAAGACGATGACGACAAGTGAGGAGGCGCCCTCCTCCTCTGA
CTGCCTCCAACGTAAAAATGTAAATATAAATTTGGTTGAGATCTGGAGGGGGGGAG
GGAGCTATTAGAGAAGGATGAGG-3'), using Lipofectamine 3000. After 48 hr, cells were single-cell sorted (BD FACSMelody) into 96-well plates and grown to confluency. Positives were identified by immunoblotting for the FLAG epitope. Genomic DNA was collected from the parental line and the LF203 cell line using the Wizard Genomic DNA Purification Kit (Promega). Genomic DNA was submitted to the Vanderbilt VANTAGE Core for whole genome sequencing to verify integration and positioning of the FLAG tag on the C-terminus of LRP6.

Organoid cultures

Wild-type mouse intestinal organoids were isolated and cultured as previously described (Li et al., 2017). Prior to infection, organoids were collected and dissociated by incubating in Gentle Cell Dissociation Reagent (StemCell Technologies) for 10 min at RT. For infection, 7,500 dissociated organoids were resuspended in a mixture containing lentivirus (MOI = 10), 8 ug/ml polybrene, and 10 μM Y27632 (StemCell Technologies) in 25% L-WRN conditioned media. The organoid-lentivirus mixtures were then spinoculated at 600 X g for 2 hr at RT, followed by incubation at 37°C for 4 hr. After incubation, organoids were pelleted, washed with Intesticult growth media (StemCell Technologies), resuspended in ice-cold Matrigel (Corning), seeded in a 48-well plate, and overlaid with Intesticult growth media. After 72 hr, the percentage of RSPO-

conditioned medium in the culture media was adjusted according to experimental design. Images were taken after 9 days using an Olympus IX51 inverted fluorescence microscope and Olympus CellSens software. The viability of organoids was assayed using Cell-Titer Glo (Promega) following manufacturer's protocol.

APC^{min} organoids were collected and digested with Gentle Cell Dissociation Reagent (Stemcell Technologies) for 10 min at RT, followed by shearing with a 25G needle once. Dissociated organoids were added to the lentiviral mixture (lentiviral particles (Dharmacon, MOI = 10), 8 ug/ml polybrene, and 10 μM Y27632 (Stemcell Technologies) in 25% L-WRN conditioned media. The organoid-lentivirus mixture was spinoculated at 600 xg for 2 hr using a tabletop centrifuge at RT, followed by incubation at 37°C for 4 hr. Infected organoids were resuspended in Matrigel (Stemcell Technologies), plated at 10,000/well in a 48-well plate, and overlaid with culture media. After 9 days, organoids were imaged, collected for RNA extraction, lysed for immunoblotting, and assayed for cell viability. Images were obtained using an Olympus IX51 inverted fluorescence microscope and Olympus CellSens software. The organoid size was measured using the Olympus CellSens software. For cell viability and immunoblotting, organoids were lysed in RIPA buffer (Thermo) supplemented with Protease/Phosphatase inhibitor cocktail (Thermo) at 4°C for 10 minutes. 1/20 of the lysates were used in Cell-Titer Glo assays (Promega) following the product's instructions to measure cell viability. The remaining lysates were boiled in SDS sample buffer for 10 min, followed by SDS-PAGE analysis and immunoblotting.

Gel filtration analysis of the USP46 deubiquitylase complex

HEK293 cells were lysed in detergent-free NDLB and sheared with a 25G needle. Lysates were spun at 13,000 RPM in a microcentrifuge for 10 min at 4^{o}C, followed by centrifugation at 100,000 X g for 20 min at 4^{o}C. Samples (normalized for protein concentration and volume) were loaded onto a Superdex 200 10/300 gel filtration column connected to a BioLogic DuoFlow System (Bio-Rad). Fractions were collected, concentrated by TCA precipitation, and pellets resuspended in sample buffer for SDS-PAGE and immunoblotting. The following standards were used for calibration: thyroglobulin (670 kDa), γ-globulin (158 kDa), ovalbumin (44 kDa), and myoglobin (17 kDa) (Bio-Rad).

Sucrose density gradient centrifugation for the USP46 deubiquitylase complex and LRP6 receptor

Equivalent amounts of whole-cell lysates in 300 uL volumes were gently layered on top of 5 ml 15-40% sucrose gradients (50 mM Tris-HCl pH 7.4, 300 mM NaCl, 0.02% Triton X-100 (w/v), 10 mM NaF, 1X PhosSTOP tablet inhibitor, 1X protease inhibitor cocktail). Gradients were spun at 43,000 RPM for 4 hr at 4^{o}C. Fractions (350 uL) were manually collected from the top of the gradient and concentrated by chloroform-methanol precipitation. Precipitated samples were resuspended in sample buffer and analyzed by SDS-PAGE and immunoblotting.

Transfections and RNAi mediated knockdowns

Plasmid transfections were performed using the calcium phosphate method unless otherwise noted. siRNA transfections for Non-targeting (NT) control, AXIN1, USP46, and UAF1 were performed using Dharmafect1 (Horizon Discovery) following the manufacturer's protocol. Knockdowns with single siRNAs or pooled siRNAs (combining siRNA #1 & siRNA #2) were performed at a final concentration of 50 nM. See Table 2-1 for siRNAs sequences.

Table 2-1. Sequences of siRNAs

siRNA	Sense Sequence (5'→3')
AXIN #1	GCGUGGAGCCUCAGAAGUUUU
AXIN #2	CCGAGGAGAAGCUGGAGGAUU
Non-targeting (NT)	UAAGGCUAUGAAGAGAUACUU
UAF1 #1	CAGCAGAGAUGUAUAGCAAUU
UAF1 #2	CCUAAGAAACCCUGACAUUUU
USP46 #1	GCAGGAUGCUCAUGAAUUUUU
USP46 #2	UCCGAAACAUCGCCUCCAUUU

Antibodies

See Table 2-2 for antibodies used and their working concentrations.

Table 2-2. Antibodies
Used for immunoblotting or immunoprecipitation.

Antibodies	Concentration	Source
Rabbit anti-XIAP	1:3	Novus Biologicals
Mouse anti-XIAP	1:1000	BD Transduction
Mouse anti-MYC	1:1000	Vanderbilt Antibody Protein Resource
Rat anti-HA	1:1000	Roche
Mouse anti-GAPDH	1:5000	Santa Cruz
Mouse anti-GAPDH	1:500	Developmental Studies Hybridoma Bank
Rabbit anti-Histone H3	1:2500	Santa Cruz
Mouse anti-β-catenin	1:5000	BD Transduction
Mouse anti-GSK3β	1:1000	BD Transduction
Rabbit IgG		Santa Cruz
Rabbit anti-USP46	1:1000	Proteintech
Rabbit anti-DYKDDDDK (FLAG)	1:2000	Proteintech
Mouse anti-Tubulin	1:1000	Vanderbilt Antibody Protein Resource
Rabbit anti-Axin1 (C76H11)	1:1000	Cell Signaling Technology
Rabbit anti-LRP6 (C5C7)	1:1000	Cell Signaling Technology
Rabbit anti-WDR20	1:2500	Bethyl Laboratories
Rabbit anti-WDR48 (UAF1)	1:1000	Proteintech
Goat anti-rat IgG H+L-HRP	1:5000	Santa Cruz
Goat anti-mouse IgG H+L-HRP	1:5000	Promega
Goat anti-mouse IgG H+L-HRP	1:5000	Promega

RNA isolation and qRT-PCR

HEK293STF cells were treated with siRNA for 48 hr followed by incubation with Wnt3a (10 ng/ml, Time Biosciences) for 8 hr. Total RNA was isolated using RNAeasy RNA extraction kit (Qiagen) and reversed transcribed to cDNA using the High-Capacity cDNA Reverse Transcription kit (Applied Biosystems). qPCR assays were performed in quadruplicate using TaqMan FAST Advanced Real-time PCR Master Mix (Applied Biosystems) and analyzed on a CFX96 Real-Time PCR system (Bio-Rad). Predesigned and validated TaqMan probes (Life Technologies) used were as follows: *GUSB* (Hs00939627_m1), *SP5* (Hs01370227_mH), and *LEF1* (Hs01547250_m1). For Xenopus and zebrafish studies, samples were homogenized in 1 ml RNA Stat-60 (Amsbio) with a disposable pestle and extracted with chloroform. All qPCR amplifications were performed in biological and technical triplicate. See Table 2-3 for sequences of PCR primers.

Table 2-3. PCR primers for qPCR

Primer	Sequence (5'→3')
*Odc*_F	GTCAATGATGGAGTGTATGGATC
*Odc*_R	TCCATTCCGCTCTCCTGAGCAC
*Chordin*_F	AACTGCCAGGACTGGATGGT
*Chordin*_R	GGCAGGATTTAGAGTTGCTTC
*Xnr3*_F	CTTCTGCACTAGATTCTG
*Xnr3*_R	CAGCTTCTGGCCAAGACT
*β-catenin*_F	CGAGCTGTCTTCCCATCCA
*β-catenin*_R	CACCAACGTAGCTGTCTTTCTG
*Lef1*_F	GAGGGAAAAGATCCAGGAAC
*Lef1*_R	AGGTTGAGAAGTCTAGCAGG
*CyclinD1*_F	GCCAAACTGCCTATACATCAG
*CyclinD1*_R	TGTCGGTGCTTTTCAGGTAC

Expression and purification of the E3 XIAP

BL21 bacterial cells transformed with MBP-XIAP or the XIAP phosphomutant, MBP-XIAP^{T180A}, plasmids were grown in a 37°C shaking incubator until cell density reached OD600 = 0.5. IPTG (300 μM) was added, and the cultures incubated at 18°C overnight. Cells were then spun down, and cell pellets lysed by sonication in Tris-NaCl-phenylmethylsulfonyl fluoride (TNP) buffer (50 mM Tris-HCl, 150 mM Nacl, 2 mM EDTA, 1 mM phenylmethylsulfonyl fluoride (PMSF), 0.1% Triton X-100). Lysates were centrifuged at 12,000 rpm at 4°C for 10 min, and supernatants incubated with amylose beads on a shaking platform for 2 hr at 4°C. Beads were then washed 3X times with 10X column volumes of TNP, and MBP-bound proteins were eluted with TNP buffer containing 1% maltose. Eluted proteins were further purified on a Mono Q anion-exchange column using the AKTA FPLC apparatus (GE Healthcare). Fractions containing the MBP fusion proteins were concentrated to 1mg/ml using Amicon Ultra Centrifugal Filter Units (EMD Millipore, Billerica, MA), and proteins were aliquoted and stored at -80°C until use.

Immunoblotting

For whole-cell lysates, cells were obtained using non-denaturing lysis buffer (NDLB) (50 mM Tris-HCl pH 7.4, 300 mM NaCl, 5 mM EDTA, and 1% Triton X-100 (w/v) supplemented with 1 mM PMSF, 1X PhosSTOP inhibitor (Roche), and 10 mM NaF). Samples were gently agitated at 4°C for 30 minutes, followed by clarification by spinning in a microfuge at 13000 RPM for 10 minutes at 4°C. For cytoplasmic fractions, cells were lysed using 10mM HEPES pH 7.8, 10 mM KCl, 2 mM $MgCl_2$, 0.1 mM EDTA,

1 mM PMSF, 1X PhosSTOP inhibitor (Roche), and 10 mM NaF, and incubated on ice for 30 minutes. Lysates were vortexed, sheared 8 times with a 25G needle, and clarified by spinning in a microfuge at 13000 RPM for 5 minutes at 4°C. Proteins were analyzed by SDS-PAGE and immunoblotting. Chemiluminescence signal was detected using a C-DiGit blot scanner (LI-COR). Obtained images and band intensity were analyzed using Image Studio (LI-COR).

Co-immunoprecipitation studies

Cells were lysed in NDLB, and lysates were diluted to 1 mg/ml and incubated with antibodies overnight at 4°C. Samples were then incubated with Protein A/G magnetic beads (Millipore) or anti-FLAG agarose beads (Sigma) for 2 hrs. Beads were washed 3X with NDLB and sample buffer added to elute the bound protein (37°C for 1 hr).

Immunofluorescence

HEK293STF cells were grown on coverslips coated with fibronectin, fixed in 4% formaldehyde, and permeabilized. Samples were then incubated with primary antibody followed by secondary antibodies conjugated to Cy3 or Alexa 488. Samples were mounted in ProLong Gold with DAPI (Invitrogen), and cells were visualized using a Cascade 512B camera mounted on a Nikon Eclipse TE2000-E confocal microscope.

In vitro phosphorylation assay

For the radioactive kinase assay, 100 ng MBP-XIAP was incubated with 100 ng TEV protease plus 250 units of GSK3 (NEB), 5 mM of cold ATP and, 5 uCi of [γ^{32}P] ATP in 1X kinase reaction buffer (50 mM Tris-HCl, 10 mM $MgCl_2$, 5 mM dithiothreitol (DTT), pH 7.5). Reactions were incubated at 30°C for 1 hr on a TOMY shaker and terminated with sample buffer. For CK1 potentiation assays, 20 uL of MBP-XIAP (~1 mg/mL) bound to amylose beads in 1X Protein Kinase buffer (NEB) containing ATP (1.5 mM) was incubated in the absence or presence of 110 ng recombinant CK1α (Thermo Fisher Scientific, Waltham, Massachusetts). Reactions were incubated at 30°C for 1 hr on a TOMY shaker. Beads were then washed 3X with 1X kinase reaction buffer prior to GSK3 radioactive kinase assay.

Mass spectrometry analysis

A kinase reaction was performed as described for the *in vitro* phosphorylation reaction except that radioactive ATP was not added. Reactions were subjected to SDS-PAGE followed by staining with Coomassie Brilliant Blue. The band corresponding to XIAP was then excised and cut into 1 mm^3 pieces prior to in-gel digestion and analysis by liquid chromatography-coupled tandem mass spectrometry. The gel pieces were treated with 45 mM DTT and available Cys residues were carbamidomethylated with 100 mM iodoacetamide. After destaining the gel pieces with 50% MeCN in 25 mM ammonium bicarbonate, proteins were digested with trypsin (10 ng/uL) in 25 mM ammonium bicarbonate overnight at 37°C. Peptides were extracted by gel dehydration (60% MeCN, 0.1% TFA), the extract was dried by speed vac centrifugation, and

peptides were reconstituted in 0.1% formic acid. The peptide solutions were then loaded onto a capillary reverse phase analytical column (360 μm O.D. x 100 μm I.D.) using an Eksigent NanoLC HPLC and autosampler. The analytical column was packed C18 reverse phase resin (Jupiter, 3 μm beads, 300Å, Phenomenox), directly into a laser-pulled emitter tip. Mobile phase solvents consisted of 0.1% formic acid, 99.9% water (solvent A) and 0.1% formic acid, 99.9% acetonitrile (solvent B). A 90-minute gradient was performed, and eluting peptides were mass analyzed on an LTQ Orbitrap mass spectrometer (Thermo Scientific), equipped with a nanoelectrospray ionization source. The instrument was operated using a data-dependent method with dynamic exclusion enabled. Full scan (m/z 400-2000) spectra were acquired with the Orbitrap, and the top 5 most abundant ions in each MS scan were selected for fragmentation via collision-induced dissociation (CID) in the LTQ. An isolation width of 2 m/z, activation time of 30 ms, and 35% normalized collision energy were used to generate MS2 spectra. Dynamic exclusion duration was set to 60 sec. For identification of peptides, tandem mass spectra were searched with Sequest (Thermo Fisher Scientific) against a human subset database created from the UniprotKB protein database (www.uniprot.org). Variable modifications of +57.0214 on Cys (carbamidomethylation), +15.9949 on Met (oxidation), and +79.9663 on Ser, Thr, and Tyr (phosphorylation) were included for database searching. Search results were assembled using Scaffold 4.3.2 (Proteome Software).

TOPFlash reporter assay

For cell-based luciferase TOPFlash assays with HEK293STF cells, cells were incubated with 10 ng/μl purified Wnt3a (Time Bioscience) for 24 hr prior to lysis with 1X

Passive Lysis buffer (Biotium) on a shaker for 15 min. Experiments were performed in duplicates, with one set used to measure luciferase activity using Steady-Glo Luciferase Assay (Promega), and the second set used to measure cell viability using the Cell-Titer Glo Assay (Promega). Luciferase signals were normalized to cell viability Cell-Titer Glo signals. For Dual-Glo (Promega) assays, lysates were prepared as above. Firefly and Renilla luciferase signal measurements were pre-formed according to the manufacturer's instructions. Firefly luciferase signals were normalized to co-transfected Renilla luciferase signals. Luminescence was detected with FLUOstar Luminometer (Optima). Assays were performed in either triplicates or quadruplicates and repeated at least 3 times.

Xenopus and zebrafish injections, immunoblotting, and microscopy

For injections, capped mRNAs were generated using mMessage mMachine (Ambion) according to the manufacturer's instructions. *Xenopus* embryos were *in vitro* fertilized, de-jellied, cultured, and injected with mRNA as previously described (Peng, 1991). Embryos were injected equatorially in the ventral blastomeres at the 4-cell stage and allowed to develop to stage 35 before phenotyping. Embryos were assessed for complete or partial duplication, and statistical analyses were performed using Fisher's exact test with Bonferroni correction. A value of $p < 0.05$ was considered statistically significant. For immunoblotting, sample buffer was added to pooled embryos from each condition and processed for SDS-PAGE. For zebrafish injections, wild-type (AB) zygotes (1 cell) were injected (1 nl) in the single cell and phenotyped at 5 days post fertilization. Scoring of the cyclopic phenotype is as described previously (Neitzel et al.,

2019). Only phenotypes observed in *n*≥3 biological repeats were reported. Embryos with severe and non-specific edema were excluded from the analysis. Embryos from *n*≥3 male/female pairs were collected per biological repeat. Morpholinos with the following sequences were purchased from Gene Tools. Standard Control MO: 5'-CCTCTTACCTCAGTTACAATTTATA-3', WDR20 MO: 5'-CTCCGCCGCCATCTTTGACATTTAC -3', UAF1 MO: 5'-GAAGCGTCGCCATCTTGCATGTTG-3', USP46 MO: 5'-CGATGTTTCTGACAGTCATTTAGTT-3'.

Bright field images were obtained using a Stemi 2000-CS microscope (Zeiss, Oberkochen, Germany) with an Olympus DP72 camera. Images were analyzed in Fiji or Photoshop. All animals in this study (*Xenopus* and zebrafish) were treated in accordance with Vanderbilt's Institutional Animal Care and Use Committee.

Ubiquitylation assays

In vitro ubiquitylation assays were carried out using the Ubiquitin Thioester/Conjugation Initiation Kit (Boston Biochem). Briefly, E1 ubiquitin-activating enzyme (1 ug), E2 UbcH5a (1 ug), ubiquitin (1 ug), XIAP or XIAP^{T180A} (1 ug) and HA-TLE3 (2 ul, generated from an *in vitro* transcription-translation reaction, Promega) were assembled in a 20 ul reaction, and samples were incubated on a TOMY shaker at 30°C for 90 min. Reactions were terminated by addition of sample buffer and ubiquitylated TLE3 products subjected to SDS-PAGE followed by immunoblotting for HA (Muratani and Tansey, 2003b). For cell-based ubiquitylation assays, cells were collected for ubiquitylation assays as described previously (Hanson et al., 2012; Salghetti et al.,

1999). Briefly, cells were spun down for 30 seconds at 10,000 RPM in a microcentrifuge at 4°C, washed in ice-cold 1X PBS, and lysed in Buffer A (6 M guanidine-HCl, 0.1 M Na2HPO4/NaH2PO4 (pH 8.0), and 10 mM imidazole). Lysates were sonicated at max power (8X at 1 second intervals), added to Ni-NTA agarose beads, and incubated for 3 hr at RT with rotation. Beads were washed with 2X Buffer A, 2X Buffer A/TI (25 mM Tris-HCl (pH 6.8), and 20 mM imidazole, 1:3 v/v), and 1X Buffer TI. Bound samples were eluted with sample buffer supplemented with 0.2 M imidazole, followed by SDS-PAGE and immunoblotting.

Cell-surface biotinylation assays

HEK293 or LF203 cells were prepared by washing 3X with pre-chilled modified PBS (1X PBS supplemented with 0.9 mM $CaCl_2$ and 0.5 mM $MgCl_2$) on ice. Biotinylation was initiated by incubating the cells with 0.5 mg/ml EZ-Link Sulfo-NHS-SS-Biotin (Thermo Fisher Scientific) in modified PBS with gentle rocking for 30 min at 4°C. The reaction was then quenched by washing the cells 2X with 50 mM Tris-HCl (pH 7.4) for 10 min. Whole-cell lysates were then collected with RIPA buffer (50 mM Tris-HCl pH 7.4, 150 mM NaCl, 1% Triton X-100, 0.5% sodium deoxycholate, 0.1% SDS, 1 mM EDTA) supplemented with 1 mM PMSF, 10 mM NaF, and 1X PhosSTOP. Lysates were gently agitated for 30 minutes at 4°C and clarified by spinning at 13000 RPM in a microcentrifuge for 10 minutes at 4°C. Biotinylated proteins were purified with Strepavidin (NEB) or Neutravidin agarose beads (Pierce). Samples were analyzed by SDS-PAGE followed by immunoblotting.

Flow cytometry analysis for Annexin V following Fas ligand-induced apoptosis

HeLa cells were transfected with vector, MYC-XIAP, or the XIAP phosphomutant, MYC-XIAP^{T180A}, to determine if MYC-XIAP^{T180A} has a reduced capacity to inhibit apoptosis. Fresh media was changed 24 hr post-transfection, and cells were incubated with 100 ng/ml recombinant Fas ligand (Sigma-Aldrich) for 24 hr. Cells released into the media and adherent cells were counted, pelleted at 400 g, and resuspended in ice-cold 1X staining media (1X PBS, 2% BSA, and 0.1% sodium azide). Cells ($1x10^6$) were then washed 2X in ice-cold 1X staining media, resuspended in 200 ul of Annexin V binding buffer (BioLegend) and stained with 2.5 ul Annexin V (BioLegend) plus 0.5 ul propidium iodide (1 mg/mL) for 15 min in the dark at room temperature. An additional 300 ul of Annexin V binding buffer was added prior to analysis on a BD Fortessa cell analyzer. Data were analyzed with FlowJo software and PRISM.

Statistics

Data were analyzed with PRISM 9 Software (GraphPad). Statistical analyses were performed in R v3.1.0. Fisher's exact test and multiple T-test (two-tailed, equal variance). Post hoc analysis of Fisher's exact test and multiple T-test tests were by Bonferroni correction. For Xenopus and zebrafish studies, sample sizes (n) are indicated as n= number of samples, with the number of the observed phenotype over the total sample number.

Chapter 3

PHOSPHORYLATION OF XIAP AT THREONINE 180 CONTROLS ITS ACTIVITY IN WNT SIGNALING

This chapter is adapted from "Phosphorylation of XIAP at threonine 180 controls its activity in Wnt signaling" published in *Journal of Cell Science* and has been reproduced with the permission of the publisher and my co-authors (Hang BI, Sawyer LM, Neitzel, LR, Crispi EE, Rose KL, Popay TM, Zhong A, Lee LA, Tansey WP, Huppert Stacey, Lee E). doi: 10.1242/jcs.210575 Link: https://jcs.biologists.org/content/131/10/jcs210575

INTRODUCTION

Cellular inhibitor of apoptosis (cIAP) protein family members, which include the X-linked inhibitor of apoptosis (XIAP), are well-known for binding caspases and inhibiting their activities (Galban and Duckett, 2010). XIAP has also been shown to have a critical role in Wnt signaling (Hanson et al., 2012). The Wnt signaling pathway plays an integral role in many developmental processes and in human cancer (Saito-Diaz et al., 2013). In the absence of a Wnt signal, cytoplasmic β-catenin is phosphorylated by casein kinase 1 (CK1) and glycogen synthase kinase 3 (GSK3) are targeted for ubiquitin-mediated degradation by the proteasome. GSK3 is a serine/threonine kinase that has been shown to be involved in multiple signaling pathways, including insulin and Hedgehog signaling (Wu and Pan, 2010). Upon Wnt activation, β-catenin accumulates in the cytoplasm, translocates into the nucleus, and displaces the co-repressor Gro/TLE from the transcription factor TCF to initiate a Wnt transcriptional program (Daniels and

Weis, 2005). The Lee Lab previously demonstrated that XIAP associates with the co-repressor complex to promote monoubiquitylation of Gro/TLE, thereby decreasing its affinity for TCF and allowing β-catenin to bind TCF (Hanson et al., 2012). How XIAP is recruited to Gro/TLE and how its activity is regulated during Wnt signaling versus during apoptosis is unknown. I now demonstrate that XIAP binds and is phosphorylated by GSK3 at threonine 180; this phosphorylation event is required for its activity in Wnt signaling, but dispensable for its role in the apoptotic pathway.

RESULTS

XIAP is a substrate of GSK3 *in vitro*

A previous study demonstrated that XIAP interacts with GSK3 in mammalian cells (Sun et al., 2009). Consistent with this result, I also showed that endogenous GSK3 co-immunoprecipitates with endogenous XIAP in several cultured cell lines, including the colorectal cancer lines, SW480 and HCT116 (Figure 3-1A). I found, however, that this interaction was not altered upon active Wnt signaling. The Lee Lab previously demonstrated that Wnt signaling did not alter the overall level of XIAP or its intracellular localization and only a small, localized pool of XIAP associated with TCF is affected (Hanson et al., 2012). Thus, the interaction between XIAP and GSK3 may be regulated similarly at a localized level. We found that XIAP was phosphorylated by GSK3 in an *in vitro* radioactive kinase assay performed by Brian Hang (Figure 3-1B & Figure 3-1C). Certain GSK3 substrates require a previous (primed) phosphorylation on a Ser or Thr residue (Beurel et al., 2015). I therefore tested whether previous

phosphorylation by CK1 could enhance the phosphorylation of XIAP by GSK3. Prior incubation with CK1α (under *in vitro* kinase conditions) dramatically increased the phosphorylation of purified XIAP by GSK3 (Figure 3-1D). This result suggests that CK1 (or possibly another kinase) may prime XIAP for GSK3 phosphorylation.

The online systems biology resource tool, PhosphoSitePlus (Hornbeck et al., 2015), curates various data sources to provide information on protein phosphorylation sites. Using this resource, I searched for previously reported phosphorylation sites on XIAP (Figure 3-2A). To determine if any of these sites represent actual GSK3 phosphorylation sites on XIAP, Brian Hang performed an *in vitro* kinase reaction with purified XIAP and GSK3 followed with liquid chromatography-mass spectrometry (LC-MS) analysis performed by Kristie Rose. One of the predicted sites, threonine 180 (T180), which is located within the Baculovirus Inhibitor of Apoptosis Repeat 2 (BIR2) domain of XIAP, is a major phosphorylation site of GSK3 *in vitro* (Figure 3-2B). This result is consistent with previous studies demonstrating that XIAP is phosphorylated on T180 in human cells (Mertins et al., 2016; Sharma et al., 2014).

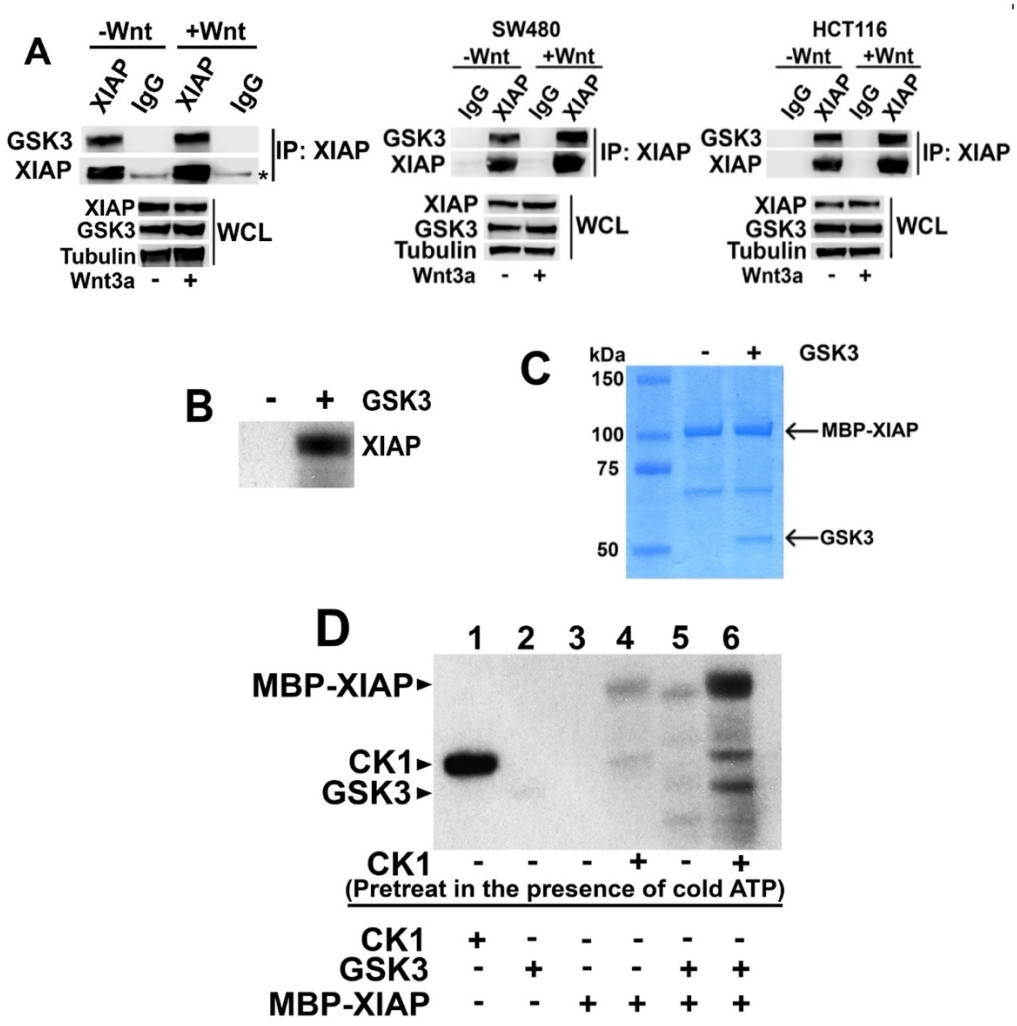

Figure 3-1. XIAP is phosphorylated by GSK3.
Figure is adapted from the publication mentioned at the beginning of this chapter. **(A)** Endogenous XIAP co-immunoprecipitates with endogenous GSK3. XIAP was immunoprecipitated from lysates of HEK293STF cells, SW480 colorectal cancer cells, or HCT116 colorectal cancer cells incubated in the absence or presence of recombinant Wnt3a followed by immunoblotting. Asterisk indicates heavy chain of IgG. WCL = whole cell lysates. IP = immunoprecipitation. Replicated at least three times. **(B)** Purified XIAP is phosphorylated by GSK3 in vitro in a [γ^{32}P] ATP kinase assay. Reactions were analyzed by SDS/PAGE followed by autoradiography. Replicated at least three times by Brian Hang. (C) Coomassie showing equal loading of MBP-XIAP from the in vitro kinase assay demonstrating equivalent amounts of XIAP protein in the reactions. **(D)** CK1 enhances XIAP phosphorylation by GSK3. XIAP-bound to beads was incubated with CK1 in a kinase reaction containing cold ATP (lanes 4 and 6). CK1 was washed away, and XIAP-bound beads incubated with GSK3 in a kinase reaction containing [γ^{32}P] ATP. Reactions were analyzed by SDS/PAGE followed by autoradiography. Kinase only lanes show CK1 and GSK3 autophosphorylation (lanes 1 and 2). Assays were performed by Brian Hang

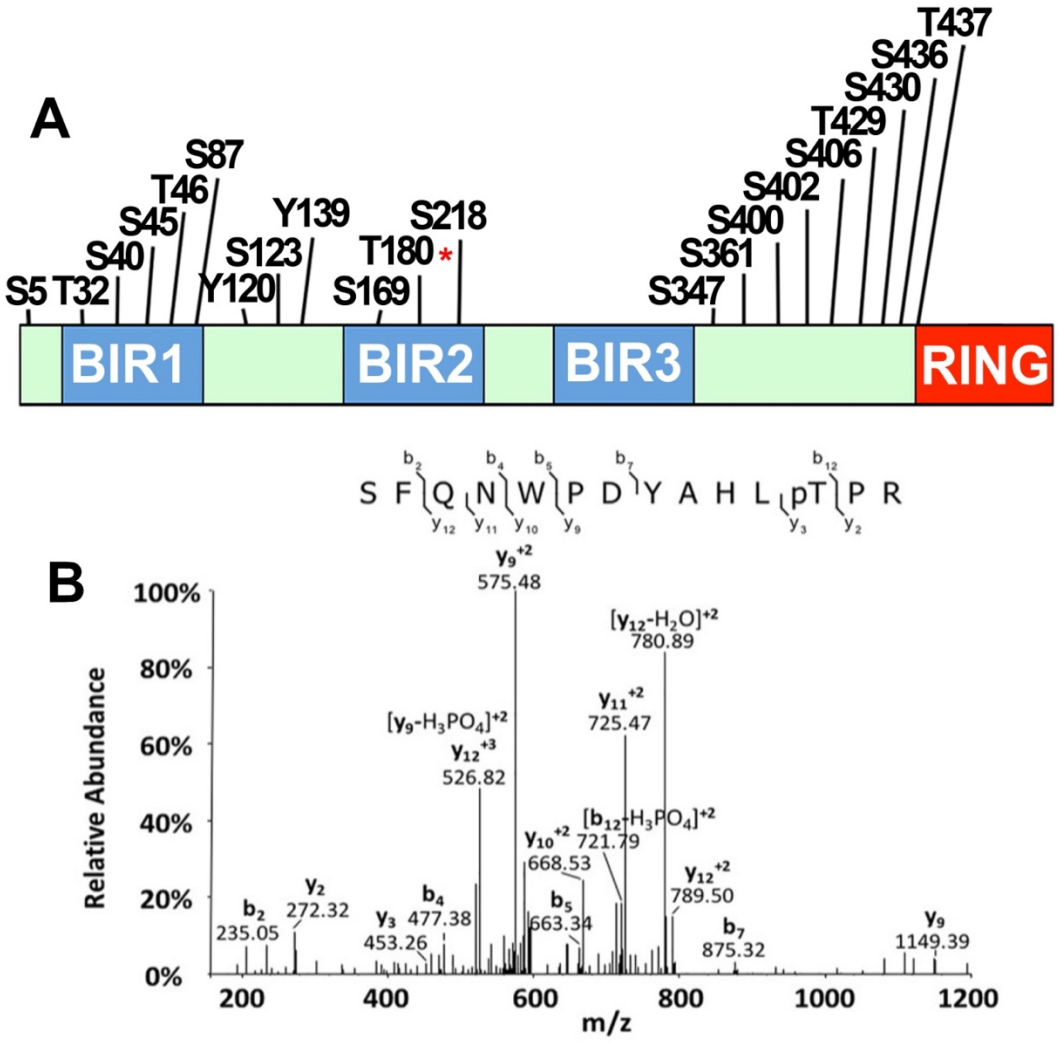

Figure 3-2. XIAP is phosphorylated by GSK3 at threonine 180.
Figure is adapted from the publication mentioned at the beginning of this chapter. **(A)** The predicted phosphorylation site on threonine 180 of XIAP is an in vitro GSK3 phosphorylated site. Predicted phosphorylation sites on XIAP curated by the PhosphoSitePlus online resource tool (Hornbeck et al., 2015). LC-MS analysis of XIAP identifies threonine 180 (asterisk) as a prominent in vitro GSK3 phosphorylation site. **(B)** Mass spectrometry analysis performed by Kristie Rose from an *in vitro* kinase reaction containing purified XIAP and GSK3 identifies phosphorylated threonine 180 on XIAP. The peptide sequence is shown above the spectrum with corresponding b and y ion splits with pT being the phosphorylated T180 site.

The XIAP^{T180A} phosphomutant exhibits decreased Wnt activity

I next tested whether an alanine mutant of XIAP at position T180 (XIAP^{T180A}) co-immunoprecipitated with GSK3 to a similar extent as wild-type XIAP (Figure 3-3A) and found that the interaction was similar. The XIAP ligase mutant, XIAP$^{H467A/F495A}$ (Damgaard et al., 2012; Gyrd-Hansen et al., 2008; Holley et al., 2002), also co-immunoprecipitated with GSK3 to a similar extent as wild-type XIAP (Figure 3-3B), suggesting that the interaction between XIAP and GSK3 does not depend on the ligase activity of XIAP. Leah Sawyer next performed immunolocalization of XIAP^{T180A} to determine if it exhibited a different localization pattern compared to wild-type XIAP. Leah Sawyer transfected MYC-tagged XIAP and XIAP^{T180A} into HEK293STF cells and performed immunostaining (Figure 3-4A). We found no differences between the cellular localization of XIAP and XIAP^{T180A} as assessed by immunofluorescence. These results were confirmed by cytoplasmic and nuclear cellular fractionation studies of HEK293STF cells expressing XIAP or XIAP^{T180A} (Figure 3-4B).

Consistent with the Lee Lab's previous studies, we found that overexpression of XIAP is insufficient to promote Wnt activation in cultured human cells (Figure 3-5A). Thus, XIAP is unlikely a limiting component of the Wnt signal transduction pathway in mammalian cells (Hanson et al., 2012). Similarly, we did not detect Wnt activity when we overexpressed XIAP^{T180A} (Figure 3-5A). We next tested whether XIAP may become limiting when the Wnt pathway is activated. Using HEK293STF cells, which contain a stably integrated luciferase-based Wnt reporter (Veeman et al., 2003), we found that overexpression of XIAP potentiates activation by Wnt3a (Figure 3-5A). The lack of change in β-catenin levels in the XIAP (or XIAP^{T180A}) plus Wnt3a condition compared to

Wnt3a treatment alone is consistent with the nuclear function of XIAP, which is downstream of the β-catenin destruction complex and would not be expected to impact steady-state β-catenin levels (Hanson et al., 2012). In contrast to XIAP, we found no enhancement of Wnt reporter activity upon overexpression of $XIAP^{T180A}$ (Figure 3-5A & Figure 3-5B), suggesting that phosphorylation at the T180 site is critical for the role of XIAP during Wnt signaling.

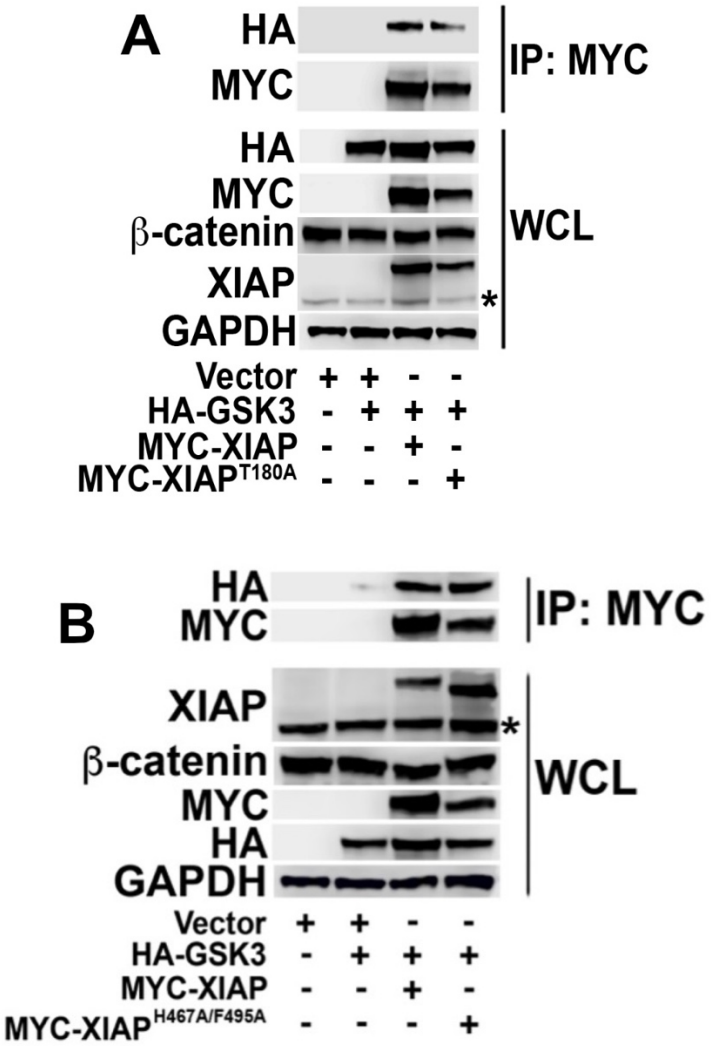

Figure 3-3. The XIAP^{T180A} and XIAP$^{H467A/F495A}$ mutants interact with GSK3.
Figure is adapted from the publication mentioned at the beginning of this chapter. **(A)** GSK3 associates with XIAP and the kinase mutant, XIAP^{T180A}, to a similar extent. HEK293STF cells were transfected with vector, HA-GSK3, MYC-XIAP, and MYC-XIAP^{T180A} as indicated, lysates were collected, and immunoprecipitation performed with anti-MYC antibody. Asterisk indicates endogenous XIAP. WCL = whole cell lysates. IP = Immunoprecipitation. **(B)** The ligase mutant, XIAP$^{H467A/F495A}$, interacts with GSK3 to a similar extent as wild-type XIAP. HEK293STF cells were transfected as indicated, lysates collected, and immunoprecipitation performed. Asterisk indicates endogenous XIAP. WCL = whole cell lysates. IP = immunoprecipitation.

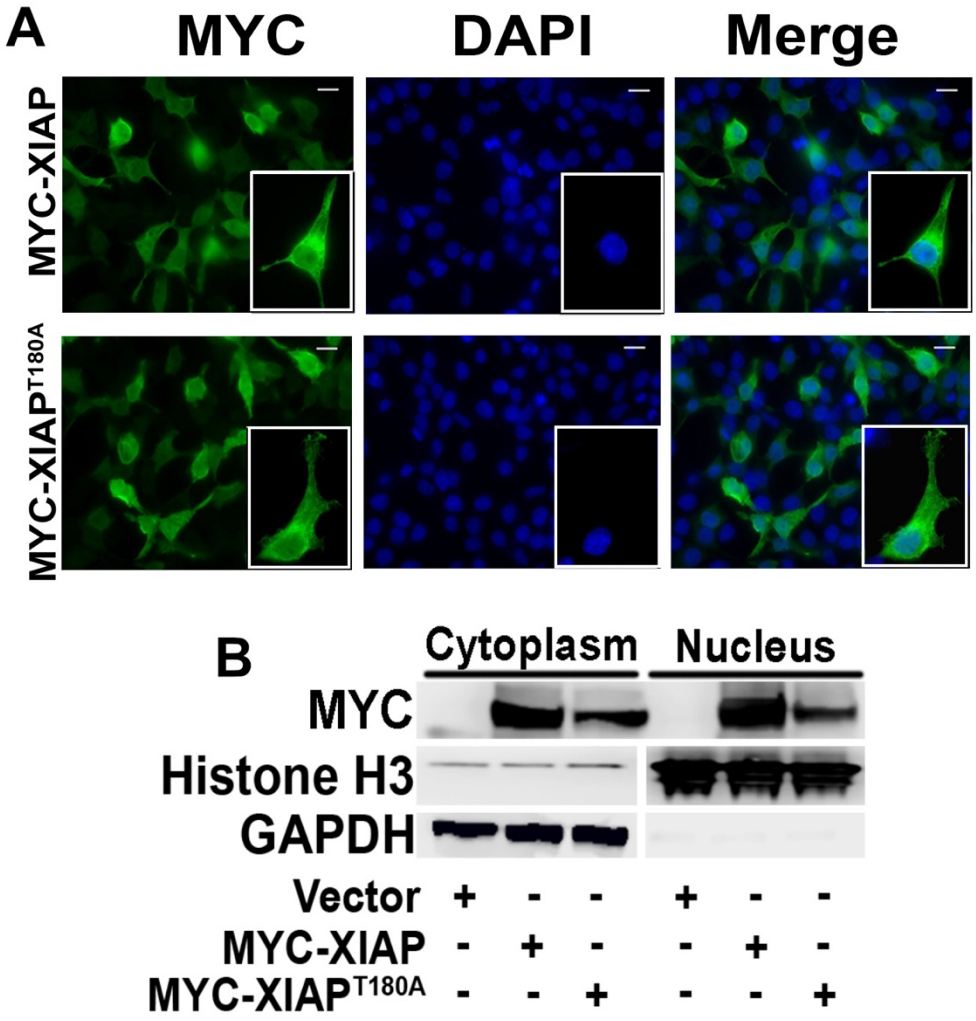

Figure 3-4. The XIAP^{T180A} mutant shares a similar localization pattern as wildtype XIAP.
Figure is adapted from the publication mentioned at the beginning of this chapter. **(A)** The XIAPT180A mutant does not exhibit localization distinct from XIAP. Left, HEK293STF cells were transfected by Leah Sawyer with MYC-XIAP or MYC-XIAPT180A, fixed, and immunostained for MYC and DNA (DAPI). Scale bar, 12.5 μm. **(B)** Cytoplasmic and nuclear fractionations were isolated from transfected cells and immunoblotted for MYC, Histone H3 (nuclear marker), and GAPDH (cytoplasmic maker).

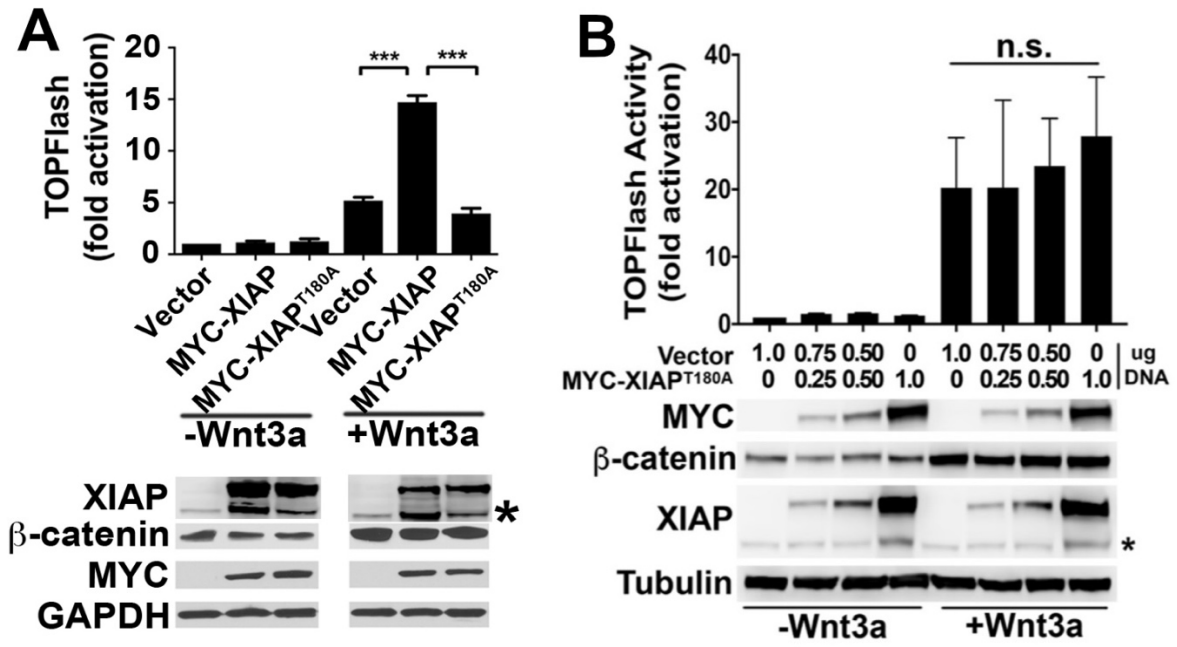

Figure 3-5. The XIAP^{T180A} mutant exhibits decreased Wnt activity in contrast to wildtype XIAP in cultured human cells.
Figure is adapted from the publication mentioned at the beginning of this chapter. **(A)** In contrast to wild-type XIAP, XIAP^{T180A} does not potentiate Wnt3a signaling. HEK293STF cells were transfected with vector, MYC-XIAP, or MYC-XIAP^{T180A} as indicated for 24 hrs, and cells incubated in the absence or presence of recombinant Wnt3a for 24 hrs. Asterisk indicates endogenous XIAP. Graph shows mean ± s.d. of TOPflash normalized to cell titer. Data was analyzed using the Student's t-test (one-tailed) in PRISM. ***p-value <0.0001. All experiments were repeated at least three times. **(B)** Overexpression of XIAPT180A fails to alter Wnt signaling. No statistically significant (as assessed by the student's t-test) increase or decrease in TOPFlash activity was detected even when XIAPT180A is expressed at high levels. Lysates were collected and immunoblotted as indicated. Asterisk indicates endogenous XIAP.

The XIAP^{T180A} phosphomutant exhibits reduced capacity to potentiate Xwnt8 activity in *Xenopus* embryos

Dorsal-anterior structure formation in *Xenopus laevis* embryos is regulated by Wnt signaling (Heasman, 2006), and induction of secondary axis formation in *Xenopus* embryos represents a powerful readout for Wnt signaling *in vivo*. The Lee Lab previously demonstrated that morpholino knockdown of XIAP resulted in severely ventralized *Xenopus* embryos, while injection of XIAP mRNA induced secondary axis formation, consistent with a positive role for XIAP in Wnt signaling (Hanson et al., 2012). The latter result suggests that XIAP is a limiting factor in the developing *Xenopus* embryo. Leif Neitzel found that *XIAP^{T180A}* induced secondary axis formation to a similar extent as *XIAP* (Figure 3-6A & Figure 3-6B). Immunoblotting confirmed that XIAP^{T180A} and XIAP were expressed at similar levels in the injected embryos (Figure 3-6C). *XIAP* synergizes with *Xwnt8* mRNA to induce axis formation in *Xenopus* embryos. In contrast, *XIAP^{T180A}* co-injection with *Xwnt8* mRNA resulted in a lower percentage of embryos with duplicated axes versus *Xwnt8* injection alone. Thus, the XIAP^{T180A} phosphomutant has impaired capacity to potentiate Wnt signaling.

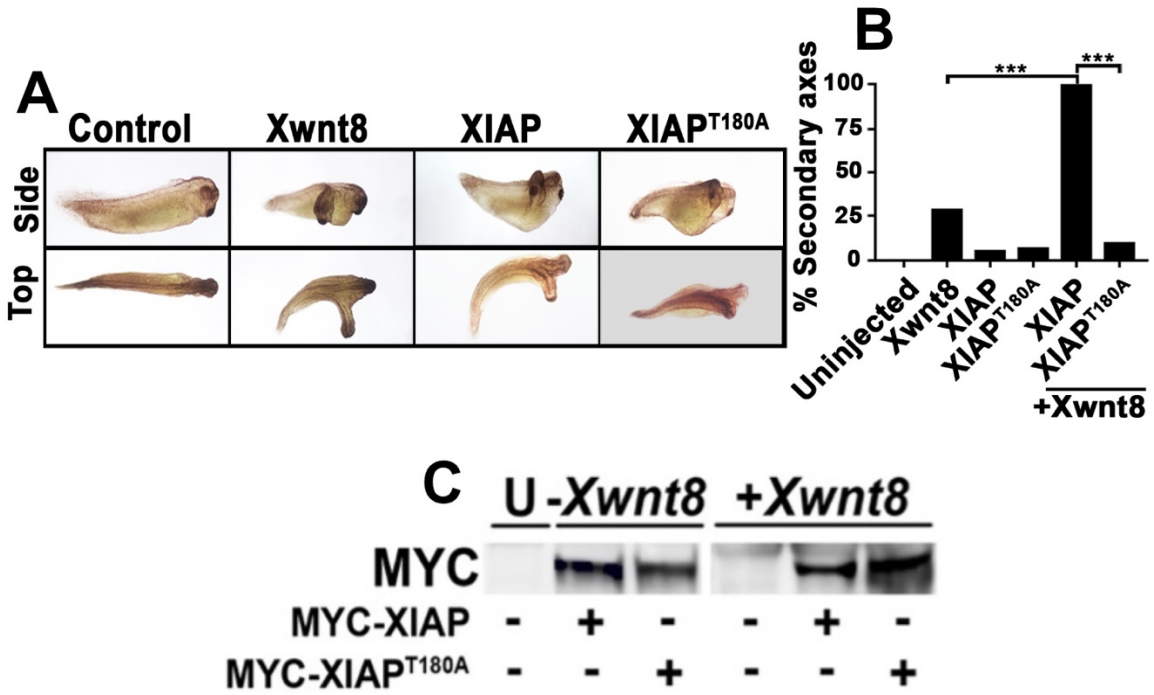

Figure 3-6. The XIAP^{T180A} mutant exhibits decreased Wnt activity in contrast to wild-type XIAP in *Xenopus* embryos.
Figure is adapted from the publication mentioned at the beginning of this chapter. **(A)** The XIAP^{T180A} mutant does not potentiate Xwnt8-induced axis formation in Xenopus embryos, in contrast to wild-type XIAP. Embryos (4-cell stage) were injected ventrally with control, XIAP^{T180A}, or XIAP mRNA (2 ng each) plus or minus Xwnt8 mRNA (0.1 ng) and allowed to develop. The percentage of embryos with secondary axis formation is graphed on the left (N≥31 per group). Data was analyzed using a Fisher's exact test, with Bonferroni Correction. ***p-value <0.0001. Replicated at least three times by Leif Neitzel. **(B)** Representative embryos of Xwnt8, XIAP, and XIAP^{T180A} injected embryos. **(C)** Injected XIAP and XIAP^{T180A} mRNAs are expressed at similar levels in Xenopus embryos. Sample buffer was added to pooled embryos from each condition and immunoblotting performed by Leah Sawyer. U = uninjected.

The XIAP^{T180A} phosphomutant exhibits decreased capacity to bind and ubiquitylate TLE3

The Lee Lab previously demonstrated that XIAP monoubiquitylates TLE3 *in vitro* and in cultured mammalian cells (Hanson et al., 2012). To test if decreased capacity of XIAP^{T180A} to potentiate Wnt signaling is due to its incapacity to ubiquitylate Gro/TLE, Brian Hang tested the capacity of XIAP^{T180A} to ubiquitylate TLE3 in an *in vitro* ubiquitylation assay. Brian Hang found that XIAP^{T180A} ubiquitylates Gro/TLE to a similar degree as wild-type XIAP (Figure 3-7A). This result suggests that XIAP^{T180A} does not have reduced intrinsic catalytic activity when compared to wild-type XIAP. In contrast, in cell-based ubiquitylation assays, the XIAP^{T180A} phosphomutant exhibited decreased capacity to ubiquitylate TLE3 when compared to wild-type XIAP (Figure 3-7B). As control, the ligase mutant XIAP$^{H467A/F495A}$ exhibited reduced capacity (similar to control transfection) to ubiquitylate TLE3 compared to wild-type XIAP (Figure 3-8A). Addition of the proteasome inhibitor, MG132, resulted in enhanced ubiquitylation of the XIAP$^{H467A/F495A}$ mutant itself (Figure S3-8B), suggesting that the decreased activity of the XIAP$^{H467A/F495A}$ mutant may be, in part, due to its rapid turnover.

I found reduced interaction between XIAP^{T180A} and TLE3 when compared to XIAP and TLE3 as assessed by co-immunoprecipitation assays. Wnt3a treatment did not significantly enhance the interaction between TLE3 and XIAP^{T180A} or XIAP (Figure 3-9). These results suggest that the decreased capacity of XIAP^{T180A} to ubiquitylate TLE3 in cultured cells is due, in part, to its decreased binding to TLE3.

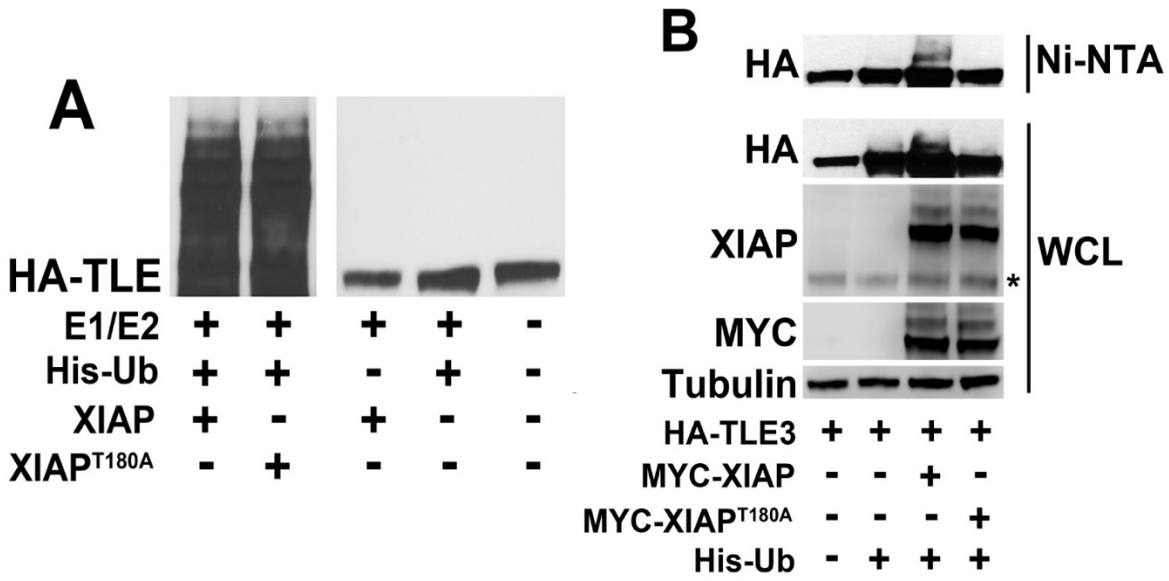

Figure 3-7. The XIAP^{T180A} mutant shows decreased ubiquitylation of TLE3. Figure is adapted from the publication mentioned at the beginning of this chapter. **(A)** XIAP^{T180A} ubiquitylates TLE3 to a similar extent as wild-type XIAP in vitro. *In vitro*-translated HA-TLE3 was incubated in an in vitro ubiquitylation reaction containing recombinant E1/E2, ubiquitin, plus XIAP or XIAP^{T180A}. Ubiquitylated TLE3 was visualized by immunoblotting with anti-HA antibody. Assays were performed by Brian Hang. **(B)** XIAP^{T180A} exhibits reduced capacity to ubiquitylate TLE3 in cultured human cells compared to wild-type XIAP. HEK293STF cells were transfected as indicated, lysed under denaturing conditions, and His-Ub modified proteins isolated by nickel affinity chromatography. XIAP and TLE3 were detected by immunoblotting with anti-MYC and anti-HA antibodies, respectively. Asterisk indicates endogenous XIAP. WCL = whole cell lysates.

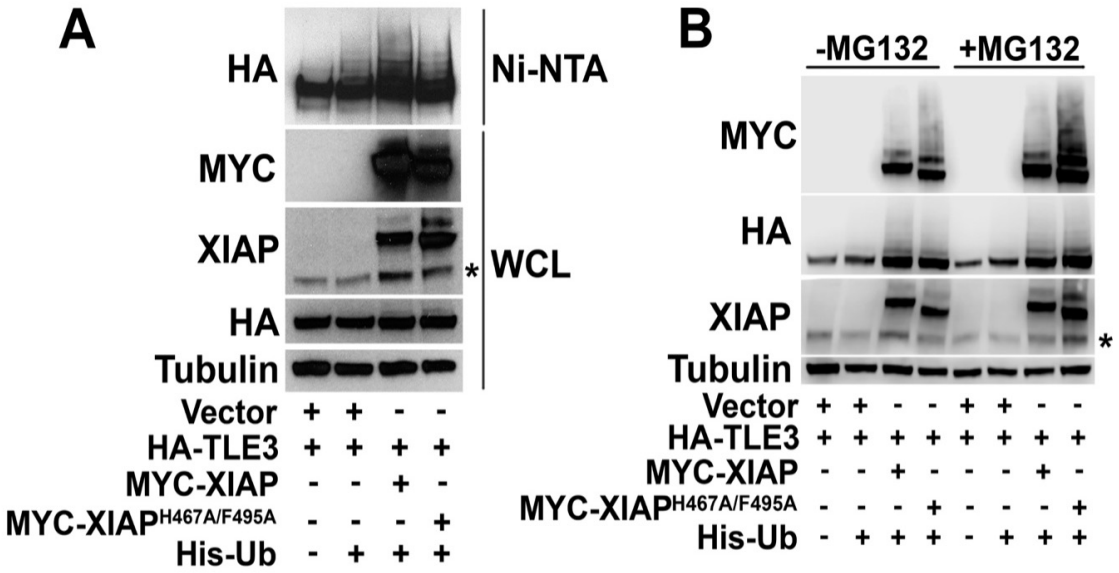

Figure 3-8. The ligase mutant, XIAP$^{H467A/F495A}$, shows decreased ubiquitylation of TLE3 and is rapidly turned over in cultured mammalian cells.
Figure is adapted from the publication mentioned at the beginning of this chapter. **A)** XIAP$^{H467A/F495A}$ is impaired in its capacity to ubiquitylate TLE3. HEK293STF cells were transfected as indicated, lysed under denaturing conditions, and His-Ub modified proteins isolated by nickel affinity chromatography. Transfected XIAP and TLE3 were detected by immunoblotting with anti-MYC and anti-HA antibodies, respectively. Asterisk indicates endogenous XIAP. (**B)** Treatment with the proteasomal inhibitor, MG132, indicate enhanced ubiquitylation of XIAP$^{H467A/F495A}$. HEK293STF cells were transfected as indicated, and cells incubated in the absence or presence of MG132. Cells were then collected, and immunoblotting performed. Transfected XIAP and TLE3 were detected by immunoblotting with anti-MYC and anti-HA antibodies, respectively. Asterisk indicates endogenous XIAP.

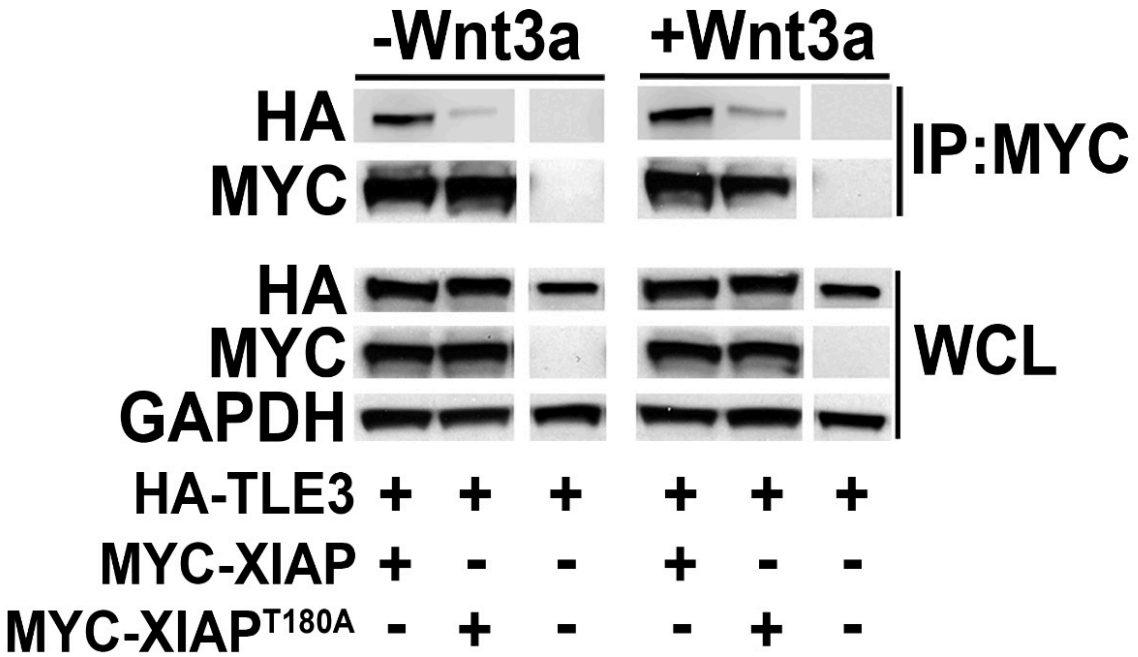

Figure 3-9. The XIAP^{T180A} mutant shows decreased binding of TLE3.
Figure is adapted from the publication mentioned at the beginning of this chapter. XIAP^{T180A} exhibits decreased affinity for HA-TLE3 compared to wild-type XIAP. HEK293STF cells were transfected for 24 hr as indicated followed by incubation in the absence or presence of recombinant Wnt3a for 24 hr. Lysates were collected and immunoprecipitated with anti-MYC antibody. Co-immunoprecipitated HA-TLE3 was detected by anti-HA antibody. WCL = whole cell lysates. IP = Immunoprecipitation.

The anti-apoptotic activity of XIAP^{T180A} is indistinguishable from that of wild-type XIAP

I next asked whether XIAP^{T180A} has reduced activity in the apoptotic pathway. One of the best-characterized substrates of XIAP is second mitochondria-derived activator of caspases (Smac) (MacFarlane et al., 2002). I found that XIAP^{T180A} interacted with Smac to a similar extent as wild-type XIAP (Figure 3-10A). Overexpression of XIAP inhibits apoptosis in cultured cells (Suzuki et al., 2001) and has been shown to specifically inhibit Fas ligand-induced apoptosis in HeLa cells (Ashkenazi and Dixit, 1998; Deveraux et al., 1999). Thus, I tested whether overexpressed XIAP^{T180A} inhibits Fas ligand-induced apoptosis in HeLa cells. There was no observable difference in the capacity of MYC-XIAP or MYC-XIAP^{T180A} to inhibit Fas ligand-induced apoptosis in HeLa cells (Figure 3-10B). Thus, phosphorylation of XIAP at the T180 site is required for the full activity of XIAP in the Wnt pathway, but not in the apoptotic pathway.

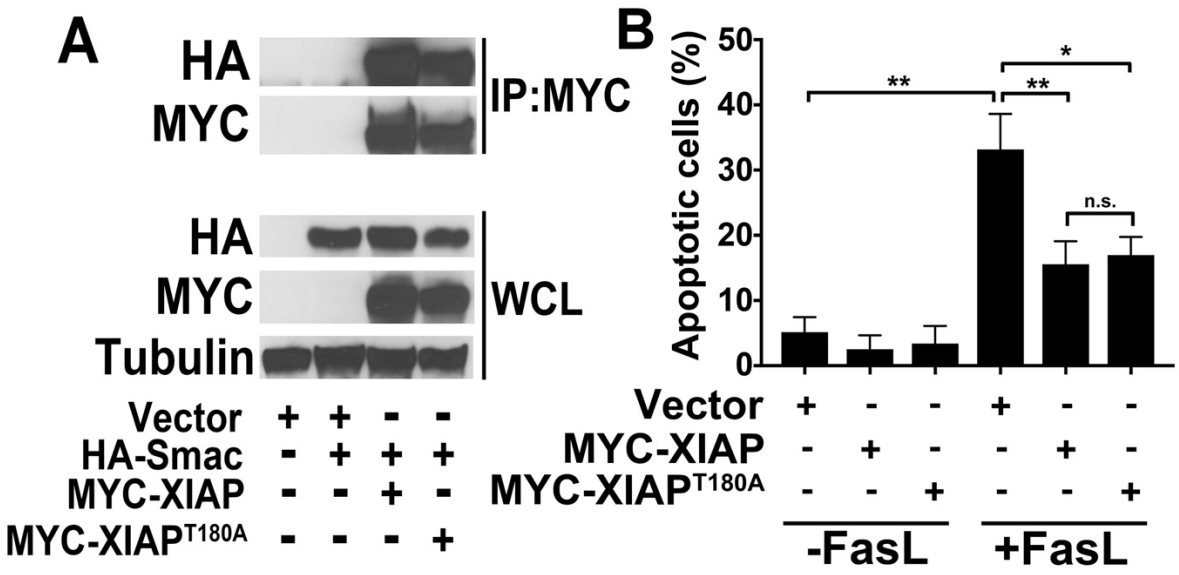

Figure 3-10. In contrast to its activity in the Wnt pathway, XIAP^{T180A} shows similar activity as wild-type XIAP in the apoptotic pathway.
Figure is adapted from the publication mentioned at the beginning of this chapter. **(A)** Smac co-immunoprecipitates with XIAP and XIAP^{T180A} to a similar extent. HEK293STF cells were transfected as indicated with vector or HA-Smac plus MYC-XIAP or MYC-XIAP^{T180A}. Lysates were collected, and immunoprecipitation performed with anti-MYC antibody followed by immunoblotting with anti-HA antibody. WCL = whole cell lysates. IP=Immunoprecipitation. **(B)** Overexpression of XIAP or XIAP^{T180A} decreases the percentage of Fas ligand-induced apoptosis to a similar extent. HeLa cells were transfected for 24 hr as indicated and incubated in the absence or presence of recombinant Fas ligand (100 ng/mL) for 24 hr. Cells were then stained with Annexin V and propidium iodide. Table shows percentage of HeLa cells undergoing early apoptosis as assessed by flow cytometry. Graph shows mean ± s.d. of percentage of apoptotic cells. Data was analyzed and processed using FlowJo and the Student's t-test (one-tailed) in PRISM. **p value <0.001, *p-value <0.01.

DISCUSSION

How the Wnt transcriptional complex is converted from a repressor complex into an activator complex is not well understood. Upon Wnt activation, XIAP is recruited onto Wnt target gene promoters to ubiquitylate Gro/TLE bound to TCF/LEF, decreasing its affinity for TCF/LEF (Hanson et al., 2012). In the same study, the Lee Lab showed that XIAP interacts with Gro/TLE in the absence or presence of Wnt stimulation, and they speculated that XIAP also decreases the pool of free Gro/TLE that can interact with TCF/LEF to inhibit transcription. Thus, Wnt signaling regulates XIAP activity by promoting its recruitment to the TCF/LEF transcriptional complex where it ubiquitylates TCF/LEF bound to Gro/TLE. I now demonstrate that XIAP is phosphorylated by GSK3, which could mediate this process. This result confirms data curated by PhosphoSitePlus from genome-scale proteomic studies indicating that XIAP is phosphorylated on T180 in human cells, although the significance of XIAP T180 phosphorylation was not clear (Mertins et al., 2016; Sharma et al., 2014). Our current data suggest that phosphorylation of T180 in XIAP is required for full Wnt activation. However, it is not clear how phosphorylation of XIAP by GSK3 is regulated by Wnt signaling, given that XIAP binds GSK3 irrespective of Wnt activation (Sun et al., 2009). One possible model is that the interaction between XIAP and Gro/TLE is facilitated by an as-yet-unidentified factor due to phosphorylation of XIAP at T180 by GSK3 (Figure 3-11). This model may explain why overexpression of $XIAP^{T180A}$ does not potentiate Wnt signaling, as it would be incapable of binding Gro/TLE and instead act to sequester the unknown factor.

The results presented in this chapter provide mechanistic insight into the regulation of XIAP activity that is Wnt pathway specific and independent of the role of XIAP in apoptosis. Historically, XIAP has been shown to be upregulated in many different types of human cancers and because of this, XIAP inhibitors are the focus of multiple clinical trials (Derakhshan et al., 2017; LaCasse et al., 2008; Schimmer et al., 2006). The idea behind XIAP inhibitors is to sensitize tumors to chemotherapeutics and radiation therapy by blocking the ability of XIAP to inhibit apoptosis (Derakhshan et al., 2017; McManus et al., 2004; Schimmer et al., 2006; Schimmer et al., 2004; Thibault et al., 2018). However, there is concern that inhibition of XIAP may promote other IAP family members such as cellular inhibitor of apoptosis (cIAP) to compensate for reduced XIAP activity (Schimmer et al., 2006). In the case of Wnt-driven cancers such as colorectal cancer, instead of using XIAP inhibitors, inhibition of kinases that phosphorylate XIAP may be a viable strategy in blocking overactive Wnt signaling. Our results show that phosphorylation of the T180 site is important for XIAP activity in the Wnt pathway and mutation of this site results in decreased Wnt signaling. The Lee Lab previously showed that expression of cIAPs does not result in ubiquitylation of Gro/TLE and that knockdown of XIAP in the colorectal cancer cell lines, SW480 and HCT116, resulted in decreased Wnt signaling in those cell lines (Hanson et al., 2012). Thus, blocking phosphorylation of XIAP could be a way to drive down Wnt signaling in cancers with hyperactive Wnt signaling without promoting compensatory activity from cIAPs. In this scenario, inhibition of the priming kinase of XIAP would likely be more effective than inhibiting the secondary kinase as the *in vitro* kinase assay showed that phosphorylated XIAP is an even better substrate for GSK3 phosphorylation than unphosphorylated

XIAP. Thus, blocking phosphorylation of XIAP alone or in combination with other therapies could be an effective strategy in treating Wnt-driven cancers.

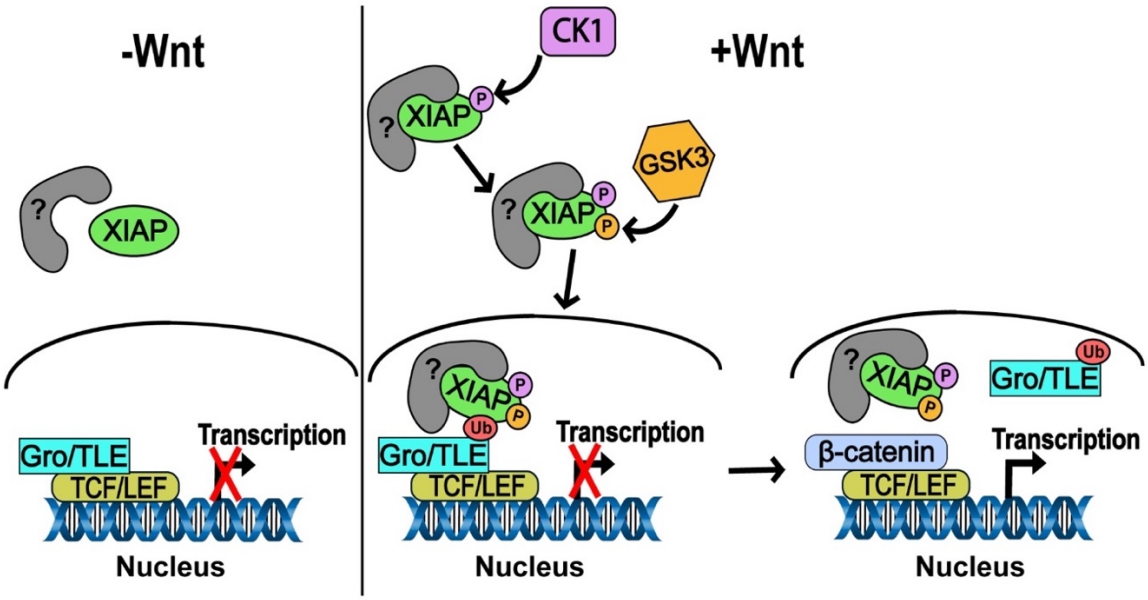

Figure 3-11. Schematic for the proposed regulation of XIAP activity in the Wnt pathway by phosphorylation at position T180.
Figure is adapted from the publication mentioned at the beginning of this chapter. In the presence of Wnt, XIAP is phosphorylated and bound to an unknown factor. XIAP phosphorylation promotes translocation to the nucleus where it binds and ubiquitylates Gro/TLE. Gro/TLE is released from TCF/LEF and β-catenin can bind TCF/LEF.

Chapter 4

THE USP46/UAF1/WDR20 COMPLEX DEUBIQUITYLATES THE WNT CO-RECEPTOR, LRP6, TO PROMOTE WNT/β-CATENIN SIGNALING

This chapter is adapted from “The USP46/UAF1/WDR20 complex deubiquitylates the Wnt co-receptor, LRP6, to promote Wnt/β-catenin signaling” currently in submission and has been reproduced with the permission of my co-authors (Spencer Z, Neitzel, LR, Shen C, Kassel SN, Kroh HK, Zhenyi An, D’Souza S, Hansen AG, Lebensohn AM, Rohatgi R, Weiss WA, Weiss VL, Williams C, Hong C, Robbins DJ, Ahmed Y, Lee E).

INTRODUCTION

The Wnt signaling pathway is an evolutionarily conserved pathway that is critical for normal development. Dysregulation of the pathway leads to human diseases such as cancer (MacDonald and He, 2012). In the absence of a Wnt ligand, cytoplasmic β-catenin is maintained at low levels via its assembly into a destruction complex composed of Axin, glycogen synthase kinase 3 (GSK3), casein kinase 1 α (CK1α), and the tumor suppressor adenomatous polyposis coli (APC). Within this complex, β-catenin is phosphorylated and undergoes ubiquitin-mediated proteasomal degradation (Liu et al., 1999; Liu et al., 2002). In the current model of Wnt activation, binding of Wnt ligands to the Frizzled (FZD) and LRP5/6 coreceptors induces phosphorylation of LRP5/6 and the formation of active aggregated receptors or "signalosomes." The formation of signalosomes inhibits cytosolic degradation of β-catenin via recruitment of Axin (Bilić et

al., 2007; Zeng et al., 2008). Accumulated cytoplasmic β-catenin translocates to the nucleus to activate a Wnt transcriptional program (Saito-Diaz et al., 2012).

In addition to its key role in controlling cytoplasmic β-catenin levels, ubiquitylation also plays a critical role in maintaining Wnt receptor homeostasis. Ubiquitylation and turnover of Frizzled and LRP5/6 occur via the transmembrane ubiquitin ligases, RNF43 and ZNRF3, which promote their turnover (Hao et al., 2012). Furthermore, conditional deletion of RNF43/ZNRF3 in mice leads to a marked expansion of intestinal crypts, indicating hyperactivation of the Wnt pathway (Koo et al., 2012). Conditional loss of ZNRF3 in the mouse leads to Wnt activation and adrenal hyperplasia (Basham et al., 2019).

Mutations in RNF43 have been found in 18% of human colorectal adenocarcinomas and endometrial carcinomas (Giannakis et al., 2014). Gene fusions involving R-spondins (RSPOs), which result in their elevated expression, have been found in ~10% of colorectal cancers (Seshagiri et al., 2012). Secreted R-spondins amplify Wnt signaling by inhibiting RNF43/ZNRF3, thereby blocking Wnt receptor ubiquitylation and turnover. Thus, regulation of Wnt receptor levels is crucial for maintaining normal Wnt pathway activity and tissue homeostasis; and their dysregulation has important implications for human disease.

The deubiquitylase(s) that oppose the action of RNF43/ZNRF3 in the Wnt pathway remains unclear. USP8 and USP6 have been shown to deubiquitylate FZD when expressed in cultured cells (Madan et al., 2016; Mukai et al., 2010). However, their activities do not appear to be regulated by Wnt signaling, and they have not been shown to specifically target LRP6. Thus, we sought to identify the deubiquitylase

involved in Wnt receptor turnover to gain further insight into how receptor homeostasis is maintained in this pathway.

Here, we demonstrate that the USP46 complex is required for Wnt signaling in cultured human cells, *Xenopus* embryos, zebrafish embryos, and mouse intestinal organoids, indicating evolutionary conservation of function. In addition, we show that in response to Wnt pathway activation, the USP46 complex is recruited to and deubiquitylates LRP6, blocking its turnover. Together with hydrodynamic studies, our data reveal a potential mechanism by which the USP46 complex acts on a newly characterized step after LRP6 receptor activation and prior to signalosome formation to control Wnt signaling at the plasma membrane. Our studies identify a new mechanism by which steady-state levels of LRP6 can be tightly regulated and further highlight the importance of receptor homeostasis in the physiological control of Wnt signaling.

RESULTS

The USP46 complex is a positive regulator of Wnt signaling

WDR20 was previously identified in a screen for uncharacterized Wnt components in haploid cells (Lebensohn et al., 2016). Based on a previous screen for ubiquitin ligase regulators of Wg/Wnt signaling (Hanson et al., 2012), we initiated a screen for deubiquitylases that regulate the Wnt pathway and identified USP46. USP46 by itself normally exhibits low catalytic activity, but its activity is enhanced significantly when bound to the WD40 repeat (WDR) proteins, WDR20 and UAF1 (Li et al., 2016b). Thus, I investigated the effects of this trimeric complex (USP46-UAF1-WDR20) on the

Wnt signaling pathway. Using human embryonic kidney (HEK) 293 cells stably transfected with the TOPFlash reporter (HEK293STF) (Xu et al., 2004), I found that expressing USP46 complex components individually (Figure 4-1A) had small effects on Wnt-stimulated reporter activity. Co-expression of two components of the USP46 complex further potentiated Wnt signaling, albeit modestly (Figure 4-1B). In contrast, expression of all three components of the USP46 complex (Tri46) stimulated Wnt signaling even in the absence of exogenous Wnt ligand (Figure 4-2A), with dramatic potentiation of signaling and stabilization of β-catenin levels in the presence of Wnt ligand (Figure 4-2B).

I next sought to determine if USP46 is required for Wnt signaling in human cells. Knockdown of USP46 with two independent short-interfering RNA (siRNA) constructs significantly blocked Wnt3a-induced TOPFlash activation (Figure 4-3A). Knockdown of USP46 also inhibited Wnt3a-induced expression of endogenous Wnt target genes (Figure 4-3B), providing further evidence that USP46 is required for Wnt-mediated transcription. Knockdown of UAF1 using two different siRNAs similarly reduced Wnt-stimulated activity (Figure 4-3C). I had difficulty knocking down WDR20 due to the lack of suitable siRNAs that could effectively target its multiple transcripts. Taken together, our experiments show that the individual components of the USP46 complex work synergistically to potentiate Wnt signaling.

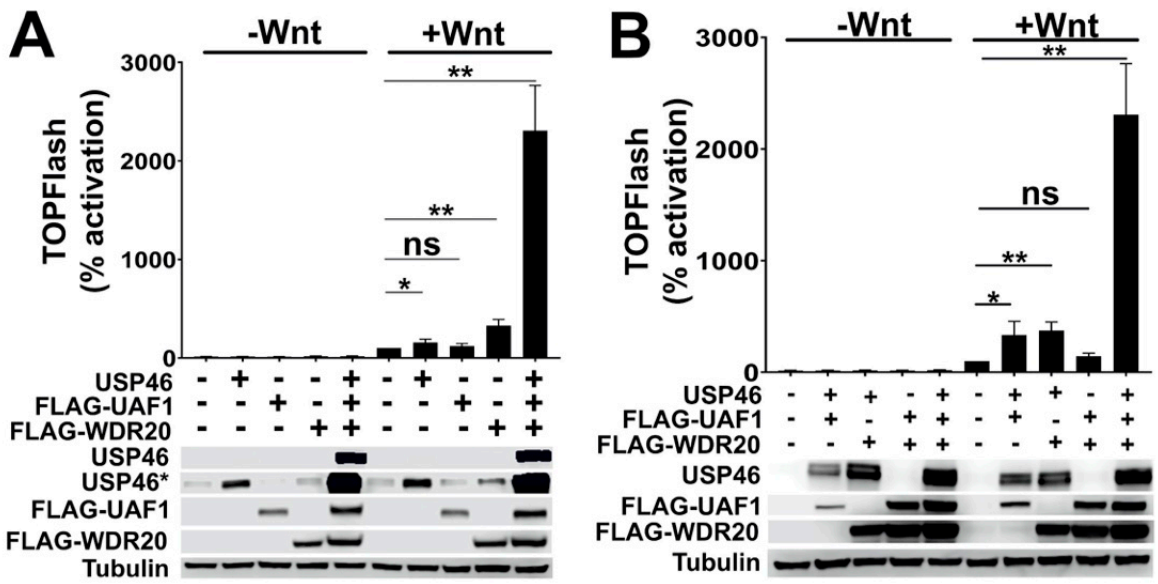

Figure 4-1. The three components of the USP46 complex synergize to potentiate Wnt signaling.

Figure is adapted from the publication mentioned at the beginning of this chapter. **(A)** Overexpression of individual components of the USP46 complex in HEK293STF cells in the presence of Wnt3a leads to low Wnt reporter (TOPFlash) activity compared to overexpression of all three members. Asterisk indicates longer exposure of blot for USP46. **(B)** Overexpression of pairwise combinations of the components of the USP46 complex in HEK293STF cells in the presence of Wnt3a leads to low Wnt reporter (TOPFlash) activity compared to overexpression of all three members. Graphs show mean ±SD of TOPFlash normalized to cell number. ns is not significant, *p-value < 0.05, **p-value < 0.01, and ***p-value < 0.001

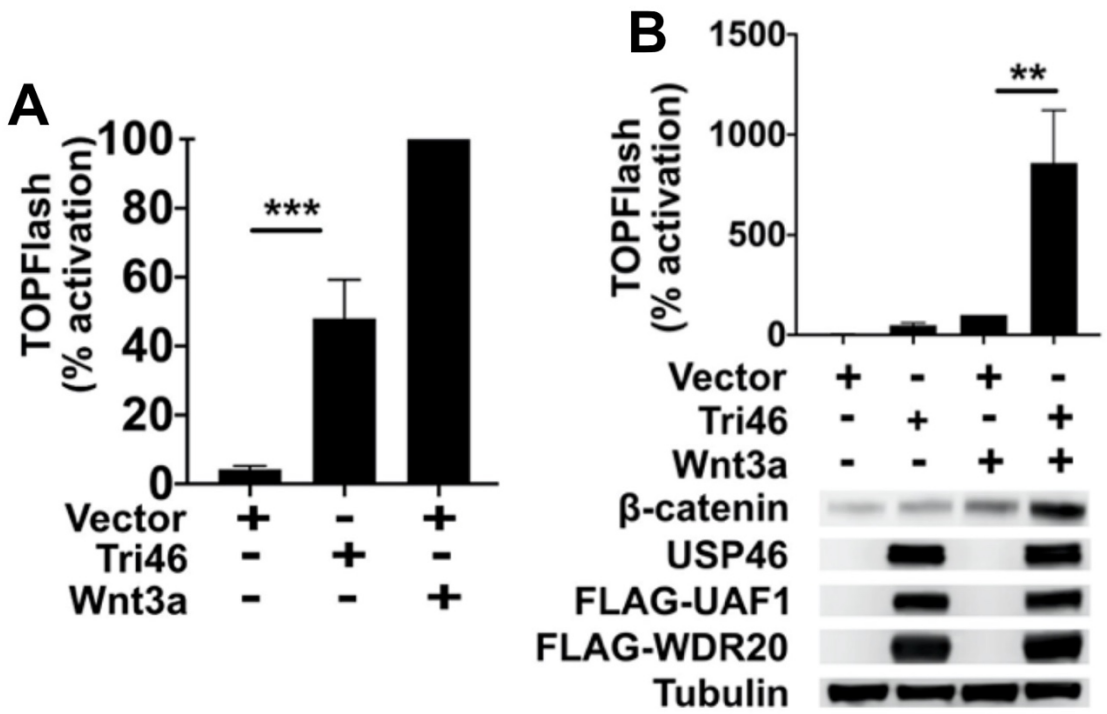

Figure 4-2. The USP46 complex increases β-catenin levels in the presence of Wnt. Figure is adapted from the publication mentioned at the beginning of this chapter. **(A)** Overexpression of the USP46 complex (Tri46) in HEK293STF cells exhibits detectable TOPFlash activity in the absence of Wnt. **(B)** Overexpression of the USP46 complex in HEK293STF cells stabilizes β-catenin in the presence of Wnt. Graphs show mean ±SD of TOPFlash normalized to cell number. *p-value < 0.05, **p-value < 0.01, and ***p-value < 0.001

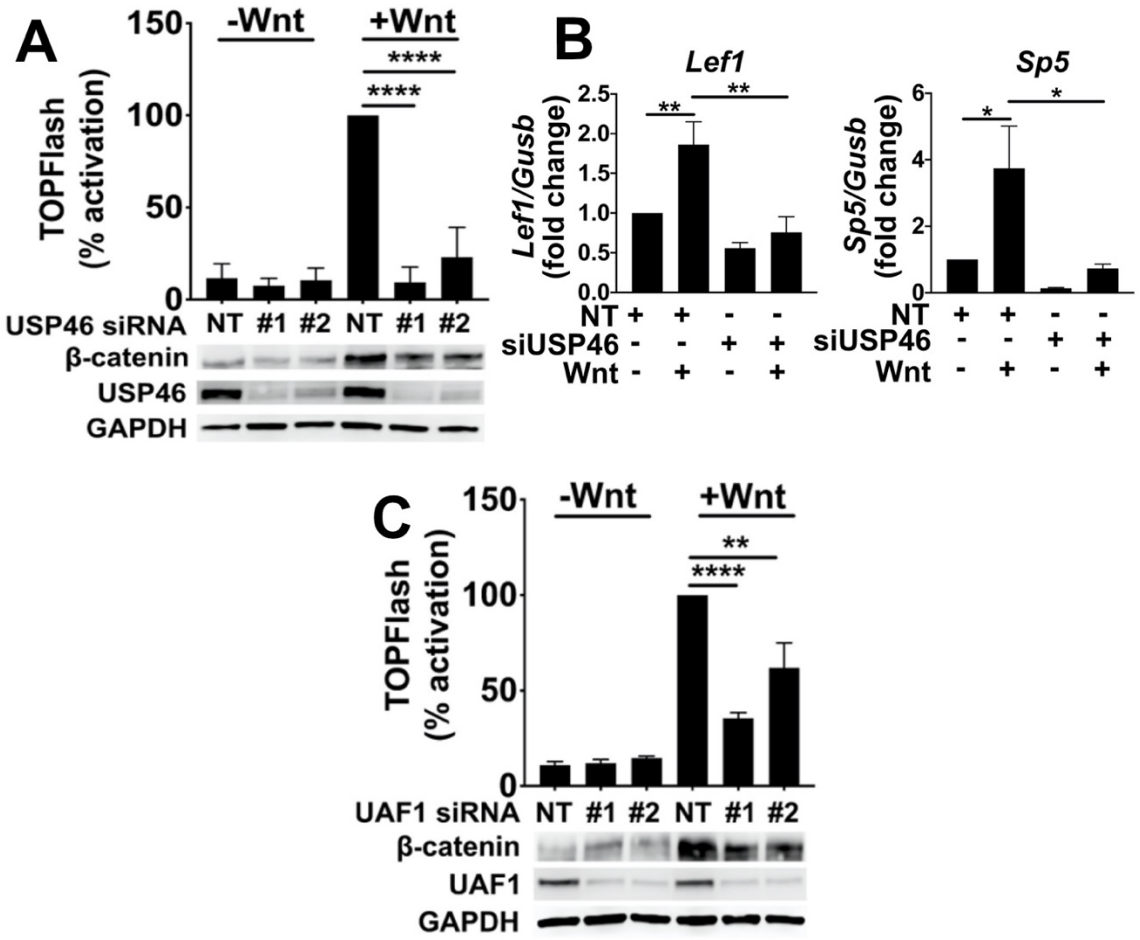

Figure 4-3. Knockdown of USP46 and UAF1 decreases Wnt signaling.
Figure is adapted from the publication mentioned at the beginning of this chapter. **(A)** Knockdown of USP46 by siRNA inhibits Wnt signaling and decreases β-catenin levels. HEK293STF cells were transfected with non-targeting control (NT) or two independent USP46 siRNAs and treated with recombinant Wnt3a. **(B)** Quantitative real-time RT-PCR of endogenous Wnt target genes in HEK293STF treated with USP46 siRNAs or non-targeting (NT) control. The graph shows a ratio of *Lef1* and *Sp5* to *Gusb* (control). Results (mean ±SD) of three independent real-time RT-PCR reactions are shown. *p-value < 0.05 and **p-value < 0.01 Assays were performed by Sara Kassel. **(C)** Knockdown of UAF1 by siRNA inhibits Wnt signaling and decreases β-catenin levels. HEK293STF cells were transfected with non-targeting control (NT) or two independent USP46 siRNAs and treated with recombinant Wnt3a. Graphs shows mean ±SD of TOPFlash normalized to cell number. **p-value < 0.01 and ****p-value < 0.0001.

The USP46 complex is required for Wnt signaling in *Xenopus* and zebrafish embryos

Next, we asked whether the USP46 complex is required for Wnt signaling in a developing organism. Dorsal-anterior structure formation in *Xenopus laevis* embryos is critically regulated by Wnt signaling (Heasman, 2006). Formation of a secondary axis occurs due to ectopic activation of the pathway, which makes this assay a robust readout for Wnt signaling *in vivo* (McMahon and Moon, 1989; Sokol et al., 1991). Leif Neitzel found that injection of mRNAs encoding individual members of the USP46 complex resulted in a significantly lower number of embryos with duplicated axes compared to embryos co-injected with all three components (Figure 4-4A), confirming my findings that all three members of the USP46 complex are required for its full Wnt-potentiating activity in mammalian cells. No duplication was observed in control embryos. These results parallel observations with *Xenopus* animal caps (which normally do not exhibit active Wnt signaling), in which injection of mRNAs for all three components significantly induced expression of the Wnt target genes, *Xnr3* and *Chordin* (Figure 4-4B).

To further assess the role of the USP46 complex in regulating Wnt signaling *in vivo*, Leif Neitzel tested the effects of the USP46 complex on Wnt signaling in zebrafish embryos. In zebrafish, inhibition of Wnt signaling leads to cyclocephaly due to failure of eye precursors to undergo migration (Thorpe and Moon, 2004). Leif Neitzel found that knockdown of each of the USP46 complex components by morpholino oligonucleotide (MO) injection resulted in cycloptic embryos (Figure 4-5A) and reduction in endogenous Wnt target gene expression (an indicator of Wnt/β-catenin signaling) (Figure 4-5B),

consistent with Wnt pathway inhibitions. Significantly, co-injection of MO with the corresponding mRNAs encoding the respective human version of the gene rescued both the cycloptic phenotype and the reduction in Wnt target gene expression (Figure 4-5A & Figure 4-5B). These results demonstrate that the USP46 complex plays a positive and conserved role in Wnt signaling during early embryonic vertebrate development.

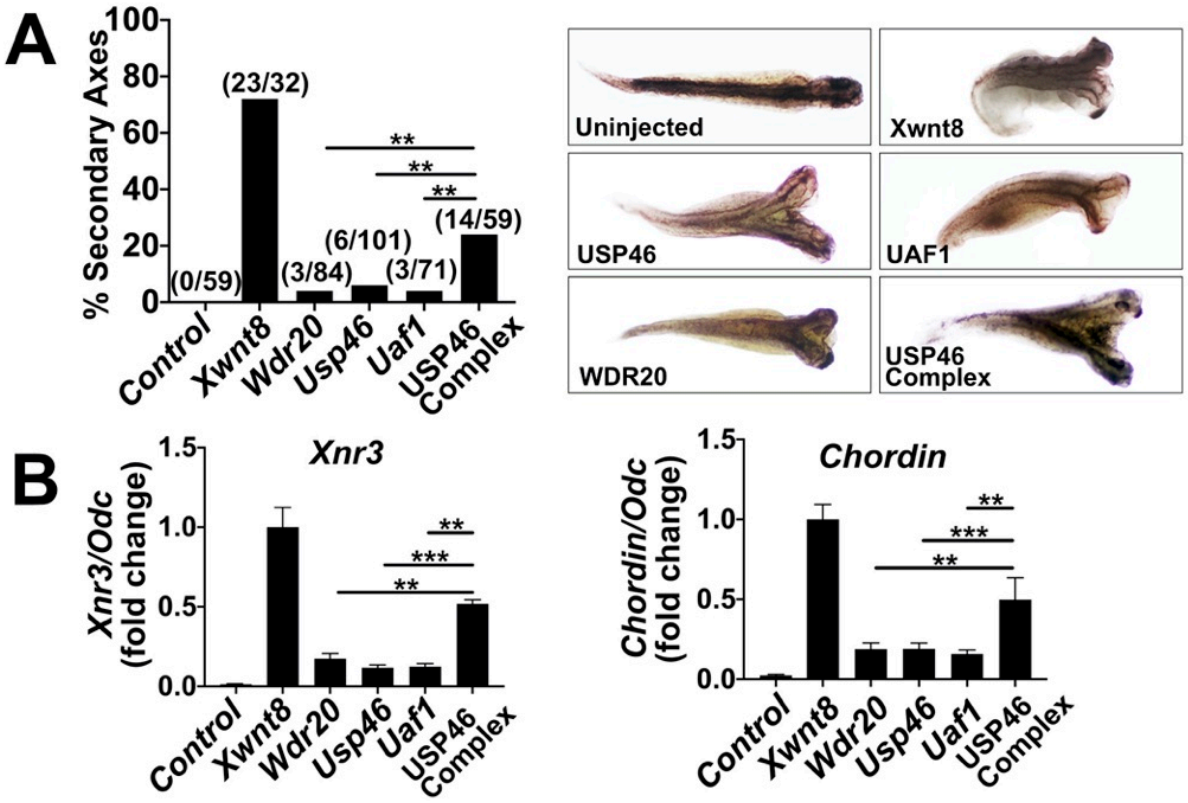

Figure 4-4. The USP46 complex induces secondary axis formation in *Xenopus laevis*.

Figure is adapted from the publication mentioned at the beginning of this chapter. **(A)** Members of the USP46 complex induce secondary body axes when overexpressed in the ventral blastomeres of *Xenopus* embryos. *Xenopus* embryos were injected ventrally at the 4-cell stage with *Xwnt8* mRNA (10 pg), individual members of the USP46 complex (1 ng), or a 1:1:1 mixture of the USP46 complex (0.33 ng each). The percentage of embryos with axis duplication is graphed on the left with absolute numbers indicated on the top of each bar. Representative images of embryos are shown on the right. **p-value $\leq$ 0.01 compares injections of individual components versus the USP46 complex. Assays were performed by Leif Neitzel. **(B)** Total RNA was extracted from animal caps of injected embryos. RT-PCR of mRNAs show induction of Xenopus Wnt target genes, *Xnr3* and *Chordin*. The graph shows expression as a ratio of *Ornithine decarboxylase* (*Odc*) normalized to *Xwnt8* injected animal caps. Control is un-injected. **p-value < 0.01 and ***p-value < 0.001. Assays were performed by Leif Neitzel.

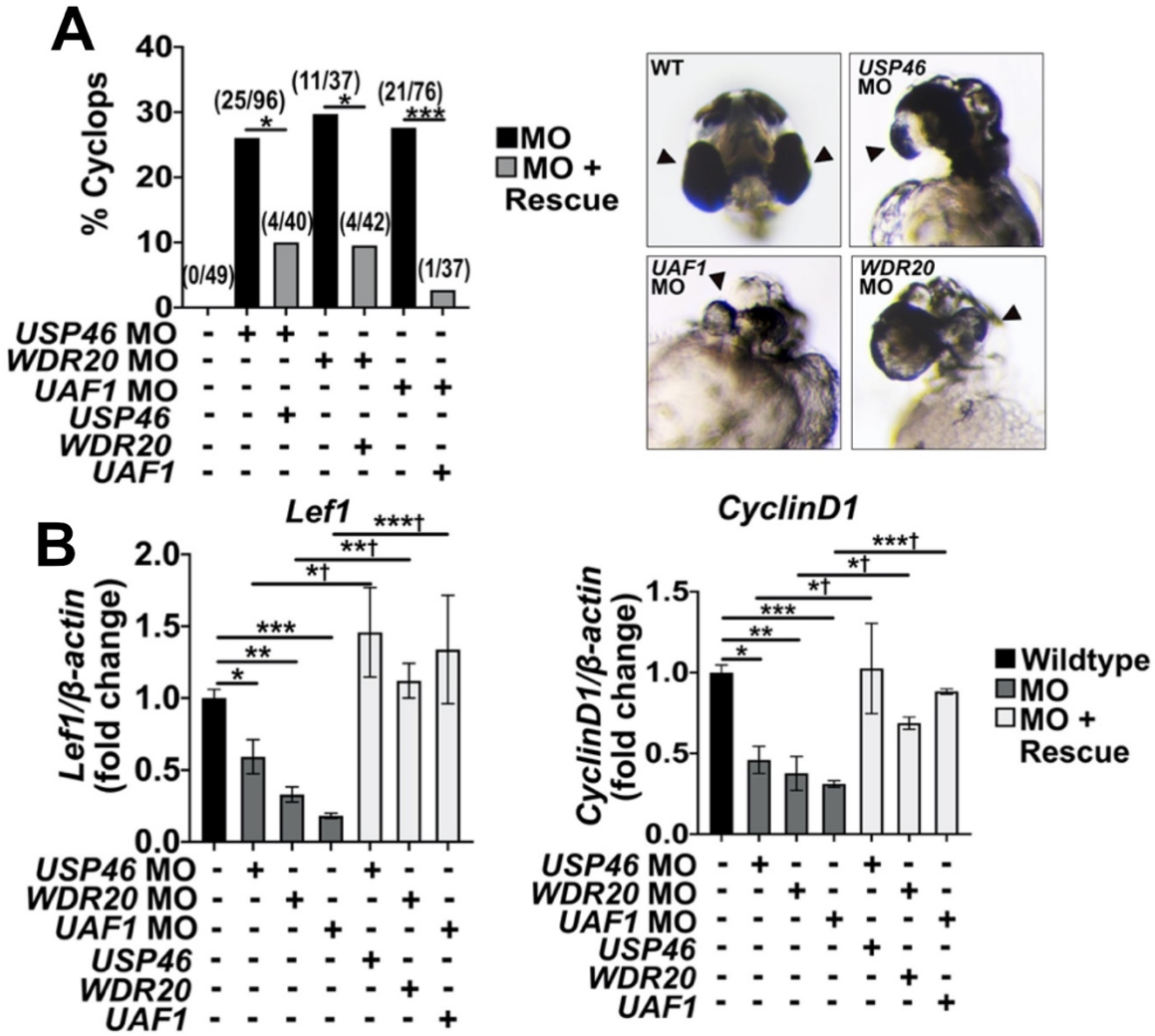

Figure 4-5. Knockdown of members of the USP46 complex results in a cyclopic phenotype in zebrafish.
Figure is adapted from the publication mentioned at the beginning of this chapter. **(A)** Embryos were injected into the yolk at the single-cell stage with morpholino oligonucleotides (MO, 3 ng) plus or minus rescue mRNAs (0.8 ng). The phenotype was assessed at the 3 dpf stage. The percentage of cyclopic embryos is graphed on the left with absolute numbers indicated on the top of each bar. Representative images are shown on the right with arrows indicating developing eyes. *p-value < 0.05 and ***p-value < 0.001. Assays were performed by Leif Neitzel. **(B)** mRNAs were isolated from injected single embryos, and *Lef1* and *CyclinD1* levels were quantified by RT-PCR. Gene expression is graphed as a ratio to β-actin control and normalized to un-injected embryos. *p-value < 0.05, **p-value < 0.01, and ***p-value < 0.001 compares Morpholino-injected versus un-injected embryos. *†p-value < 0.05, **†p-value < 0.01, and ***†p-value < 0.001 compares morpholino-injected versus corresponding rescued embryos. Assays were performed by Leif Neitzel.

The USP46 complex acts upstream of the destruction complex to increase the steady-state levels of LRP6

Having demonstrated that the USP46 complex is required for Wnt signaling in vertebrates, I addressed the molecular mechanism of its function in the Wnt pathway. Based on my studies with cultured mammalian cells demonstrating decreased β-catenin levels upon knockdown of USP46 or UAF1, it is likely that the USP46 complex acts at or above the level of the β-catenin destruction complex. To test the former possibility, I initially used the GSK3 inhibitor, CHIR99021, to activate Wnt signaling by blocking GSK3-mediated phosphorylation of β-catenin, thereby stabilizing its levels (Cline et al., 2002; Cohen and Goedert, 2004; Ring et al., 2003). Overexpression of the USP46 complex did not potentiate CHIR99021-mediated activation of Wnt signaling (Figure 4-6). To further test the potential roles for USP46 in the destruction complex, I activated the Wnt pathway by Axin knockdown, which is required for assembly of the β-catenin destruction complex. As expected, knockdown of Axin increased β-catenin levels (Figure 4-7A). However, in contrast to Wnt3a activation, knockdown of USP46 did not reduce β-catenin levels in Axin knockdown cells. Tankyrase inhibitors increase steady-state levels of Axin to promote β-catenin degradation and inhibit Wnt signaling (Huang et al., 2009a). The tankyrase inhibitor, XAV939, blocked the increase in β-catenin levels in cells expressing the USP46 complex in the absence and presence of Wnt3a (Figure 4-7B). As a control, XAV939 did not affect the level of an N-terminal truncated form of β-catenin resistant to degradation by the destruction complex (Figure 4-7C). These experiments show that the USP46 complex potentiates Wnt signaling upstream of the destruction complex.

Given that the USP46 complex acts upstream of the destruction complex, I next interrogated the Wnt receptor complex. I was unable to observe any effect on the levels of FZD or Dishevelled when we expressed the USP46 complex, although I cannot rule out small changes not detectable by our methods. In contrast, I detected increased and decreased levels of LRP6 upon expression and knockdown, respectively, of USP46 in HEK293 cells (Figure 4-8A & Figure 4-8B). USP46 is highly expressed in the brain (Hodul et al., 2017). An analysis of the Cancer Genome Atlas (TCGA) (Cancer Genome Atlas Research et al., 2013) showed that the expression of USP46 correlated with both WDR20 and UAF1 expression in glioblastoma (Figure 4-9A). To determine whether the observed effects on LRP6 were specific to HEK293 cells, I performed USP46 knockdowns in the glioblastoma cell lines A172 and U87 and similarly found significant decreases in LRP6 levels in both cell lines (Figure 4-9B). Thus, the USP46 complex regulates LRP6 levels in the absence of exogenous Wnt.

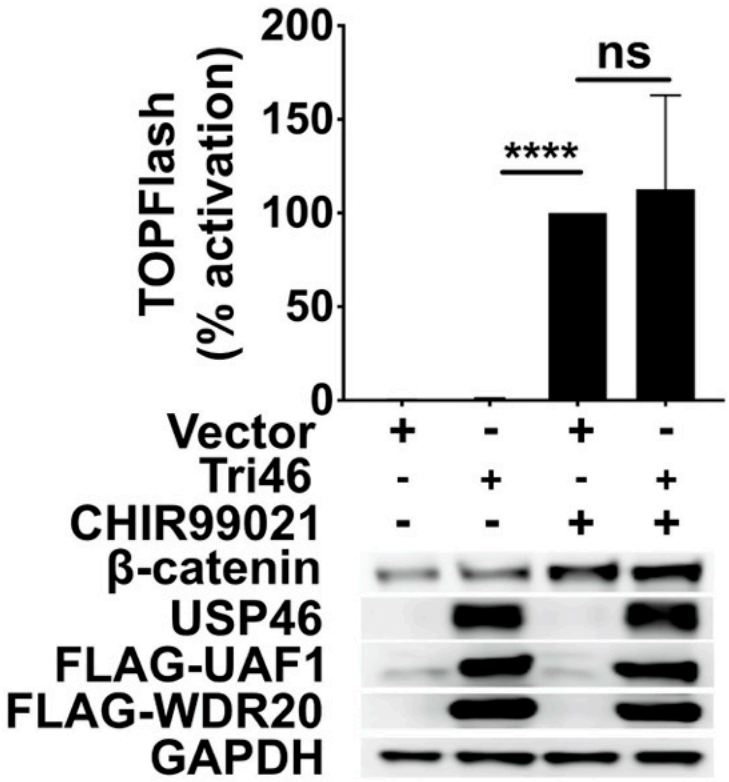

Figure 4-6. The USP46 complex does not potentiate activation of Wnt signaling by GSK3 inhibition.
Figure is adapted from the publication mentioned at the beginning of this chapter. Activation of Wnt signaling by CHIR99021 is not potentiated by the USP46 complex. HEK293STF cells were transfected with the USP46 complex and treated with CHIR99021 (2 mM) overnight. Graphs shows mean ±SD of TOPFlash normalized to cell number. ns compares CHIR99021-treated cells that were transfected with vector control or USP46 complex. ****p-value < 0.0001 compares CHIR99021-treated cells with USP46 complex-transfected cells.

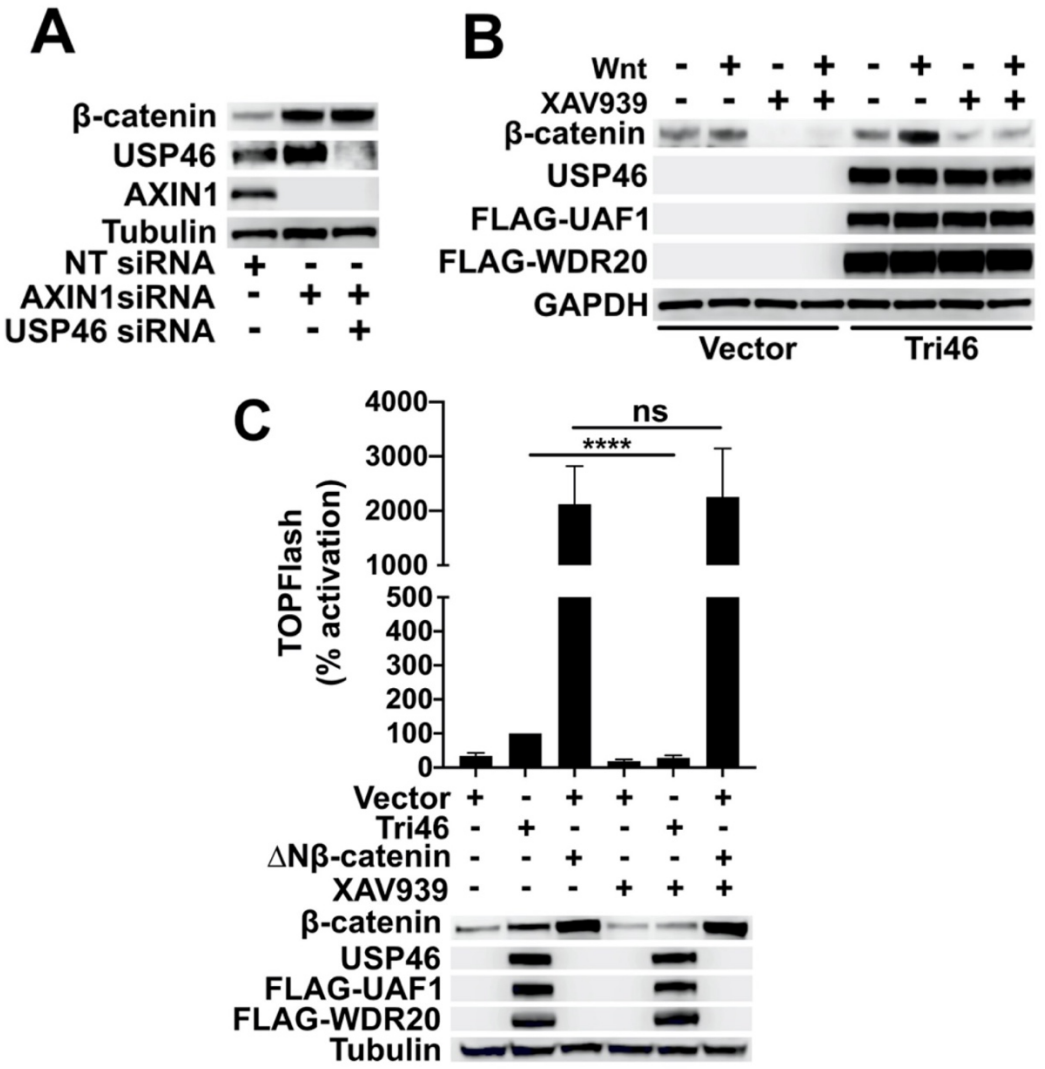

Figure 4-7. The USP46 complex acts upstream of the destruction complex. Figure is adapted from the publication mentioned at the beginning of this chapter. **(A)** USP46 depletion does not block stabilization of β-catenin upon AXIN1 siRNA knockdown. HEK293 cells were transfected with USP46 and AXIN1 siRNAs as indicated and immunoblotted for β-catenin. Immunoblotting for AXIN1 and USP46 confirmed their knockdown. **(B)** The tankyrase inhibitor, XAV939, which stabilizes AXIN to promote β-catenin degradation, inhibits β-catenin stabilization mediated by the USP46 complex. Cells were transfected and treated with Wnt3a in the absence or presence of XAV939 (1 mM) as indicated and immunoblotted for β-catenin, USP46, FLAG-UAF1, and FLAG-WDR20. **(C)** The AXIN stabilizer, XAV939, inhibits Wnt signaling stimulated by the USP46 complex but not by a non-degradable form of β-catenin (ΔN-β-catenin). Cells were transfected as indicated and treated with or without XAV939 (1 mM) overnight. Graphs shows mean ±SD of TOPFlash normalized to cell number. ns is not significant, ****p-value < 0.0001.

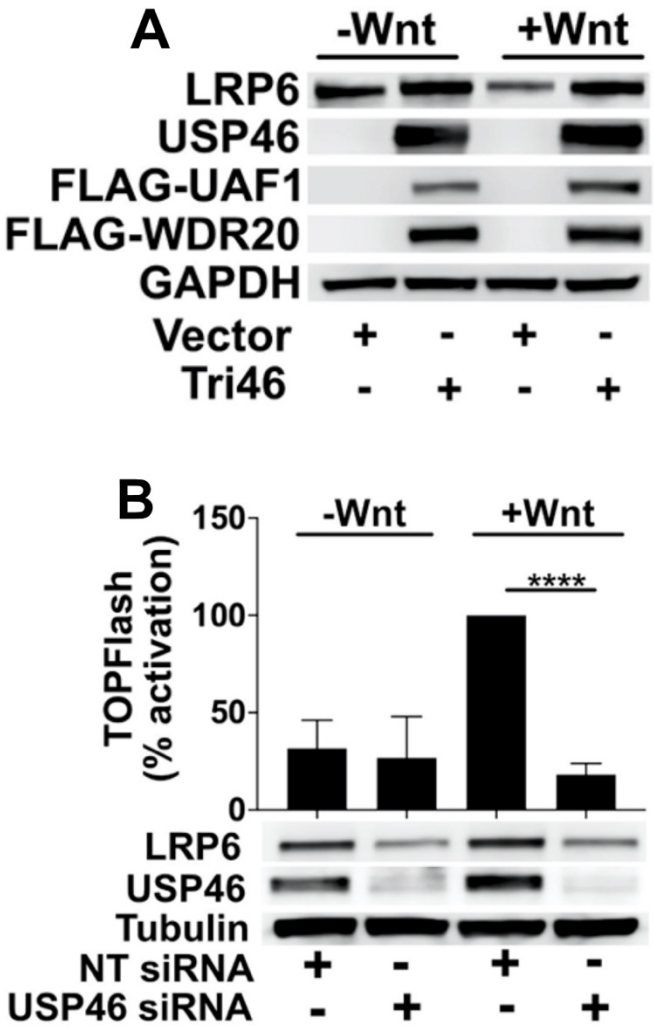

Figure 4-8. The USP46 complex regulates steady-state levels of LRP6.
Figure is adapted from the publication mentioned at the beginning of this chapter. **(A)** Overexpression of the USP46 complex increases steady-state levels of LRP6. HEK293STF cells were transfected with vector or the USP46 complex in the absence or presence of Wnt. **(B)** Knockdown of USP46 reduces LRP6 steady-state levels. HEK293STF cells were transfected with non-targeting (NT) or pooled USP46 siRNAs. Graph shows mean ±SD of TOPFlash normalized to cell number. ****p-value $\leq$ 0.0001.

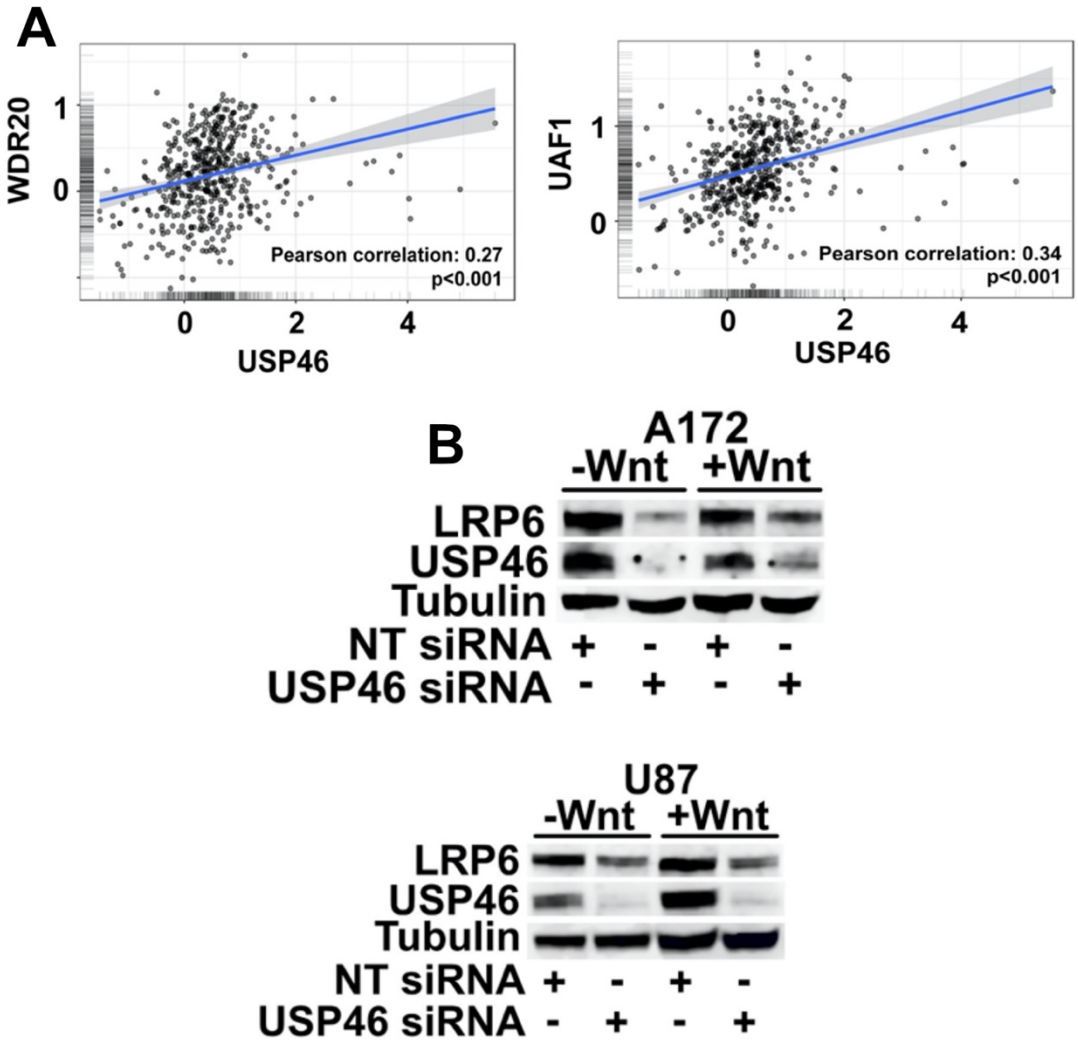

Figure 4-9. The USP46 complex regulates levels of LRP6 in glioblastoma. Figure is adapted from the publication mentioned at the beginning of this chapter. **(A)** USP46 positively correlates with expression of UAF1 and WDR20 in glioblastoma (TCGA-GBM Agilent platform). Correlation analysis between indicated genes (left, USP46 and WDR20 and right, USP46 and UAF1) was performed using the TCGA-GBM mRNA expression data from the Agilent-4502A platform (http://gliovis.bioinfo.cnio.es/). Pearson correlation coefficient and p-value were calculated and indicated in each panel. Analysis was performed by Zhenyi An. **(B)** USP46 regulates steady-state levels of LRP6 in glioblastoma cell lines. Pooled siRNA knockdown of USP46 decreased steady-state levels of LRP6 in A172 and U87 glioblastoma cell lines.

Binding of the USP46 complex to LRP6 is enhanced by Wnt signaling

Given its effect on LRP6 levels, I explored whether the USP46 complex interacted with LRP6. Using either tagged UAF1 and/or WDR20, I found that LRP6 co-immunoprecipitated with the USP46 complex using either tagged UAF1 and/or WDR20 (Figure 4-10A) and that co-immunoprecipitation of LRP6 was significantly enhanced in the presence of Wnt3a (Figure 4-10B). I was unable to perform USP46 co-immunoprecipitation due to the limitations of our USP46 antibody and tagging USP46 at its amino or carboxyl termini inactivated the protein in my Wnt assays.

To determine whether the USP46 complex acts on the pool of LRP6 at the plasma membrane, I performed cell-surface biotinylation assays. In this assay, cell-surface proteins were labeled with biotin and affinity purified with Neutravidin or Streptavidin beads. I observed that expression of the USP46 complex increased the cell-surface levels of LRP6 but not the insulin receptor control (Figure 4-11A). To facilitate detection of endogenous LRP6, I generated a HEK293 cell line, LF203, in which a FLAG tag was knocked into the C-terminal end of LRP6 by CRISPR-Cas9-mediated editing (Figure 4-12A-C). Consistent with a model in which the USP46 complex acts on the plasma membrane pool of LRP6, I found that USP46, UAF1, and WDR20 co-immunoprecipitated with cell-surface proteins in the biotinylation assay in both LF203 cells (Figure 4-11B) and parental HEK293 cells (Figure 4-11C). These results show that Wnt signaling facilitates the recruitment of the USP46 complex to the pool of LRP6 at the plasma membrane.

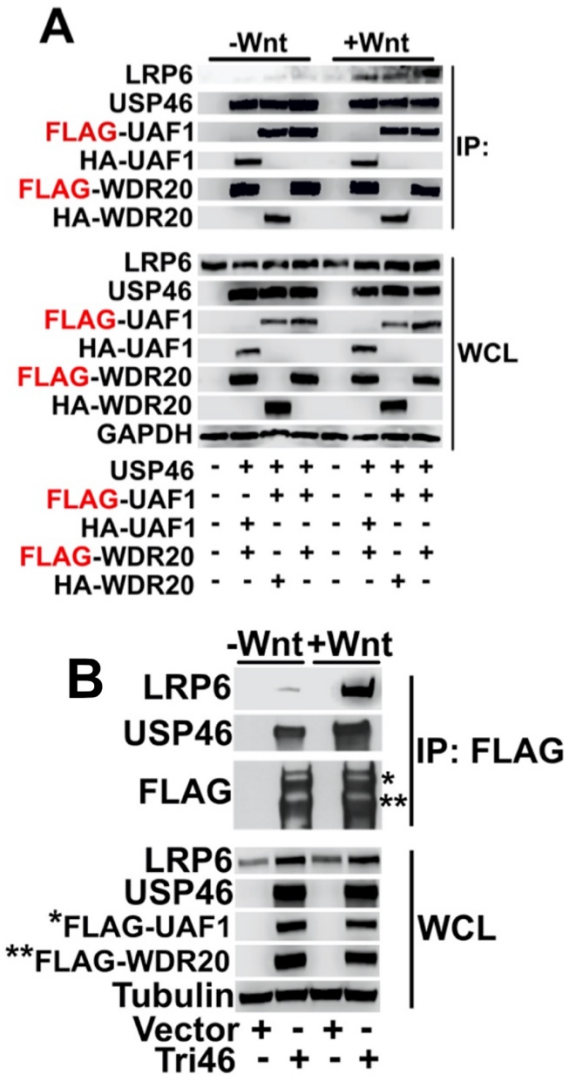

Figure 4-10. The USP46 complex interacts with LRP6.
Figure is adapted from the publication mentioned at the beginning of this chapter. **(A)** Endogenous LRP6 co-immunoprecipitates with FLAG-tagged WDR20 or UAF1. HEK293 cells were transfected as indicated and treated with Wnt3a (10 ng/ml) overnight. Cells were lysed, proteins immunoprecipitated with anti-FLAG conjugated beads, and immunoblotting performed. **(B)** Wnt signaling promotes the association between the USP46 complex and endogenous LRP6. HEK293 cells were transfected with USP46 complex components and treated with Wnt3a as indicated, FLAG-UAF1 (*) and FLAG-WDR20 (**) immunoprecipitated (IP) with anti-FLAG conjugated beads, and co-immunoprecipitated LRP6 detected by immunoblotting. WCL = whole cell lysates.

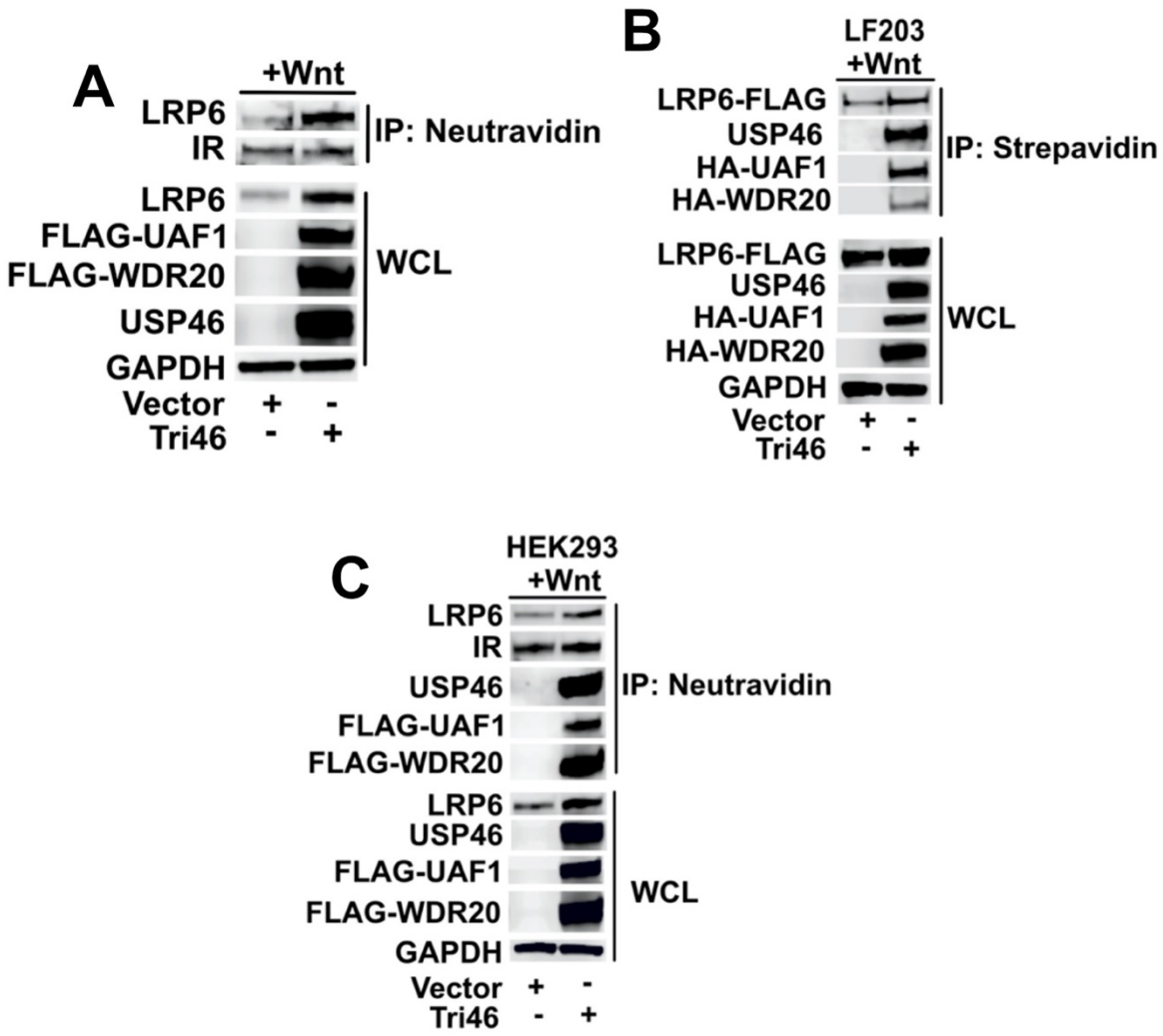

Figure 4-11. The USP46 complex increases cell-surface levels of LRP6.
Figure is adapted from the publication mentioned at the beginning of this chapter. **(A)** Overexpression of the USP46 complex increases cell-surface levels of LRP6. HEK293 cells were transfected with USP46 complex components and treated with Wnt3a, as indicated. Cells were then surface biotinylated, lysates subjected to neutravidin-pulldown, and immunoblotted for endogenous LRP6 and insulin (IR, control) receptors. **(B)** The USP46 complex co-precipitates with LRP6-FLAG in LF203 cells. **(C)** The USP46 complex co-precipitates with and LRP6 in HEK293 cells. Cells transfected with the USP46 complex and treated overnight with Wnt3a were subjected to surface biotinylation, lysis, avidin-pulldown, and immunoblotting.

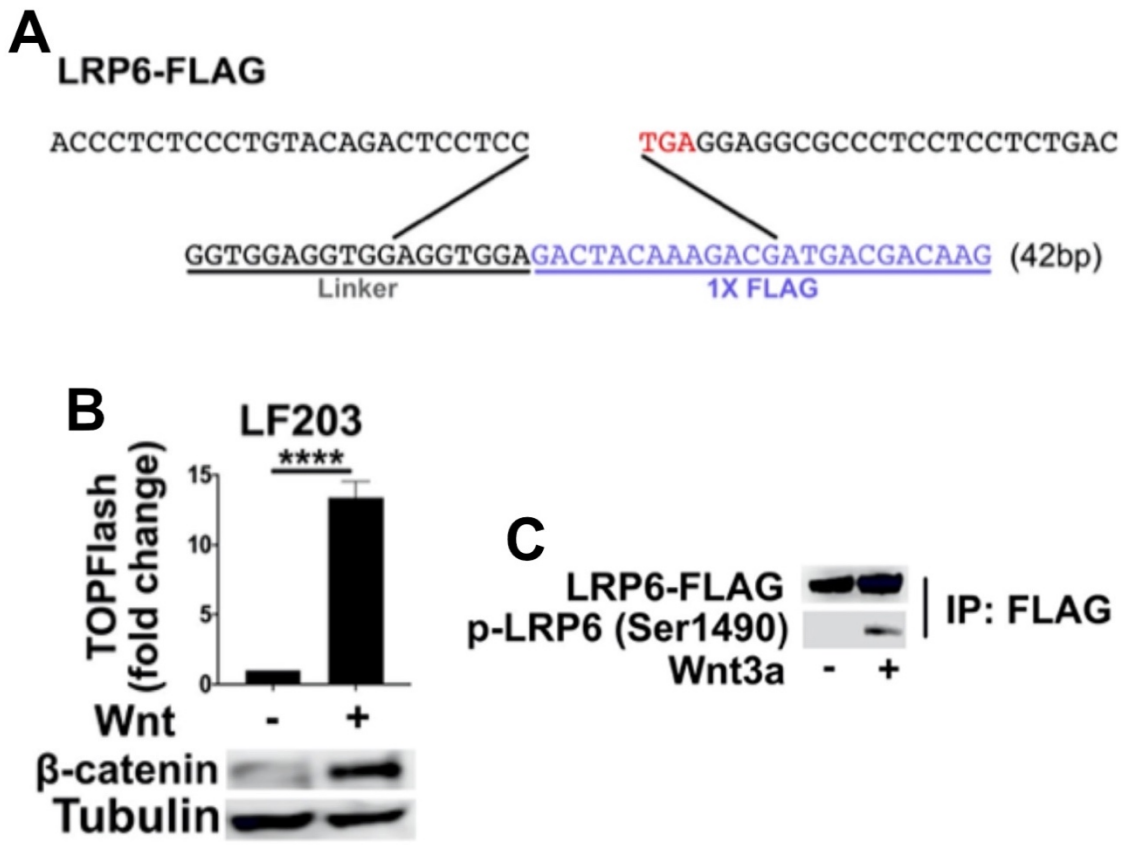

Figure 4-12. Generation and validation of the LF203 cell line.
Figure is adapted from the publication mentioned at the beginning of this chapter. **(A)** Genomic sequencing confirms correct in-frame insertion of the FLAG tag into endogenous LRP6. **(B)** Activation of Wnt signaling in LF203 cells by Wnt3a. Cells were transfected with TOPFlash and Renilla Luciferase control reporter plasmids and treated with Wnt3a (10 ng/ml) overnight. Firefly and Renilla luciferase activities were assessed by the Dual-Glo Luciferase Assay. Graph shows mean ±SD of TOPFlash normalized to cell number. ****p-value $\leq$ 0.0001 compares non-treated and Wnt3a-treated cells. **(C)** LRP6-FLAG is activated by Wnt3a in LF203 cells. LF203 cells were treated overnight with or without Wnt3a, lysed, and subjected to immunoprecipitation with anti-FLAG conjugated beads. Samples were analyzed by immunoblotting for total LRP6 and p-LRP6 (Ser1490), which detects the activated receptor.

Activation of Wnt signaling induces the assembly of USP46, UAF1, and WDR20 into large cytoplasmic complexes but not into LRP6 signalosomes

I performed gel filtration studies on the cytosolic fraction from HEK293 cells to assess USP46 complex formation in the absence and presence of Wnt signaling. In the absence of Wnt signaling, USP46, UAF1, and WDR20 migrated in a peak corresponding to the predicted size (~150 kDa) of a globular trimeric complex (Figure 4-13A). In the presence of Wnt signaling, however, the peak was broadened in a manner consistent with the formation of larger molecular weight complex(es) or a significant change in complex size. Thus, Wnt signaling induced a physical alteration of the USP46 complex in the cytoplasm.

Because the association of the USP46 complex with LRP6 was enhanced in the presence of Wnt signaling, I tested whether the USP46 complex interacted with LRP6 receptor aggregates in signalosomes that could be readily detected in sucrose density gradients (Bilić et al., 2007). Signalosomes contain activated Wnt receptors and are critical for the stabilization of β-catenin (Bilic et al., 2007). HEK293 cells treated with Wnt3a showed a shift in the migration of LRP6 into the denser sucrose density fractions of lysates compared to untreated cells (Figure 4-13B). The migration of USP46 did not change, however: it remained in the lighter fractions, even in the presence of Wnt3a. Based on these findings, we conclude that the USP46 complex associates with activated LRP6 receptors but not signalosome LRP6 aggregates.

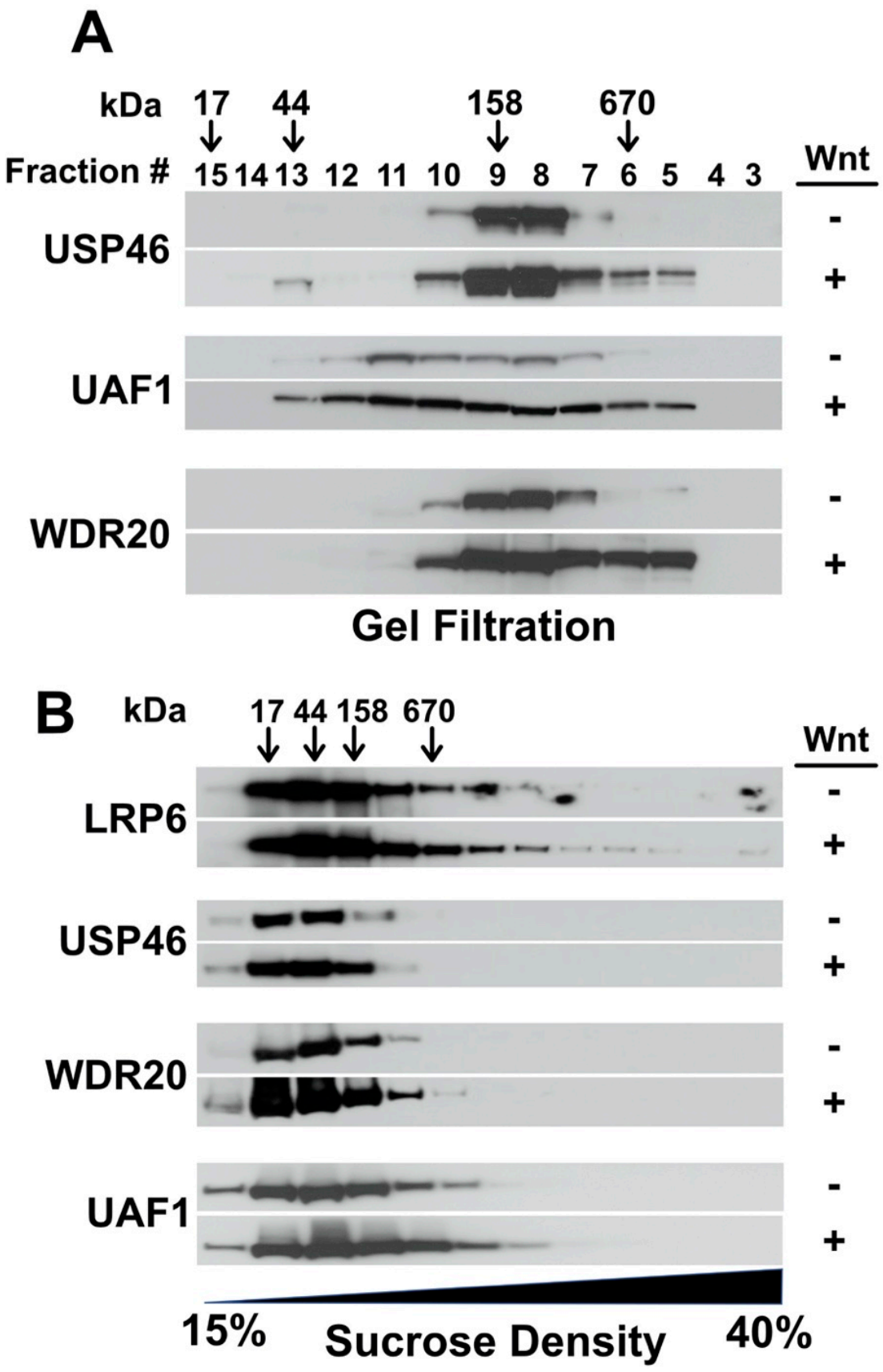
A
kDa
17
44
158
670
Fraction #
15 14 13 12 11 10 9 8 7 6 5 4 3
Wnt
USP46
UAF1
WDR20
-
+
Gel Filtration
B
kDa
17 44 158 670
Wnt
LRP6
USP46
WDR20
UAF1
15%
Sucrose Density
40%

Figure 4-13. The USP46 complex associates into large complexes independent of LRP6 signalosomes in the presence of Wnt.
Figure is adapted from the publication mentioned at the beginning of this chapter. **(A)** Wnt signaling induces the formation of high molecular weight USP46 complexes as assessed by size exclusion chromatography. HEK293 cells were treated in the absence or presence of Wnt3a (10 ng/ml), lysates prepared, and high-speed (100,000 x g) supernatants passed over a Superdex 200 FPLC column. Fractions obtained were subjected to TCA precipitation followed by immunoblotting. **(B)** The USP46 complex does not co-fractionate with high molecular weight LRP6 aggregates (signalosomes) on sucrose gradient centrifugation. HEK293 cells were incubated in the absence or presence of Wnt3a (10 ng/ml), Triton X-100 lysates collected, and sucrose density gradient (15-40%) sedimentation performed. Fractions were precipitated with chloroform-methanol extraction and analyzed by immunoblotting. The predicted kDa is based on the elution profile of a set of protein standards.

USP46 inhibits the ubiquitylation of LRP6

The enzymatic activity of USP46 is required for its Wnt activity, as a catalytically inactive version of USP46, USP46^{C44S}, did not increase LRP6 levels (Figure 4-14A) or potentiate Wnt signaling in HEK293STF cells (Figure 4-14B). The decreases in LRP6 levels and Wnt reporter activity suggest that USP46^{C44S} may be acting in a dominant-negative fashion. To ensure that the differences in the Wnt activity of wild-type USP46 and USP46^{C44S} were not due to differences in expression levels, I performed a titration study. I found that, in contrast to wild-type USP46, USP46^{C44S} was inactive at all of the concentrations tested (Figure 4-14C). I similarly found that a mutant of UAF1, UAF1^{S170Y}, which disrupts its interaction with USP46 (Yin et al., 2015), also failed to increase LRP6 levels (Figure 4-15A) and exhibited reduced Wnt activity (Figure 4-15B). Thus, the enzymatic activity of the USP46 complex is required for its regulation of LRP6 levels.

Next, I examined if the USP46 complex increases LRP6 levels by promoting its deubiquitylation and opposing the activity of RNF43, an E3 that targets Wnt receptors. I found that expression of RNF43 in HEK293 and LF203 cells increased ubiquitylation of LRP6 and LRP6-FLAG, respectively, an effect that was countered by the USP46 complex (Figure 4-16A & Figure 4-16B). Conversely, knockdown of USP46 in LF203 cells leads to increased ubiquitylation of LRP6-FLAG that was readily detected in whole-cell lysates as a dramatic broadening of the LRP6-FLAG bands (Figure 4-16C). These results indicate that the USP46 complex promotes the deubiquitylation of LRP6 at the plasma membrane, thereby increasing its stabilization and opposing the action of the Wnt receptor ubiquitin ligase, RNF43.

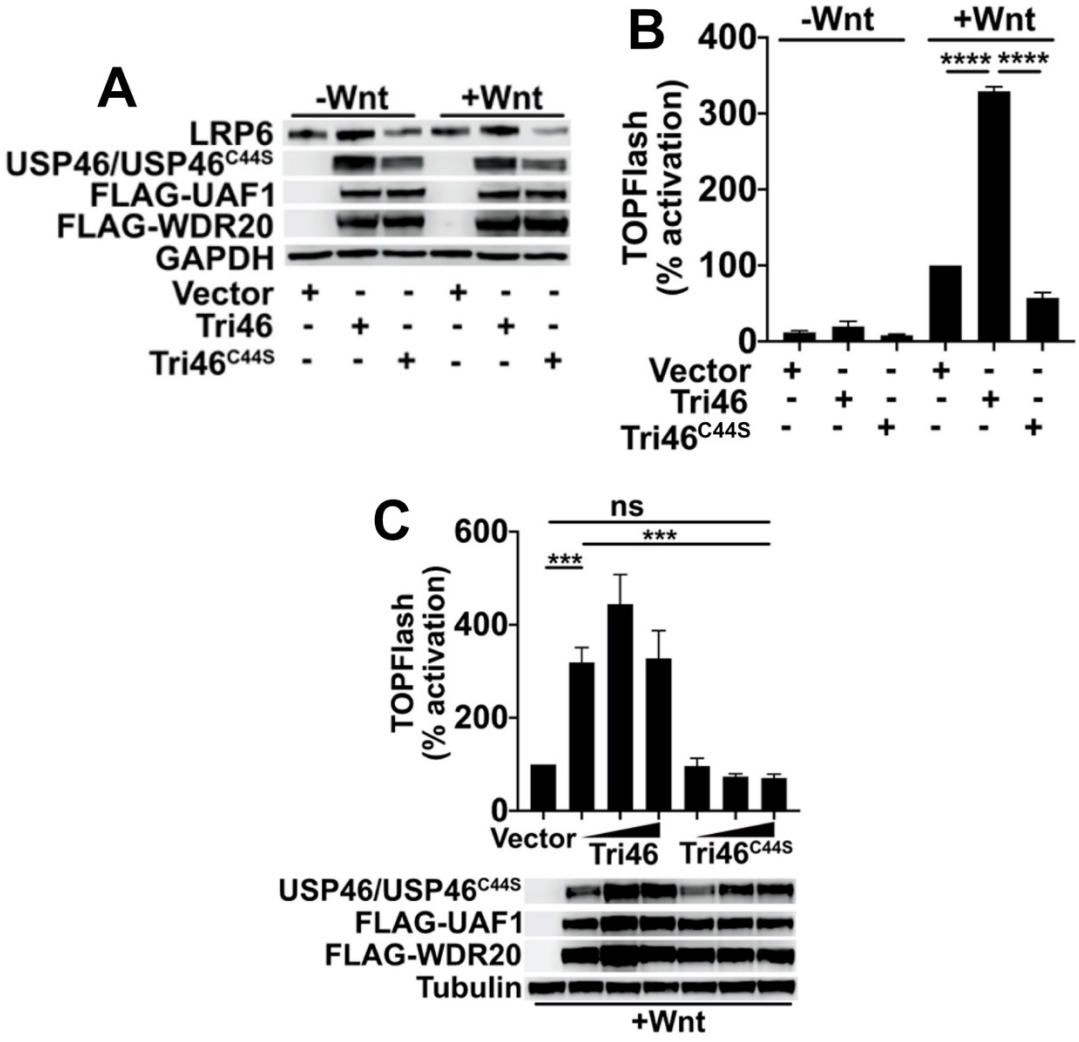

Figure 4-14. The catalytically inactive USP46 mutant, USP46^{C44S}, cannot potentiate Wnt signaling.

Figure is adapted from the publication mentioned at the beginning of this chapter. **(A)** Overexpression of the USP46 complex containing the catalytically dead USP46^{C44S} (Tri46^{C44S}) does not increase LRP6 levels. **(B)** Overexpression of catalytically dead USP46^{C44S} fails to potentiate Wnt signaling as assessed by Wnt reporter assay. ****p-value < 0.0001. **(C)** Titration of increasing amounts of catalytically dead USP46^{C44S} complex fails to potentiate Wnt signaling as assessed by Wnt reporter assay and β-catenin stabilization. ns compares vector-transfected cells with the highest amount of USP46^{C44S} complex-transfected cells. ***p-value < 0.001.

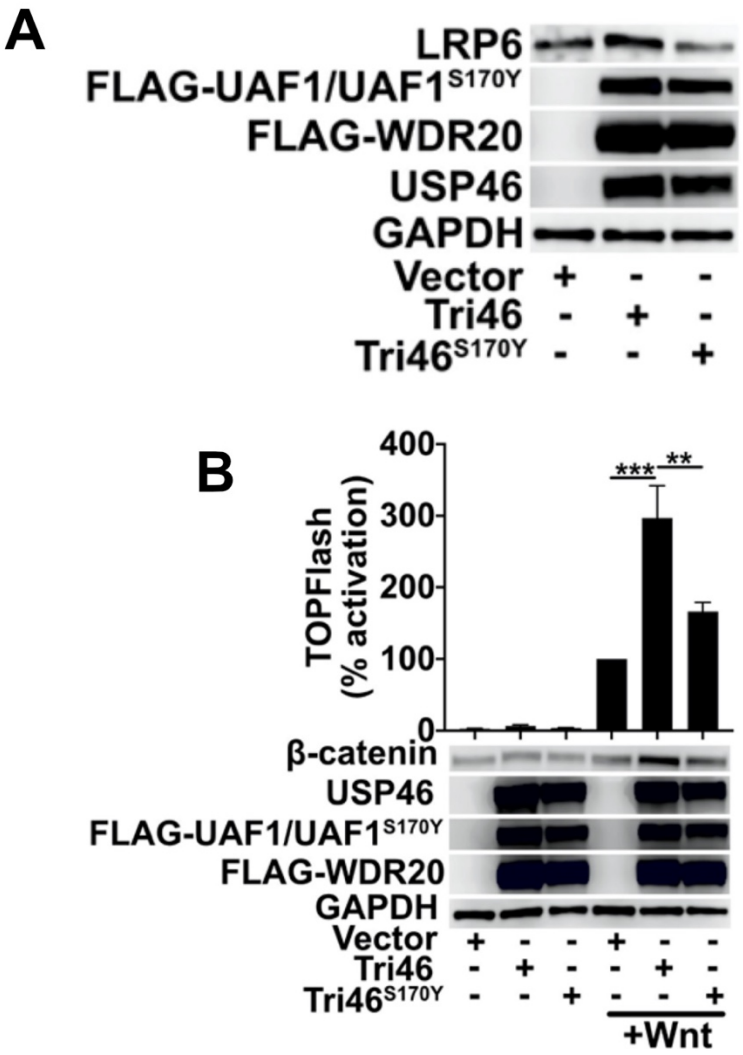

Figure 4-15. The USP46^{S170Y} complex has reduced capacity to potentiate Wnt signaling.
Figure is adapted from the publication mentioned at the beginning of this chapter. **(A)** Overexpression of the USP46 complex containing the USP46 binding mutant, FLAG-UAF1^{S170Y}, does not increase LRP6 levels. GAPDH is loading control.
(B) The USP46^{S170Y} complex exhibits reduced activity. **p-value $\leq$ 0.01 compares Wnt-treated cells transfected with active USP46 complex or USP46^{S170Y}- complex. ***p-value $\leq$ 0.001 compares Wnt-treated cells transfected with vector or USP46 complex. Graphs show mean $\pm$SD of TOPFlash normalized to cell number.

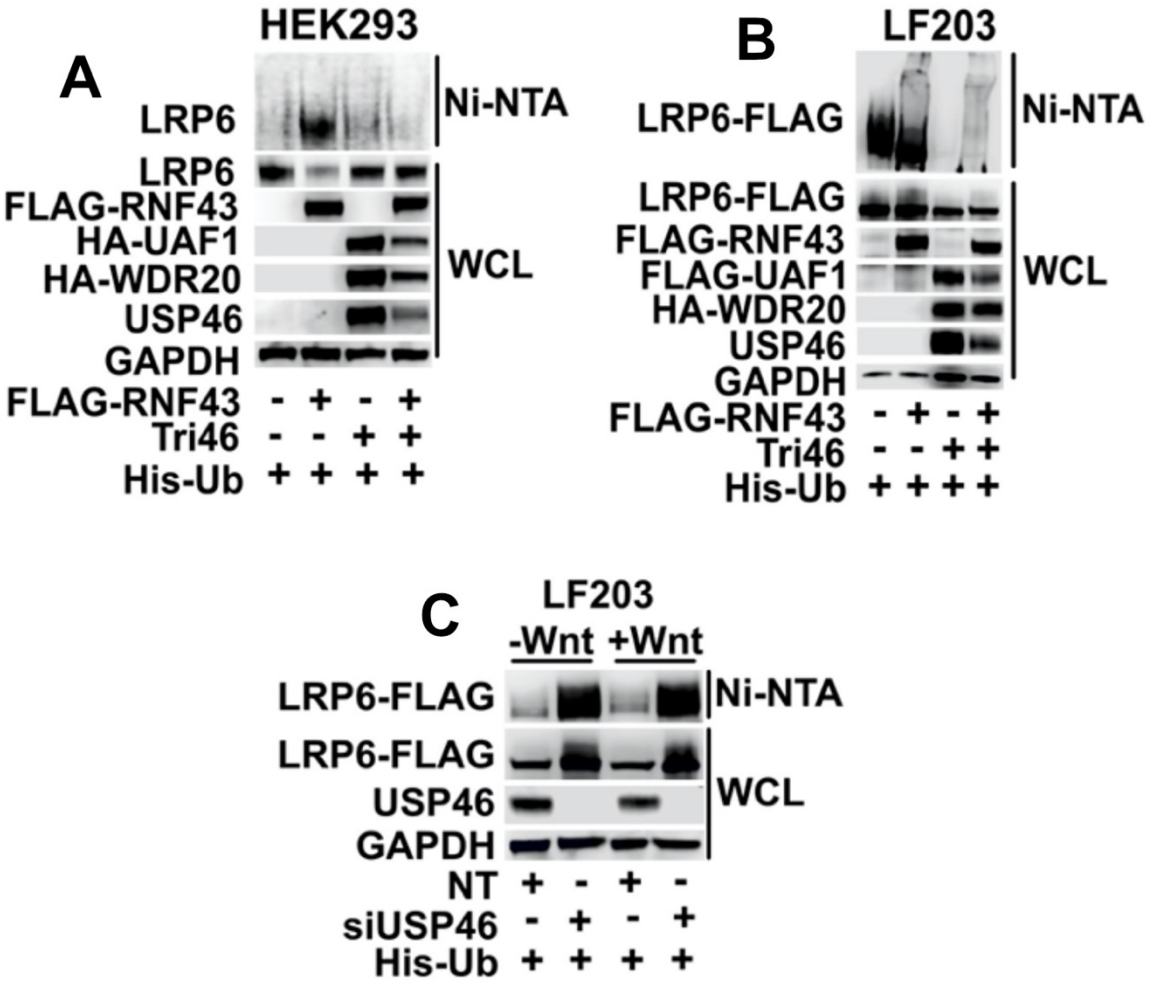

Figure 4-16. The USP46 complex deubiquitylates LRP6.
Figure is adapted from the publication mentioned at the beginning of this chapter. **(A)** The USP46 complex can counter RNF43-mediated ubiquitylation. In a His ubiquitylation assay, expression of FLAG-RNF43 promotes endogenous ubiquitylation of LRP6, which is opposed by expression of the USP46 complex. His-Ub modified proteins isolated by nickel affinity purification (Ni-NTA). Ubiquitylated LRP6 was detected by LRP6 antibody. **(B)** Overexpression of FLAG-RNF43 in LF203 cells similarly promotes LRP6-FLAG ubiquitylation, which is opposed by overexpression of the USP46 complex. His-Ub modified proteins isolated by nickel affinity purification. Ubiquitylated LRP6-FLAG was detected by FLAG antibody. **(C)** Knockdown of USP46 enhances LRP6-FLAG ubiquitylation. His-Ub modified proteins isolated by nickel affinity purification. Ubiquitylated LRP6-FLAG was detected by FLAG antibody. WCL = whole cell lysates.

USP46 promotes the growth of intestinal organoids

Intestinal organoids rely on Wnt signaling for their growth and represent a powerful *ex vivo* model to study the modulation of the Wnt pathway in a physiologically relevant context (Merenda et al., 2020). RSPOs, which increase levels of Frizzled and LRP6, are critical factors required for the culture of intestinal organoids (Hao et al., 2012; Koo et al., 2012; Sato et al., 2011; Sato et al., 2009). Because the USP46 complex opposes the action of RNF43, loss of USP46 would be expected to potentiate the activities of RNF43/ZNRF3, thereby decreasing the effectiveness of RSPO in maintaining intestinal organoid growth. Chen Shen found that knockdown of USP46 decreased the viability of intestinal organoids (Figure 4-17A) and that this effect was more evident at lower concentrations of RSPO (higher levels of RNF43/ZNRF3 activity) (Figure 4-17A & Figure 4-17B). Intestinal organoids derived from the intestinal epithelium of APC^{min} mice do not require exogenous Wnt for growth (Sato et al., 2011). The growth of these APC^{min} organoids, however, is sensitive to the level of LRP6, and knockdown of LRP6 blocks their growth (Saito-Diaz et al., 2018). Consistent with a role regulating LRP6 levels in intestinal organoids, knockdown of USP46 similarly resulted in β–catenin decreased β-catenin levels and cell viability of APC^{min} organoids (Figure 4-18A & Figure 4-18B). Given the role of Wnt signaling as a major driver of tissue growth, we asked whether USP46 is altered in human cancers. Using the cBioPortal to assess 9,125 tumor samples across 33 cancer types in The Cancer Genome Atlas (Cancer Genome Atlas Research et al., 2013; Tang et al., 2017), Vivian Weiss found a significant correlation between USP46 gene alterations and decreased overall cancer patient survival (Figure 4-19A), and high levels of USP46 correlated with reduced

survival of patients with cancers such as invasive breast cancer (Figure 4-19B). Alterations in USP46 mostly consisted of amplification and were commonly observed in glioblastoma multiforme and lung squamous cell carcinomas (Figure 4-19C).

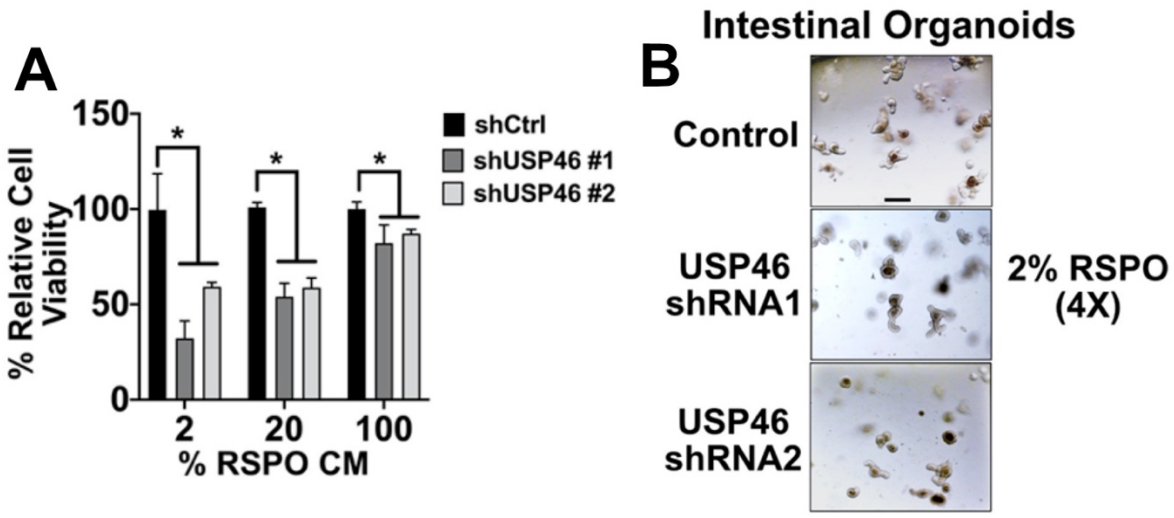

Figure 4-17. Viability of intestinal organoids in low RSPO conditions decreases following USP46 depletion.
Figure is adapted from the publication mentioned at the beginning of this chapter. **(A)** The sensitivity of intestinal organoids to USP46 depletion is RSPO-dependent. Exogenous RSPO is essential for culturing intestinal organoids in vitro. Intestinal organoids infected with a control lentivirus or two independent lentiviruses expressing USP46 shRNAs were grown in decreasing concentrations of RSPO conditioned media (CM). Viability was assessed by Cell-Titer Glo. *p-value < 0.05. GAPDH is loading control. Assays were performed by Chen Shen. **(B)** Representative images of intestinal organoids treated with USP46 shRNA 1 or 2 and grown in the presence of 2% RSPO-CM. Scale bar = 200 μM. Assays were performed by Chen Shen.

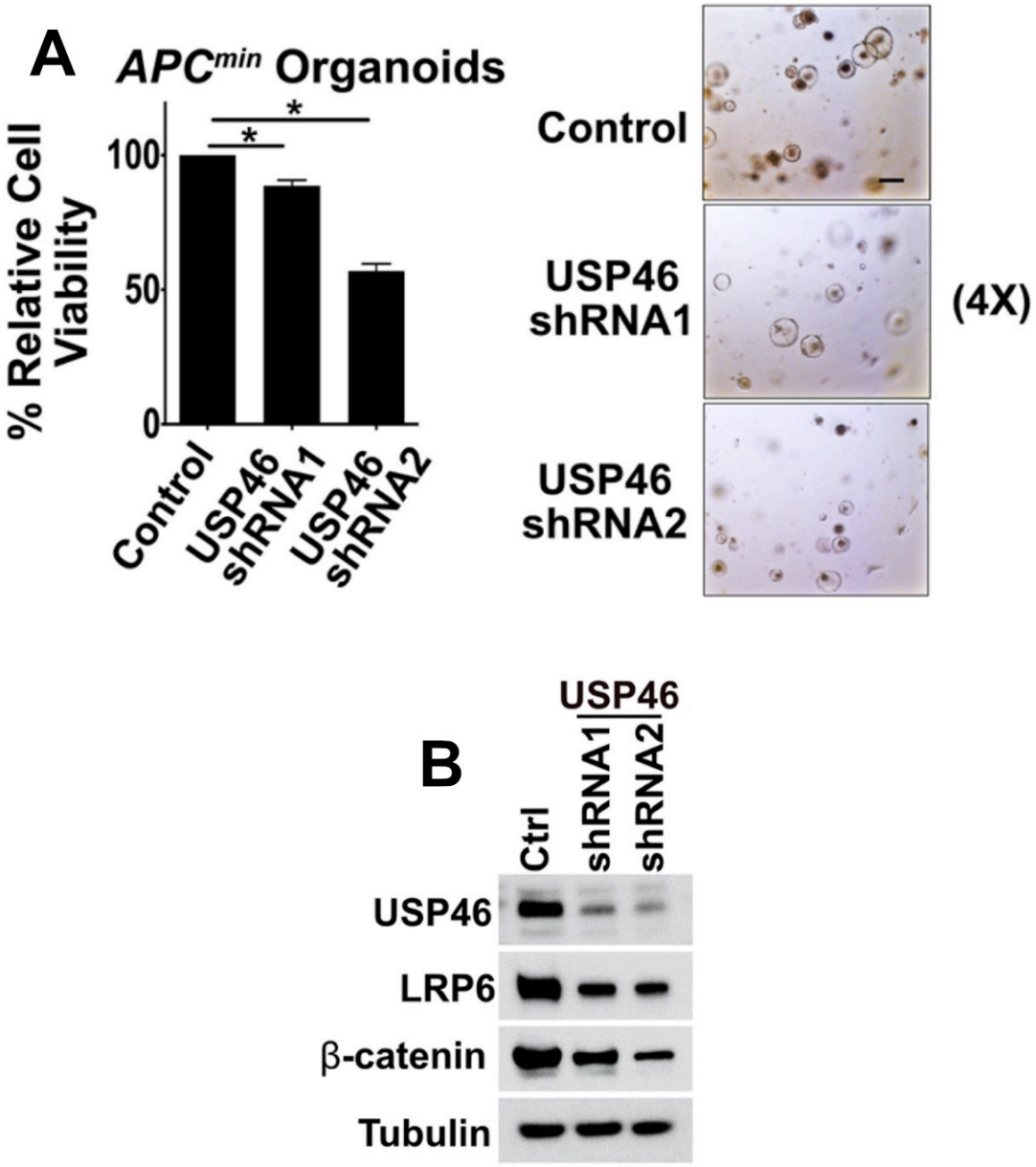

Figure 4-18. Knockdown of USP46 decreases cell viability of *APC^{min}* organoids. Figure is adapted from the publication mentioned at the beginning of this chapter. **(A)** Following knockdown of USP46 with individual USP46 shRNA lentivirus, organoids have reduced cell viability. Percentage relative viability (control represents 100% viability) is shown on the left with representative images on the right. Graph shows mean ±SD of Cell-Titer Glo. *p-value $\leq$ 0.05 compares control-treated with USP46 shRNA 1 or 2–treated *APC^{min}* organoids. Scale bar = 200 μM. Assays were performed by Chen Shen. **(B)** Immunoblot confirms decreased USP46, LRP6, and β-catenin in *APC^{min}* organoids with USP46 shRNA 1 or 2 treatment. Assays were performed by Chen Shen.

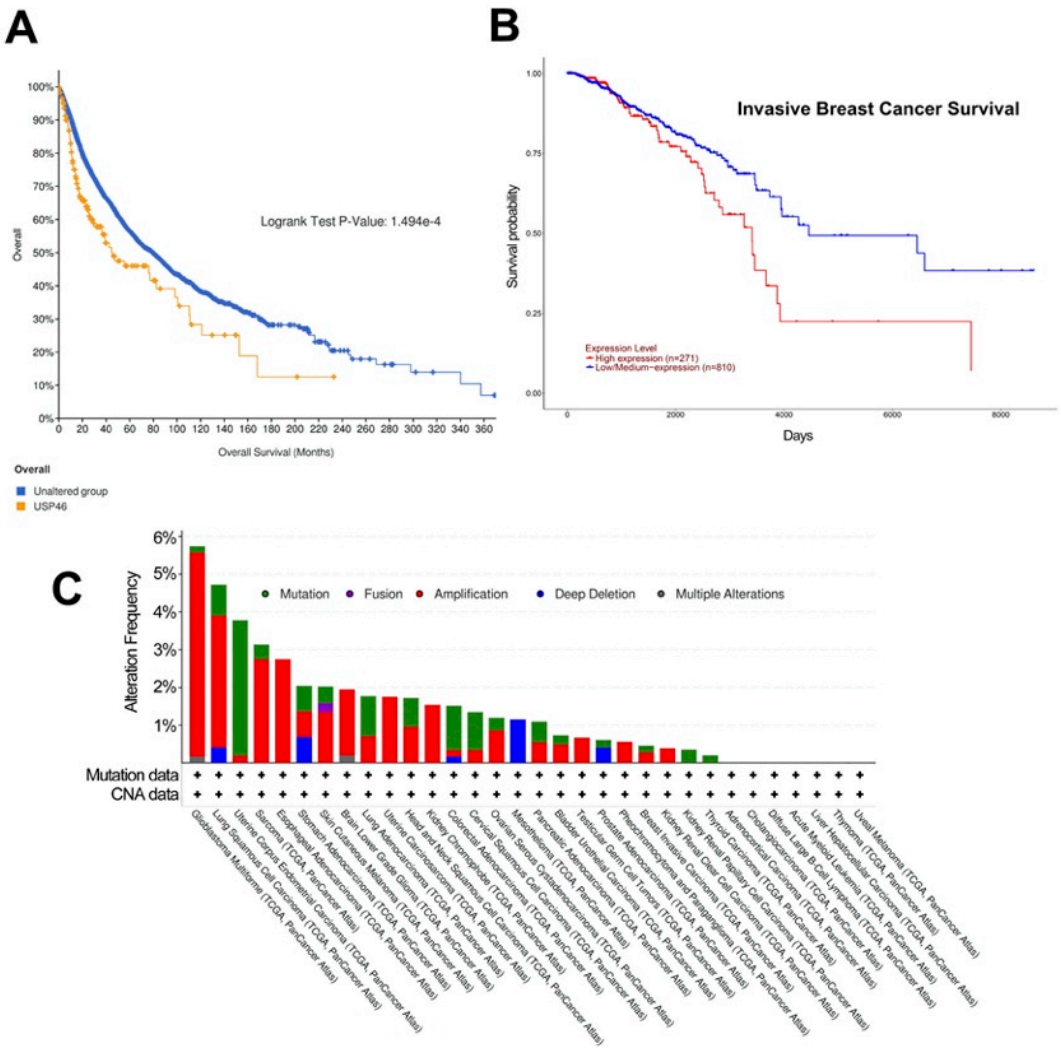

Figure 4-19. USP46 expression is upregulated in cancer and associated with a poorer prognosis.
Figure is adapted from the publication mentioned at the beginning of this chapter. **(A)** Altered USP46 expression in cancer is associated with decreased overall survival. The median overall survival of patients with USP46 alterations was 45.14 months (N=178) compared to 79.46 months (N=10,623) for the unaltered group across tumor types. Analysis was performed by Vivian Weiss. **(B)** High USP46 mRNA expression levels in the TCGA correlate with decreased overall survival in invasive breast cancer (p-value $\leq$ 0.02). Decreased survival were also observed for liver hepatocellular carcinoma (p-value $\leq$ 0.02), and sarcoma (p-value $\leq$ 0.05). Analysis was performed by Vivian Weiss. **(C)** Gene amplification of USP46 is commonly observed in human cancers. Altered group: fusions, deletions, amplifications, and mutations. CNA copy number alteration. Analyses of TCGA gene expression data were pre-formed using the UALCAN interactive web-portal tool (Chandrashekar et al., 2017). Analysis was performed by Vivian Weiss.

DISCUSSION

In the current study, we identify the USP46 deubiquitylase complex as an evolutionarily conserved positive regulator of Wnt signaling in vertebrates. Full activity of the USP46 complex in Wnt signaling requires all three components: USP46, UAF1, and WDR20. I show that this trimeric complex maintains the steady-state level of LRP6 by inhibiting its turnover (opposes the action of the ubiquitin ligase, RNF43), thereby increasing cell surface levels of LRP6 (Figure 4-20A). Consistent with my data demonstrating that USP46 regulated LRP6 levels, USP46 was identified in a genome-wide screen as a member of a group of novel genes involved in network rewiring at the level of (or above) the Wnt receptors (Billmann et al., 2018).

I found that the USP46 complex is recruited to LRP6 and that knockdown of USP46 does not result in further decreases in LRP6 levels upon Wnt stimulation. Ubiquitylated Dishevelled (Dvl), a positive regulator of the Wnt pathway, was found to block its oligomerization *in vitro*, and it was proposed that deubiquitylation of Dvl is required to promote its polymerization and its subsequent role in signalosome formation (Madrzak et al., 2015). I speculate that, similarly, activated, ubiquitylated LRP6 cannot be assembled into signalosomes (possibly due to steric hindrance). Based on my sucrose density gradient experiments, the USP46 complex does not associate with signalosomes, although I cannot rule out low affinity, transient interactions. Thus, Wnt ligand-stimulated recruitment of the USP46 complex may represent a "pruning" step to maximally increase the availability of active LRP6 receptors for signalosome assembly and subsequent pathway activation (Figure 4-20B).

In accompanying work, the Ahmed Lab describe the characterization of the USP46 complex in *Drosophila*, which provides *in vivo* evidence for an evolutionarily conserved role of the USP46 complex in regulating Arrow/LRP6 levels during Wg/Wnt signaling. In contrast to my results in vertebrate cells, however, the USP46 complex does not appear to regulate steady-state levels of Arrow in the Wnt unstimulated state. Rather, regulation of Arrow levels is dependent on active Wg signaling. Thus, in *Drosophila*, regulation of Arrow levels and pruning by the USP46 complex may occur simultaneously.

USP46 knockdowns in the glioblastoma cell lines, U87 and A172, significantly reduced LRP6 levels. There is increasing evidence that suggests misregulated Wnt signaling is involved in the formation of gliomas (McCord et al., 2017). However, the mechanisms involved are not clear. Using the cBioPortal resource, the database shows that USP46 is amplified in roughly 5-6% of glioblastomas (Figure 4-19C). Glioblastomas are the most aggressive form of gliomas with a five-year survival rate of less than 5% of patients (Davis, 2016). High expression of USP46 could be a biomarker of a subset of glioblastomas that have overactive Wnt signaling and may respond to Wnt-specific therapeutics. It is possible that the USP46 complex in this context maintains elevated levels of Wnt signaling that drives tumorigenesis in this subset of glioblastomas.

Analysis of USP46 mRNA expression in the TCGA database shows high USP46 mRNA expression in invasive breast cancer and this correlates with decreased survival (Figure 4-19B). High expression of LRP6 has been found in a subset of breast cancers and treatment of breast cancer cell lines expressing high levels of LRP6 with an LRP6 antagonist reduced Wnt signaling and decreased cell proliferation (Liu et al., 2010). It is

possible that tumors expressing high levels of USP46 mRNA may also have high levels of LRP6. If these tumors do have high levels of LRP6, then it is possible that they may be sensitive to treatment with novel LRP6 antibodies. These novel LRP6 antibodies bind LRP6 domains to block binding of Wnt ligands to LRP6. They have been shown to inhibit growth of Wnt-driven tumors (Ettenberg et al., 2010; Jackson et al., 2016).

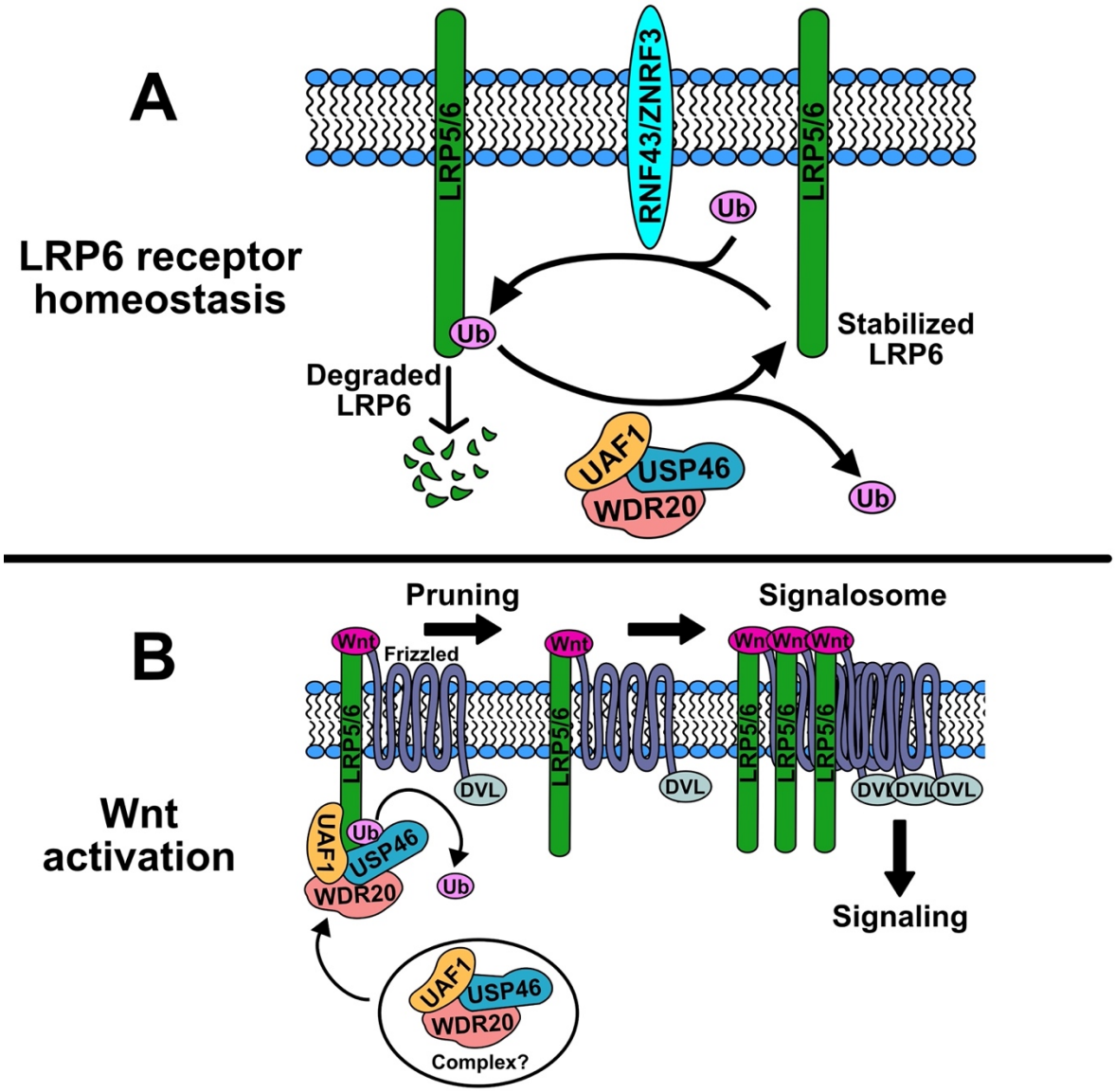

Figure 4-20. Model of the mechanism of the USP46 complex in Wnt signaling Figure is adapted from the publication mentioned at the beginning of this chapter. **(A)** The basal function of the USP46 complex. **(B)** In the presence of Wnt, there is increased recruitment of the USP46 complex to ubiquitylated LRP6 receptors.

Chapter 5

FUTURE DIRECTIONS

Phosphorylation of XIAP in Wnt signaling

Given the likely small pool of phosphorylated nuclear XIAP involved in Wnt signaling, we were unable to detect this form of XIAP in cell extracts using conventional biochemical methods. The development of a XIAP phospho-T180 specific antibody would be a powerful tool to further assess the *in vivo* importance of this phosphorylated form of XIAP. It is not clear whether GSK3 phosphorylates XIAP in the cytoplasm or the nucleus. Although it is abundant in the cytoplasm, GSK3 has been shown to also localize in the nucleus and also contains a nuclear localization signal (Bijur and Jope, 2001; Meares and Jope, 2007). Using this antibody, we could determine whether phosphorylation occurs in the cytoplasm or nucleus.

It is possible that the interaction between XIAP and Gro/TLE may be facilitated by another protein that is recruited to XIAP following phosphorylation. One way to examine this is to perform mass spectrometry analysis comparing samples from co-immunoprecipitations with wildtype XIAP or the $XIAP^{T180A}$ mutant in the presence or absence of Wnt treatment. This would allow us to examine changes in protein-protein interactions and give us candidates for Wnt-dependent interactions that are lost with the T180A mutation.

While we have shown that GSK3 phosphorylates XIAP at the T180 it is not clear whether Wnt signaling promotes phosphorylation of XIAP on the appropriate site(s) or

primes the GSK3 site(s) on XIAP via regulation of another kinase (e.g., CK1). The latter option is particularly attractive given that CK1 has been shown to prime GSK3 sites on both β-catenin and LRP6 to inhibit and activate Wnt signaling, respectively (Liu et al., 2002; Zeng et al., 2005). Based on the results, it is clear that sequential phosphorylation by CK1α and then GSK3 promotes phosphorylation of XIAP in *in vitro* kinase assays. One potential priming phosphorylation site for GSK3 is serine 186. Although the optimal distance between a primed site and a GSK3 target is four amino acids, greater distances have also been demonstrated (Cole et al., 2004). To explore phosphorylation by CK1α, an *in vitro* kinase reaction with CK1α and XIAP followed by liquid chromatography-mass spectrometry (LC-MS) would identify potential phosphorylation sites. Though CK1 is likely to confer priming phosphorylation on XIAP, it is also possible that XIAP may be phosphorylated by nuclear kinases such as mitogen-activated protein kinases (MAPKs) to affect the activity of XIAP in Wnt signaling. MAPKs have been shown to phosphorylate nuclear proteins and transcription factors to control nuclear events (Turjanski et al., 2007). I could explore this possibility by expressing a construct that contains a biotin ligase (BioID) fused to XIAP in cells, treating with or without Wnt ligand, and then treating with biotin to induce proximity-based biotinylation of interactors of the BioID fused-XIAP. Biotinylated proteins would be isolated with avidin purification and identified by mass spectrometry.

When we performed the liquid chromatography-mass spectrometry (LC-MS) analysis on samples from the *in vitro* kinase assay with XIAP and GSK3, other phosphosites were also identified. It is possible that other sites might be important for XIAP activity in Wnt signaling. For example, activation of the Wnt co-receptor LRP6

following binding of Wnt ligand involves the cooperativity of five different phosphosites. Likewise, ubiquitylation of β-catenin occurs after phosphorylation of four different sites on β-catenin. Thus, it is possible that a combination of phosphosites could regulate XIAP and this could be explored through mutagenesis of these sites in pairwise combination with the T180A mutation.

All of our studies were performed using overexpression of a $XIAP^{T180A}$ mutant, but it would be better to perform CRISPR/Cas9-mediated mutagenesis of the T180 site to alanine in the endogenous XIAP gene to fully understand the effect of phosphorylation at the T180 site. This would be useful in eliminating any potential background activity coming from wildtype XIAP. We showed that $XIAP^{T180A}$ has decreased affinity for TLE3, but the interaction is not completely lost. This could be because another phosphosite on XIAP is also involved in the interaction with Gro/TLE. Another possibility is that XIAP can form oligomers and in the case of residual binding of TLE3, $XIAP^{T180A}$ might have dimerized with wildtype XIAP which we know interacts with TLE3. It has been shown that cIAP forms dimers in their RING domains and XIAP can form dimers in their BIR domain and RING domain (Feltham et al., 2011; Lu et al., 2007; Nakatani et al., 2013). It has not been determined whether XIAP forms dimers prior to ubiquitylating Gro/TLE and whether dimerization is necessary for XIAP activity in the Wnt pathway.

Beyond its role in apoptosis, there is increasing evidence that XIAP can participate in a variety of signaling pathways. For example, in addition to our previous studies demonstrating the role of XIAP in the Wnt pathway, a number of studies have shown that XIAP overexpression is also capable of activating the NF-kB pathway

(Barkett et al., 1997). How XIAP is recruited differentially to regulate NF-κB and/or Wnt signaling, as opposed to its apoptotic function has remained a mystery. Further investigation would provide insight into the roles of additional post-translational modifications (e.g., ubiquitylation and sumoylation) on the activity of XIAP in other signaling pathways and apoptosis.

The USP46 complex in Wnt signaling

Though we have uncovered a mechanism for the USP46 complex in regulating Wnt signaling by modulating LRP6 co-receptors, many questions still remain about its mechanism of action and what other components may be involved. These questions include: How does recruitment of the USP46 complex to LRP6 occur in a Wnt-dependent manner? Does the USP46 complex bind LRP6 as a pre-formed trimer or does it proceed through stepwise recruitment of individual subunits? Are other components necessary in the Wnt-dependent recruitment of the USP46? Does assembly of these components onto LRP6 form a larger macromolecular structure on LRP6 outside of the signalosome? I will discuss some of these questions and how we can address them here.

USP46 shares about 89% sequence identity with the deubiquitylase ubiquitin specific protease 12 (USP12). WDR20 and UAF1 also bind USP12 to allosterically activate the deubiquitylase (Li et al., 2016a). Thus, it is possible that USP12 may have some activity in Wnt signaling and might even regulate LRP6 levels. However, my preliminary overexpression studies in HEK293STF cells suggests that overexpression of the USP12 complex does not potentiate the Wnt pathway when compared to

overexpression of the USP46 complex. To further confirm that USP12 does not act on LRP6, immunoprecipitation of the LRP6 receptor and immunoblotting for USP12 would determine whether it interacts with LRP6. Additionally, knockdown of USP12 would demonstrate effects on the steady-state levels of LRP6. A knockdown of USP12 followed by an *in vivo* ubiquitylation assay would allow us to assess the ubiquitylation status of LRP6. While we expect these assays to show that the USP12 complex has no effect on LRP6 and its ubiquitylation, this does not exclude the possibility that USP12 itself or that the USP12 complex may have some other regulatory mechanism in the Wnt pathway. However, this would demonstrate a level of substrate specificity between the two highly similar deubiquitylases.

I have shown that mutation of the catalytic cysteine of USP46 to a serine ($USP46^{C44S}$) results in a decrease in Wnt reporter activity and LRP6 steady-state levels, indicating that the catalytic activity of USP46 is involved in potentiating the Wnt pathway. However, it still remains to be confirmed that the $USP46^{C44S}$ mutant is incapable of deubiquitylating LRP6. One way to demonstrate this would be with overexpression of the mutant followed by an *in vivo* ubiquitylation assay. To ensure that this is a direct effect on LRP6 ubiquitylation, the ideal experiment would be to immunoprecipitate ubiquitylated LRP6 from cells and perform an *in vitro* deubiquitylation assay using purified WDR20, UAF1, and USP46 or $USP46^{C44S}$. This would confirm that USP46 is a bona fide deubiquitylase for LRP6.

Based on my biotinylation and immunoprecipitation experiments, it is clear that overexpression of the USP46 complex can interact with and increase cell-surface levels of LRP6. It is possible that the USP46 complex could mediate this through interactions

with another protein that interacts with LRP6. I can determine if the components of the USP46 complex closely bind LRP6 by performing a proximity ligation assay (PLA) as successful PLAs typically require the proteins to have a distance of 40 nm or less. This would also allow us to visualize the localization of this interaction and determine if it is indeed at the plasma membrane. Another way to assess recruitment would be to perform a CRISPR-mediated knock-in of a C-terminal Halo tag on the endogenous LRP6 gene and overexpress members of the USP46 complex that have been tagged with a SNAP tag. Following treatment with Halo and SNAP ligands that are attached to fluorophores, we would treat with Wnt ligand and perform live cell imaging to visualize Wnt-dependent recruitment of the USP46 complex to the LRP6 co-receptor. This would allow us to determine if activation of the Wnt pathway promotes an increase in recruitment of the USP46 complex to LRP6 co-receptors to drive receptor availability.

Our data supports the idea that the USP46 complex “prunes” LRP6 prior to its assembly into signalosomes. Signalosomes contain LRP6 and phospho-LRP6 aggregates that are in higher molecular weight fractions following sucrose density gradient ultracentrifugation (Bilic et al., 2007; Kim et al., 2013). It is not known whether ubiquitylated LRP6 exists in signalosomes. To address this, I would need perform to sucrose density gradient ultracentrifugation on lysates from cells treated with or without Wnt ligand and perform immunoprecipitations using MBP-tagged tandem ubiquitin binding entity (TUBE) protein conjugated to beads from pooled light fractions and heavy fractions, respectively. TUBE protein recognizes and binds endogenous ubiquitin chains, which makes it a powerful tool in studying endogenous ubiquitylation activity (Yoshida et al., 2015). Second, I have shown evidence that the USP46 complex is not a

component of signalosomes. To further confirm this, I would need to perform to sucrose density gradient ultracentrifugation on lysates from cells expressing the USP46 complex treated with or without Wnt ligand and perform immunoprecipitations of LRP6 from pooled light fractions and heavy fractions, respectively, to look for binding of the USP46 complex. If the USP46 complex binds LRP6 outside of signalosomes, I expect the USP46 complex to co-immunoprecipitate with LRP6 mostly in the light fractions. If the results show that the USP46 complex associates with ubiquitylated LRP6 outside of signalosomes, the next question to ask is whether the USP46 complex is necessary for formation of these signalosomes. I can accomplish this by either siRNA knockdown of USP46 or generate a USP46 CRISPR interference (CRISPRi) cell line and perform sucrose density gradient ultracentrifugation experiments to assess signalosome formation. This work would provide more mechanistic insight into how the USP46 complex regulates LRP6 assembly into signalosomes.

Our studies focused on LRP6 co-receptors, but many E3s and DUBs identified for the Wnt receptors focused primarily on Frizzleds (Hao et al., 2012; Koo et al., 2012; Madan et al., 2016). It is possible that the USP46 complex could also bind and deubiquitylate Frizzled receptors. This could be determined with a simple co-immunoprecipitation and *in vivo* ubiquitylation assay.

I have shown that the USP46 complex can counter RNF43-mediated ubiquitylation of LRP6, but it is possible that the USP46 can counter LRP6 ubiquitylation by another unknown E3 as well. While RNF43/ZNRF3 ubiquitylates Wnt receptors and has significant roles in Wnt signaling in vertebrates, there is no RNF43/ZNRF3 homolog in *Drosophila*. In contrast, the homolog for USP46 in *Drosophila* is USP12-46 and as

mentioned previously, regulates Arrow/LRP6 during active Wg/Wnt signaling. Thus, there is likely to be an as yet unidentified E3 that targets Arrow/LRP6 in *Drosophila*. The E3 ITCH (homolog in *Drosophila* is Su(dx)) has been shown to ubiquitylate LRP6 at its extracellular LDLR repeat regions and has also been shown to ubiquitylate DVL to negatively regulate Wnt signaling (Vijayakumar et al., 2017; Wei et al., 2012). I could test if the USP46 complex can counter ITCH-mediated LRP6 ubiquitylation with an *in vivo* His-ubiquitylation assay, but it is very possible that out of the hundreds of E3s, there is another evolutionarily conserved E3 that can ubiquitylate LRP6.

Previously, it was shown that DVL serves as an adaptor for RNF43/ZNRF3 in recognizing the Wnt receptors as their substrates (Jiang et al., 2015). It is not clear if the USP46 complex also requires DVL to bind and recognize LRP6 as its substrate. It is thought that the scaffolding proteins, WDR20 and UAF1, in the USP46 complex bind USP46 to increase the catalytic activity of USP46 and are not necessarily involved in substrate recognition (Faesen et al., 2011; Yin et al., 2015). If WDR20 and UAF1 are not involved in substrate recognition, then it is possible that the ubiquitin modification on LRP6 is recognized by USP46 alone. Alternatively, the USP46 complex could be recruited to LRP6 through DVL. We could explore this option using a DVL triple knockout (DVLTKO) cell line where all three isoforms have been knocked out using CRISPR-mediated gene editing. Using the DVLTKO cell line, we would overexpress the USP46 complex and immunoprecipitate the complex to assess LRP6 interaction.

The focus of our work is mainly on the role of the USP46 complex in canonical Wnt signaling, but it remains to be determined whether the USP46 complex regulates or can be regulated by RSPO enhancement of Wnt signaling. RSPO enhances Wnt

signaling by inhibiting RNF43/ZNRF3 through its binding to the E3s and the leucine rich repeat containing G protein-coupled receptors (LGRs) (de Lau et al., 2014). There is evidence that RSPO binds LGR4 which regulates the IQ motif containing GTPase Activating Protein 1 (IQGAP1) to potentiate canonical Wnt signaling (Carmon et al., 2014). Using BioGRID, which is a database of curated interactions, one of the proteins that interacts with USP46 was shown to be IQGAP1 (Oughtred et al., 2021). As mentioned earlier in this section, the USP46 complex may use an adaptor to recognize its substrate and it is possible that the USP46 complex may use IQGAP1 to recognize ubiquitylated LRP6 as its substrate. If this is the case, then the USP46 complex may directly bridge signaling through RSPO and canonical Wnt signaling.

REFERENCES

1. Aberle, H., Bauer, A., Stappert, J., Kispert, A., and Kemler, R. (1997). beta-catenin is a target for the ubiquitin-proteasome pathway. EMBO J *16*, 3797-3804.

2. Amit, S., Hatzubai, A., Birman, Y., Andersen, J.S., Ben-Shushan, E., Mann, M., Ben-Neriah, Y., and Alkalay, I. (2002). Axin-mediated CKI phosphorylation of beta-catenin at Ser 45: a molecular switch for the Wnt pathway. Genes Dev *16*, 1066-1076.

3. Anthony, C.C., Robbins, D.J., Ahmed, Y., and Lee, E. (2020). Nuclear Regulation of Wnt/beta-Catenin Signaling: It's a Complex Situation. Genes (Basel) *11*.

4. Ashkenazi, A., and Dixit, V.M. (1998). Death receptors: signaling and modulation. Science *281*, 1305-1308.

5. Bafico, A., Liu, G., Yaniv, A., Gazit, A., and Aaronson, S.A. (2001). Novel mechanism of Wnt signalling inhibition mediated by Dickkopf-1 interaction with LRP6/Arrow. Nat Cell Biol *3*, 683-686.

6. Baig-Lewis, S., Peterson-Nedry, W., and Wehrli, M. (2007). Wingless/Wnt signal transduction requires distinct initiation and amplification steps that both depend on Arrow/LRP. Dev Biol *306*, 94-111.

7. Baker, N.E. (1987). Molecular cloning of sequences from wingless, a segment polarity gene in Drosophila: the spatial distribution of a transcript in embryos. EMBO J *6*, 1765-1773.

8. Banziger, C., Soldini, D., Schutt, C., Zipperlen, P., Hausmann, G., and Basler, K. (2006). Wntless, a conserved membrane protein dedicated to the secretion of Wnt proteins from signaling cells. Cell *125*, 509-522.

9. Bao, J., Zheng, J.J., and Wu, D. (2012). The structural basis of DKK-mediated inhibition of Wnt/LRP signaling. Sci Signal *5*, pe22.

10. Barkett, M., Xue, D., Horvitz, H.R., and Gilmore, T.D. (1997). Phosphorylation of I B- Inhibits Its Cleavage by Caspase CPP32 in Vitro. Journal of Biological Chemistry *272*, 29419-29422.

11. Bartscherer, K., Pelte, N., Ingelfinger, D., and Boutros, M. (2006). Secretion of Wnt ligands requires Evi, a conserved transmembrane protein. Cell *125*, 523-533.

12. Basham, K.J., Rodriguez, S., Turcu, A.F., Lerario, A.M., Logan, C.Y., Rysztak, M.R., Gomez-Sanchez, C.E., Breault, D.T., Koo, B.K., Clevers, H.*, et al.* (2019). A ZNRF3-dependent Wnt/beta-catenin signaling gradient is required for adrenal homeostasis. Genes Dev *33*, 209-220.

13. Behrens, J., von Kries, J.P., Kuhl, M., Bruhn, L., Wedlich, D., Grosschedl, R., and Birchmeier, W. (1996). Functional interaction of beta-catenin with the transcription factor LEF-1. Nature *382*, 638-642.

14. Beurel, E., Grieco, S.F., and Jope, R.S. (2015). Glycogen synthase kinase-3 (GSK3): regulation, actions, and diseases. Pharmacol Ther *148*, 114-131.

15. Bhanot, P., Brink, M., Samos, C.H., Hsieh, J.C., Wang, Y., Macke, J.P., Andrew, D., Nathans, J., and Nusse, R. (1996). A new member of the frizzled family from Drosophila functions as a Wingless receptor. Nature *382*, 225-230.

16. Bijur, G.N., and Jope, R.S. (2001). Proapoptotic stimuli induce nuclear accumulation of glycogen synthase kinase-3 beta. J Biol Chem *276*, 37436-37442.

17. Bilic, J., Huang, Y.L., Davidson, G., Zimmermann, T., Cruciat, C.M., Bienz, M., and Niehrs, C. (2007). Wnt induces LRP6 signalosomes and promotes dishevelled-dependent LRP6 phosphorylation. Science *316*, 1619-1622.

18. Billmann, M., Chaudhary, V., ElMaghraby, M.F., Fischer, B., and Boutros, M. (2018). Widespread Rewiring of Genetic Networks upon Cancer Signaling Pathway Activation. Cell Syst *6*, 52-64 e54.

19. Blair, S.S. (1994). A role for the segment polarity gene shaggy-zeste white 3 in the specification of regional identity in the developing wing of Drosophila. Dev Biol *162*, 229-244.

20. Bourhis, E., Tam, C., Franke, Y., Bazan, J.F., Ernst, J., Hwang, J., Costa, M., Cochran, A.G., and Hannoush, R.N. (2010). Reconstitution of a frizzled8.Wnt3a.LRP6 signaling complex reveals multiple Wnt and Dkk1 binding sites on LRP6. J Biol Chem *285*, 9172-9179.

21. Bovolenta, P., Esteve, P., Ruiz, J.M., Cisneros, E., and Lopez-Rios, J. (2008). Beyond Wnt inhibition: new functions of secreted Frizzled-related proteins in development and disease. J Cell Sci *121*, 737-746.

22. Brantjes, H., Roose, J., van De Wetering, M., and Clevers, H. (2001). All Tcf HMG box transcription factors interact with Groucho-related co-repressors. Nucleic Acids Res *29*, 1410-1419.

23. Cabrera, C.V., Alonso, M.C., Johnston, P., Phillips, R.G., and Lawrence, P.A. (1987). Phenocopies induced with antisense RNA identify the wingless gene. Cell *50*, 659-663.

24. Cadigan, K.M., and Waterman, M.L. (2012). TCF/LEFs and Wnt signaling in the nucleus. Cold Spring Harb Perspect Biol *4*.

25. Callow, M.G., Tran, H., Phu, L., Lau, T., Lee, J., Sandoval, W.N., Liu, P.S., Bheddah, S., Tao, J., Lill, J.R.*, et al.* (2011). Ubiquitin ligase RNF146 regulates tankyrase and Axin to promote Wnt signaling. PLoS One *6*, e22595.

26. Cancer Genome Atlas, N. (2012). Comprehensive molecular characterization of human colon and rectal cancer. Nature *487*, 330-337.

27. Cancer Genome Atlas Research, N., Weinstein, J.N., Collisson, E.A., Mills, G.B., Shaw, K.R.M., Ozenberger, B.A., Ellrott, K., Shmulevich, I., Sander, C., and Stuart, J.M. (2013). The Cancer Genome Atlas Pan-Cancer analysis project. Nature Genetics *45*, 1113-1120.

28. Carmon, K.S., Gong, X., Yi, J., Thomas, A., and Liu, Q. (2014). RSPO-LGR4 functions via IQGAP1 to potentiate Wnt signaling. Proc Natl Acad Sci U S A *111*, E1221-1229.

29. Cavallo, R.A., Cox, R.T., Moline, M.M., Roose, J., Polevoy, G.A., Clevers, H., Peifer, M., and Bejsovec, A. (1998). Drosophila Tcf and Groucho interact to repress Wingless signalling activity. Nature *395*, 604-608.

30. Chacon-Martinez, C.A., Koester, J., and Wickstrom, S.A. (2018). Signaling in the stem cell niche: regulating cell fate, function and plasticity. Development *145*.

31. Chandrashekar, D.S., Bashel, B., Balasubramanya, S.A.H., Creighton, C.J., Ponce-Rodriguez, I., Chakravarthi, B., and Varambally, S. (2017). UALCAN: A Portal for Facilitating Tumor Subgroup Gene Expression and Survival Analyses. Neoplasia *19*, 649-658.

32. Chen, S., Bubeck, D., MacDonald, B.T., Liang, W.X., Mao, J.H., Malinauskas, T., Llorca, O., Aricescu, A.R., Siebold, C., He, X.*, et al.* (2011). Structural and functional studies of LRP6 ectodomain reveal a platform for Wnt signaling. Dev Cell *21*, 848-861.

33. Chitalia, V.C., Foy, R.L., Bachschmid, M.M., Zeng, L., Panchenko, M.V., Zhou, M.I., Bharti, A., Seldin, D.C., Lecker, S.H., Dominguez, I.*, et al.* (2008). Jade-1 inhibits Wnt signalling by ubiquitylating beta-catenin and mediates Wnt pathway inhibition by pVHL. Nat Cell Biol *10*, 1208-1216.

34. Ciechanover, A., Elias, S., Heller, H., and Hershko, A. (1982). "Covalent affinity" purification of ubiquitin-activating enzyme. J Biol Chem *257*, 2537-2542.

35. Clevers, H., Loh, K.M., and Nusse, R. (2014). Stem cell signaling. An integral program for tissue renewal and regeneration: Wnt signaling and stem cell control. Science *346*, 1248012.

36. Clevers, H., and Nusse, R. (2012). Wnt/beta-catenin signaling and disease. Cell *149*, 1192-1205.

37. Cline, G.W., Johnson, K., Regittnig, W., Perret, P., Tozzo, E., Xiao, L., Damico, C., and Shulman, G.I. (2002). Effects of a novel glycogen synthase kinase-3 inhibitor on insulin-stimulated glucose metabolism in Zucker diabetic fatty (fa/fa) rats. Diabetes *51*, 2903-2910.

38. Cohen, P., and Goedert, M. (2004). GSK3 inhibitors: development and therapeutic potential. Nat Rev Drug Discov *3*, 479-487.

39. Cole, A.R., Knebel, A., Morrice, N.A., Robertson, L.A., Irving, A.J., Connolly, C.N., and Sutherland, C. (2004). GSK-3 phosphorylation of the Alzheimer

epitope within collapsin response mediator proteins regulates axon elongation in primary neurons. J Biol Chem *279*, 50176-50180.

40. Cong, F., Schweizer, L., and Varmus, H. (2004). Wnt signals across the plasma membrane to activate the beta-catenin pathway by forming oligomers containing its receptors, Frizzled and LRP. Development *131*, 5103-5115.

41. Cong, F., and Varmus, H. (2004). Nuclear-cytoplasmic shuttling of Axin regulates subcellular localization of beta-catenin. Proc Natl Acad Sci U S A *101*, 2882-2887.

42. Coudreuse, D., and Korswagen, H.C. (2007). The making of Wnt: new insights into Wnt maturation, sorting and secretion. Development *134*, 3-12.

43. Cselenyi, C.S., Jernigan, K.K., Tahinci, E., Thorne, C.A., Lee, L.A., and Lee, E. (2008). LRP6 transduces a canonical Wnt signal independently of Axin degradation by inhibiting GSK3's phosphorylation of beta-catenin. Proc Natl Acad Sci U S A *105*, 8032-8037.

44. Damgaard, R.B., Nachbur, U., Yabal, M., Wong, W.W., Fiil, B.K., Kastirr, M., Rieser, E., Rickard, J.A., Bankovacki, A., Peschel, C.*, et al.* (2012). The ubiquitin ligase XIAP recruits LUBAC for NOD2 signaling in inflammation and innate immunity. Mol Cell *46*, 746-758.

45. Daniels, D.L., and Weis, W.I. (2005). Beta-catenin directly displaces Groucho/TLE repressors from Tcf/Lef in Wnt-mediated transcription activation. Nat Struct Mol Biol *12*, 364-371.

46. DaRosa, P.A., Wang, Z., Jiang, X., Pruneda, J.N., Cong, F., Klevit, R.E., and Xu, W. (2015). Allosteric activation of the RNF146 ubiquitin ligase by a poly(ADP-ribosyl)ation signal. Nature *517*, 223-226.

47. Davidson, G., Wu, W., Shen, J., Bilic, J., Fenger, U., Stannek, P., Glinka, A., and Niehrs, C. (2005). Casein kinase 1 gamma couples Wnt receptor activation to cytoplasmic signal transduction. Nature *438*, 867-872.

48. Davis, M.E. (2016). Glioblastoma: Overview of Disease and Treatment. Clin J Oncol Nurs *20*, S2-8.

49. De Ferrari, G.V., and Moon, R.T. (2006). The ups and downs of Wnt signaling in prevalent neurological disorders. Oncogene *25*, 7545-7553.

50. de Lau, W., Peng, W.C., Gros, P., and Clevers, H. (2014). The R-spondin/Lgr5/Rnf43 module: regulator of Wnt signal strength. Genes Dev *28*, 305-316.

51. Derakhshan, A., Chen, Z., and Van Waes, C. (2017). Therapeutic Small Molecules Target Inhibitor of Apoptosis Proteins in Cancers with Deregulation of Extrinsic and Intrinsic Cell Death Pathways. Clin Cancer Res *23*, 1379-1387.

52. Deshaies, R.J., and Joazeiro, C.A. (2009). RING domain E3 ubiquitin ligases. Annu Rev Biochem *78*, 399-434.

53. Deveraux, Q.L., Leo, E., Stennicke, H.R., Welsh, K., Salvesen, G.S., and Reed, J.C. (1999). Cleavage of human inhibitor of apoptosis protein XIAP results in fragments with distinct specificities for caspases. EMBO J *18*, 5242-5251.

54. Ding, Y., Zhang, Y., Xu, C., Tao, Q.H., and Chen, Y.G. (2013). HECT domain-containing E3 ubiquitin ligase NEDD4L negatively regulates Wnt signaling by targeting dishevelled for proteasomal degradation. J Biol Chem *288*, 8289-8298.

55. Ettenberg, S.A., Charlat, O., Daley, M.P., Liu, S., Vincent, K.J., Stuart, D.D., Schuller, A.G., Yuan, J., Ospina, B., Green, J.*, et al.* (2010). Inhibition of tumorigenesis driven by different Wnt proteins requires blockade of distinct ligand-binding regions by LRP6 antibodies. Proc Natl Acad Sci U S A *107*, 15473-15478.

56. Faesen, A.C., Luna-Vargas, M.P., Geurink, P.P., Clerici, M., Merkx, R., van Dijk, W.J., Hameed, D.S., El Oualid, F., Ovaa, H., and Sixma, T.K. (2011). The differential modulation of USP activity by internal regulatory domains, interactors and eight ubiquitin chain types. Chem Biol *18*, 1550-1561.

57. Feltham, R., Bettjeman, B., Budhidarmo, R., Mace, P.D., Shirley, S., Condon, S.M., Chunduru, S.K., McKinlay, M.A., Vaux, D.L., Silke, J.*, et al.* (2011). Smac mimetics activate the E3 ligase activity of cIAP1 protein by promoting RING domain dimerization. J Biol Chem *286*, 17015-17028.

58. Fevr, T., Robine, S., Louvard, D., and Huelsken, J. (2007). Wnt/beta-catenin is essential for intestinal homeostasis and maintenance of intestinal stem cells. Mol Cell Biol *27*, 7551-7559.

59. Finley, D., and Chau, V. (1991). Ubiquitination. Annual Review of Cell Biology *7*, 25-69.

60. Foulquier, S., Daskalopoulos, E.P., Lluri, G., Hermans, K.C.M., Deb, A., and Blankesteijn, W.M. (2018). WNT Signaling in Cardiac and Vascular Disease. Pharmacol Rev *70*, 68-141.

61. Galban, S., and Duckett, C.S. (2010). XIAP as a ubiquitin ligase in cellular signaling. Cell Death Differ *17*, 54-60.

62. Gerhart, J. (1999). 1998 Warkany lecture: signaling pathways in development. Teratology *60*, 226-239.

63. Giannakis, M., Hodis, E., Jasmine Mu, X., Yamauchi, M., Rosenbluh, J., Cibulskis, K., Saksena, G., Lawrence, M.S., Qian, Z.R., Nishihara, R.*, et al.* (2014). RNF43 is frequently mutated in colorectal and endometrial cancers. Nat Genet *46*, 1264-1266.

64. Gomperts, B.D., Tatham, P.E.R., and Kramer, I.M. (2009). Signal transduction (Burlington, M.A. ; London: Elsevier/Academic Press,), pp. xxvii, 810 p.

65. Graham, T.A., Weaver, C., Mao, F., Kimelman, D., and Xu, W. (2000). Crystal structure of a beta-catenin/Tcf complex. Cell *103*, 885-896.

66. Griffin, J.N., Del Viso, F., Duncan, A.R., Robson, A., Hwang, W., Kulkarni, S., Liu, K.J., and Khokha, M.K. (2018). RAPGEF5 Regulates Nuclear Translocation of beta-Catenin. Dev Cell *44*, 248-260 e244.

67. Gyrd-Hansen, M., Darding, M., Miasari, M., Santoro, M.M., Zender, L., Xue, W., Tenev, T., da Fonseca, P.C., Zvelebil, M., Bujnicki, J.M.*, et al.* (2008). IAPs contain an evolutionarily conserved ubiquitin-binding domain that regulates NF-kappaB as well as cell survival and oncogenesis. Nat Cell Biol *10*, 1309-1317.

68. Haas, A.L., Warms, J.V., Hershko, A., and Rose, I.A. (1982). Ubiquitin-activating enzyme. Mechanism and role in protein-ubiquitin conjugation. J Biol Chem *257*, 2543-2548.

69. Handley, P.M., Mueckler, M., Siegel, N.R., Ciechanover, A., and Schwartz, A.L. (1991). Molecular cloning, sequence, and tissue distribution of the human ubiquitin-activating enzyme E1. Proc Natl Acad Sci U S A *88*, 258-262.

70. Hanson, A.J., Wallace, H.A., Freeman, T.J., Beauchamp, R.D., Lee, L.A., and Lee, E. (2012). XIAP monoubiquitylates Groucho/TLE to promote canonical Wnt signaling. Mol Cell *45*, 619-628.

71. Hao, H.X., Xie, Y., Zhang, Y., Charlat, O., Oster, E., Avello, M., Lei, H., Mickanin, C., Liu, D., Ruffner, H.*, et al.* (2012). ZNRF3 promotes Wnt receptor turnover in an R-spondin-sensitive manner. Nature *485*, 195-200.

72. Hart, M., Concordet, J.P., Lassot, I., Albert, I., del los Santos, R., Durand, H., Perret, C., Rubinfeld, B., Margottin, F., Benarous, R.*, et al.* (1999). The F-box protein beta-TrCP associates with phosphorylated beta-catenin and regulates its activity in the cell. Curr Biol *9*, 207-210.

73. He, X., Semenov, M., Tamai, K., and Zeng, X. (2004). LDL receptor-related proteins 5 and 6 in Wnt/beta-catenin signaling: arrows point the way. Development *131*, 1663-1677.

74. Heasman, J. (2006). Patterning the early Xenopus embryo. Development *133*, 1205-1217.

75. Henderson, B.R., and Fagotto, F. (2002). The ins and outs of APC and beta-catenin nuclear transport. EMBO Rep *3*, 834-839.

76. Hendriksen, J., Jansen, M., Brown, C.M., van der Velde, H., van Ham, M., Galjart, N., Offerhaus, G.J., Fagotto, F., and Fornerod, M. (2008). Plasma membrane recruitment of dephosphorylated beta-catenin upon activation of the Wnt pathway. J Cell Sci *121*, 1793-1802.

77. Hicke, L. (2001). Protein regulation by monoubiquitin. Nat Rev Mol Cell Biol *2*, 195-201.

78. Hirai, H., Matoba, K., Mihara, E., Arimori, T., and Takagi, J. (2019). Crystal structure of a mammalian Wnt-frizzled complex. Nat Struct Mol Biol *26*, 372-379.

79. Hodul, M., Dahlberg, C.L., and Juo, P. (2017). Function of the Deubiquitinating Enzyme USP46 in the Nervous System and Its Regulation by WD40-Repeat Proteins. Front Synaptic Neurosci *9*, 16.

80. Holley, C.L., Olson, M.R., Colon-Ramos, D.A., and Kornbluth, S. (2002). Reaper eliminates IAP proteins through stimulated IAP degradation and generalized translational inhibition. Nat Cell Biol *4*, 439-444.

81. Hornbeck, P.V., Zhang, B., Murray, B., Kornhauser, J.M., Latham, V., and Skrzypek, E. (2015). PhosphoSitePlus, 2014: mutations, PTMs and recalibrations. Nucleic Acids Res *43*, D512-520.

82. Huang, S.M., Mishina, Y.M., Liu, S., Cheung, A., Stegmeier, F., Michaud, G.A., Charlat, O., Wiellette, E., Zhang, Y., Wiessner, S.*, et al.* (2009a). Tankyrase inhibition stabilizes axin and antagonizes Wnt signalling. Nature *461*, 614-620.

83. Huang, X., Langelotz, C., Hetfeld-Pechoc, B.K., Schwenk, W., and Dubiel, W. (2009b). The COP9 signalosome mediates beta-catenin degradation by deneddylation and blocks adenomatous polyposis coli destruction via USP15. J Mol Biol *391*, 691-702.

84. Hunter, T. (2007). The age of crosstalk: phosphorylation, ubiquitination, and beyond. Mol Cell *28*, 730-738.

85. Ismail, I.H., Gagne, J.P., Genois, M.M., Strickfaden, H., McDonald, D., Xu, Z., Poirier, G.G., Masson, J.Y., and Hendzel, M.J. (2015). The RNF138 E3 ligase displaces Ku to promote DNA end resection and regulate DNA repair pathway choice. Nat Cell Biol *17*, 1446-1457.

86. Jackson, H., Granger, D., Jones, G., Anderson, L., Friel, S., Rycroft, D., Fieles, W., Tunstead, J., Steward, M., Wattam, T.*, et al.* (2016). Novel Bispecific Domain Antibody to LRP6 Inhibits Wnt and R-spondin Ligand-Induced Wnt Signaling and Tumor Growth. Mol Cancer Res *14*, 859-868.

87. Janda, C.Y., Waghray, D., Levin, A.M., Thomas, C., and Garcia, K.C. (2012). Structural basis of Wnt recognition by Frizzled. Science *337*, 59-64.

88. Ji, L., Jiang, B., Jiang, X., Charlat, O., Chen, A., Mickanin, C., Bauer, A., Xu, W., Yan, X., and Cong, F. (2017). The SIAH E3 ubiquitin ligases promote Wnt/beta-catenin signaling through mediating Wnt-induced Axin degradation. Genes Dev *31*, 904-915.

89. Jiang, X., Charlat, O., Zamponi, R., Yang, Y., and Cong, F. (2015). Dishevelled promotes Wnt receptor degradation through recruitment of ZNRF3/RNF43 E3 ubiquitin ligases. Mol Cell *58*, 522-533.

90. Jiang, X., Hao, H.X., Growney, J.D., Woolfenden, S., Bottiglio, C., Ng, N., Lu, B., Hsieh, M.H., Bagdasarian, L., Meyer, R.*, et al.* (2013). Inactivating mutations of RNF43 confer Wnt dependency in pancreatic ductal adenocarcinoma. Proc Natl Acad Sci U S A *110*, 12649-12654.

91. Jung, H., Kim, B.G., Han, W.H., Lee, J.H., Cho, J.Y., Park, W.S., Maurice, M.M., Han, J.K., Lee, M.J., Finley, D.*, et al.* (2013). Deubiquitination of Dishevelled by Usp14 is required for Wnt signaling. Oncogenesis *2*, e64.

92. Kadowaki, T., Wilder, E., Klingensmith, J., Zachary, K., and Perrimon, N. (1996). The segment polarity gene porcupine encodes a putative multitransmembrane protein involved in Wingless processing. Genes Dev *10*, 3116-3128.

93. Kawano, Y., and Kypta, R. (2003). Secreted antagonists of the Wnt signalling pathway. J Cell Sci *116*, 2627-2634.

94. Kee, Y., Yang, K., Cohn, M.A., Haas, W., Gygi, S.P., and D'Andrea, A.D. (2010). WDR20 regulates activity of the USP12 x UAF1 deubiquitinating enzyme complex. J Biol Chem *285*, 11252-11257.

95. Kim, I., Pan, W., Jones, S.A., Zhang, Y., Zhuang, X., and Wu, D. (2013). Clathrin and AP2 are required for PtdIns(4,5)P2-mediated formation of LRP6 signalosomes. J Cell Biol *200*, 419-428.

96. Kim, J., Han, W., Park, T., Kim, E.J., Bang, I., Lee, H.S., Jeong, Y., Roh, K., Kim, J., Kim, J.S.*, et al.* (2020). Sclerostin inhibits Wnt signaling through tandem interaction with two LRP6 ectodomains. Nat Commun *11*, 5357.

97. Kimelman, D., and Xu, W. (2006). beta-catenin destruction complex: insights and questions from a structural perspective. Oncogene *25*, 7482-7491.

98. Kinzler, K.W., Nilbert, M.C., Su, L.K., Vogelstein, B., Bryan, T.M., Levy, D.B., Smith, K.J., Preisinger, A.C., Hedge, P., McKechnie, D.*, et al.* (1991). Identification of FAP locus genes from chromosome 5q21. Science *253*, 661-665.

99. Kinzler, K.W., and Vogelstein, B. (1996). Lessons from hereditary colorectal cancer. Cell *87*, 159-170.

100. Klaus, A., and Birchmeier, W. (2008). Wnt signalling and its impact on development and cancer. Nat Rev Cancer *8*, 387-398.

101. Klingensmith, J., Nusse, R., and Perrimon, N. (1994). The Drosophila segment polarity gene dishevelled encodes a novel protein required for response to the wingless signal. Genes Dev *8*, 118-130.

102. Komander, D. (2009). The emerging complexity of protein ubiquitination. Biochem Soc Trans *37*, 937-953.

103. Komander, D., Clague, M.J., and Urbe, S. (2009). Breaking the chains: structure and function of the deubiquitinases. Nat Rev Mol Cell Biol *10*, 550-563.

104. Komekado, H., Yamamoto, H., Chiba, T., and Kikuchi, A. (2007). Glycosylation and palmitoylation of Wnt-3a are coupled to produce an active form of Wnt-3a. Genes Cells *12*, 521-534.

105. Koo, B.K., Spit, M., Jordens, I., Low, T.Y., Stange, D.E., van de Wetering, M., van Es, J.H., Mohammed, S., Heck, A.J., Maurice, M.M.*, et al.* (2012). Tumour suppressor RNF43 is a stem-cell E3 ligase that induces endocytosis of Wnt receptors. Nature *488*, 665-669.

106. Korinek, V., Barker, N., Moerer, P., van Donselaar, E., Huls, G., Peters, P.J., and Clevers, H. (1998). Depletion of epithelial stem-cell compartments in the small intestine of mice lacking Tcf-4. Nat Genet *19*, 379-383.

107. Kramps, T., Peter, O., Brunner, E., Nellen, D., Froesch, B., Chatterjee, S., Murone, M., Zullig, S., and Basler, K. (2002). Wnt/wingless signaling requires BCL9/legless-mediated recruitment of pygopus to the nuclear beta-catenin-TCF complex. Cell *109*, 47-60.

108. Krieghoff, E., Behrens, J., and Mayr, B. (2006). Nucleo-cytoplasmic distribution of beta-catenin is regulated by retention. J Cell Sci *119*, 1453-1463.

109. LaCasse, E.C., Mahoney, D.J., Cheung, H.H., Plenchette, S., Baird, S., and Korneluk, R.G. (2008). IAP-targeted therapies for cancer. Oncogene *27*, 6252-6275.

110. Latres, E., Chiaur, D.S., and Pagano, M. (1999). The human F box protein beta-Trcp associates with the Cul1/Skp1 complex and regulates the stability of beta-catenin. Oncogene *18*, 849-854.

111. Lebensohn, A.M., Dubey, R., Neitzel, L.R., Tacchelly-Benites, O., Yang, E., Marceau, C.D., Davis, E.M., Patel, B.B., Bahrami-Nejad, Z., Travaglini, K.J.*, et al.* (2016). Comparative genetic screens in human cells reveal new regulatory mechanisms in WNT signaling. Elife *5*.

112. Lee, E., Salic, A., Kruger, R., Heinrich, R., and Kirschner, M.W. (2003). The roles of APC and Axin derived from experimental and theoretical analysis of the Wnt pathway. PLoS Biol *1*, E10.

113. Lento, W., Congdon, K., Voermans, C., Kritzik, M., and Reya, T. (2013). Wnt signaling in normal and malignant hematopoiesis. Cold Spring Harb Perspect Biol *5*.

114. Li, H., Lim, K.S., Kim, H., Hinds, T.R., Jo, U., Mao, H., Weller, C.E., Sun, J., Chatterjee, C., D'Andrea, A.D.*, et al.* (2016a). Allosteric Activation of Ubiquitin-Specific Proteases by beta-Propeller Proteins UAF1 and WDR20. Mol Cell *63*, 249-260.

115. Li, H., Lim, K.S., Kim, H., Hinds, T.R., Jo, U., Mao, H., Weller, C.E., Sun, J., Chatterjee, C., D'Andrea, A.D.*, et al.* (2016b). Allosteric Activation of Ubiquitin-Specific Proteases by beta-Propeller Proteins UAF1 and WDR20. Mol Cell *63*, 249-260.

116. Li, V.S., Ng, S.S., Boersema, P.J., Low, T.Y., Karthaus, W.R., Gerlach, J.P., Mohammed, S., Heck, A.J., Maurice, M.M., Mahmoudi, T.*, et al.* (2012). Wnt signaling through inhibition of beta-catenin degradation in an intact Axin1 complex. Cell *149*, 1245-1256.

117. Li, X., Zhang, Y., Kang, H., Liu, W., Liu, P., Zhang, J., Harris, S.E., and Wu, D. (2005). Sclerostin binds to LRP5/6 and antagonizes canonical Wnt signaling. J Biol Chem *280*, 19883-19887.

118. Licchesi, J.D., Mieszczanek, J., Mevissen, T.E., Rutherford, T.J., Akutsu, M., Virdee, S., El Oualid, F., Chin, J.W., Ovaa, H., Bienz, M.*, et al.* (2012). An ankyrin-repeat ubiquitin-binding domain determines TRABID's specificity for atypical ubiquitin chains. Nat Struct Mol Biol *19*, 62-71.

119. Lim, X., and Nusse, R. (2013). Wnt signaling in skin development, homeostasis, and disease. Cold Spring Harb Perspect Biol *5*.

120. Liu, C., Kato, Y., Zhang, Z., Do, V.M., Yankner, B.A., and He, X. (1999). beta-Trcp couples beta-catenin phosphorylation-degradation and regulates Xenopus axis formation. Proc Natl Acad Sci U S A *96*, 6273-6278.

121. Liu, C., Li, Y., Semenov, M., Han, C., Baeg, G.H., Tan, Y., Zhang, Z., Lin, X., and He, X. (2002). Control of beta-catenin phosphorylation/degradation by a dual-kinase mechanism. Cell *108*, 837-847.

122. Liu, C.C., Prior, J., Piwnica-Worms, D., and Bu, G. (2010). LRP6 overexpression defines a class of breast cancer subtype and is a target for therapy. Proc Natl Acad Sci U S A *107*, 5136-5141.

123. Liu, J., Stevens, J., Rote, C.A., Yost, H.J., Hu, Y., Neufeld, K.L., White, R.L., and Matsunami, N. (2001). Siah-1 mediates a novel beta-catenin degradation pathway linking p53 to the adenomatous polyposis coli protein. Mol Cell *7*, 927-936.

124. Liu, X., Rubin, J.S., and Kimmel, A.R. (2005). Rapid, Wnt-induced changes in GSK3beta associations that regulate beta-catenin stabilization are mediated by Galpha proteins. Curr Biol *15*, 1989-1997.

125. Logan, C.Y., and Nusse, R. (2004). The Wnt signaling pathway in development and disease. Annu Rev Cell Dev Biol *20*, 781-810.

126. Lu, M., Lin, S.C., Huang, Y., Kang, Y.J., Rich, R., Lo, Y.C., Myszka, D., Han, J., and Wu, H. (2007). XIAP induces NF-kappaB activation via the BIR1/TAB1 interaction and BIR1 dimerization. Mol Cell *26*, 689-702.

127. Lui, T.T., Lacroix, C., Ahmed, S.M., Goldenberg, S.J., Leach, C.A., Daulat, A.M., and Angers, S. (2011). The ubiquitin-specific protease USP34 regulates axin stability and Wnt/beta-catenin signaling. Mol Cell Biol *31*, 2053-2065.

128. Luis, T.C., Ichii, M., Brugman, M.H., Kincade, P., and Staal, F.J. (2012). Wnt signaling strength regulates normal hematopoiesis and its deregulation is involved in leukemia development. Leukemia *26*, 414-421.

129. Luis, T.C., Weerkamp, F., Naber, B.A., Baert, M.R., de Haas, E.F., Nikolic, T., Heuvelmans, S., De Krijger, R.R., van Dongen, J.J., and Staal, F.J. (2009). Wnt3a deficiency irreversibly impairs hematopoietic stem cell self-renewal and leads to defects in progenitor cell differentiation. Blood *113*, 546-554.

130. Ma, P., Yang, X., Kong, Q., Li, C., Yang, S., Li, Y., and Mao, B. (2014). The ubiquitin ligase RNF220 enhances canonical Wnt signaling through USP7-mediated deubiquitination of beta-catenin. Mol Cell Biol *34*, 4355-4366.

131. Ma, W., Chen, M., Kang, H., Steinhart, Z., Angers, S., He, X., and Kirschner, M.W. (2020). Single-molecule dynamics of Dishevelled at the plasma membrane and Wnt pathway activation. Proc Natl Acad Sci U S A *117*, 16690-16701.

132. MacDonald, B.T., and He, X. (2012). Frizzled and LRP5/6 receptors for Wnt/beta-catenin signaling. Cold Spring Harb Perspect Biol *4*.

133. MacDonald, B.T., Tamai, K., and He, X. (2009). Wnt/beta-catenin signaling: components, mechanisms, and diseases. Dev Cell *17*, 9-26.

134. MacDonald, B.T., Yokota, C., Tamai, K., Zeng, X., and He, X. (2008). Wnt signal amplification via activity, cooperativity, and regulation of multiple intracellular PPPSP motifs in the Wnt co-receptor LRP6. J Biol Chem *283*, 16115-16123.

135. MacFarlane, M., Merrison, W., Bratton, S.B., and Cohen, G.M. (2002). Proteasome-mediated degradation of Smac during apoptosis: XIAP promotes Smac ubiquitination in vitro. J Biol Chem *277*, 36611-36616.

136. Madan, B., Walker, M.P., Young, R., Quick, L., Orgel, K.A., Ryan, M., Gupta, P., Henrich, I.C., Ferrer, M., Marine, S.*, et al.* (2016). USP6 oncogene promotes Wnt signaling by deubiquitylating Frizzleds. Proc Natl Acad Sci U S A.

137. Madrzak, J., Fiedler, M., Johnson, C.M., Ewan, R., Knebel, A., Bienz, M., and Chin, J.W. (2015). Ubiquitination of the Dishevelled DIX domain blocks its head-to-tail polymerization. Nat Commun *6*, 6718.

138. Mao, B., Wu, W., Li, Y., Hoppe, D., Stannek, P., Glinka, A., and Niehrs, C. (2001a). LDL-receptor-related protein 6 is a receptor for Dickkopf proteins. Nature *411*, 321-325.

139. Mao, J., Wang, J., Liu, B., Pan, W., Farr, G.H., 3rd, Flynn, C., Yuan, H., Takada, S., Kimelman, D., Li, L.*, et al.* (2001b). Low-density lipoprotein receptor-related protein-5 binds to Axin and regulates the canonical Wnt signaling pathway. Mol Cell *7*, 801-809.

140. Martinez Arias, A. (2003). Wnts as morphogens? The view from the wing of Drosophila. Nat Rev Mol Cell Biol *4*, 321-325.

141. McCord, M., Mukouyama, Y.S., Gilbert, M.R., and Jackson, S. (2017). Targeting WNT Signaling for Multifaceted Glioblastoma Therapy. Front Cell Neurosci *11*, 318.

142. McMahon, A.P., and Moon, R.T. (1989). Ectopic expression of the proto-oncogene int-1 in Xenopus embryos leads to duplication of the embryonic axis. Cell *58*, 1075-1084.

143. McManus, D.C., Lefebvre, C.A., Cherton-Horvat, G., St-Jean, M., Kandimalla, E.R., Agrawal, S., Morris, S.J., Durkin, J.P., and Lacasse, E.C. (2004). Loss of XIAP protein expression by RNAi and antisense approaches sensitizes cancer cells to functionally diverse chemotherapeutics. Oncogene *23*, 8105-8117.

144. Meares, G.P., and Jope, R.S. (2007). Resolution of the nuclear localization mechanism of glycogen synthase kinase-3: functional effects in apoptosis. J Biol Chem *282*, 16989-17001.

145. Merenda, A., Fenderico, N., and Maurice, M.M. (2020). Wnt Signaling in 3D: Recent Advances in the Applications of Intestinal Organoids. Trends Cell Biol *30*, 60-73.

146. Mertins, P., Mani, D.R., Ruggles, K.V., Gillette, M.A., Clauser, K.R., Wang, P., Wang, X., Qiao, J.W., Cao, S., Petralia, F.*, et al.* (2016). Proteogenomics connects somatic mutations to signalling in breast cancer. Nature *534*, 55-62.

147. Metzger, M.B., Hristova, V.A., and Weissman, A.M. (2012). HECT and RING finger families of E3 ubiquitin ligases at a glance. J Cell Sci *125*, 531-537.

148. Mikels, A.J., and Nusse, R. (2006). Wnts as ligands: processing, secretion and reception. Oncogene *25*, 7461-7468.

149. Mosimann, C., Hausmann, G., and Basler, K. (2009). Beta-catenin hits chromatin: regulation of Wnt target gene activation. Nat Rev Mol Cell Biol *10*, 276-286.

150. Mukai, A., Yamamoto-Hino, M., Awano, W., Watanabe, W., Komada, M., and Goto, S. (2010). Balanced ubiquitylation and deubiquitylation of Frizzled regulate cellular responsiveness to Wg/Wnt. EMBO J *29*, 2114-2125.

151. Muratani, M., and Tansey, W.P. (2003a). How the ubiquitin-proteasome system controls transcription. Nat Rev Mol Cell Biol *4*, 192-201.

152. Muratani, M., and Tansey, W.P. (2003b). How the ubiquitin–proteasome system controls transcription. Nature Reviews Molecular Cell Biology *4*, 192-201.

153. Nakatani, Y., Kleffmann, T., Linke, K., Condon, S.M., Hinds, M.G., and Day, C.L. (2013). Regulation of ubiquitin transfer by XIAP, a dimeric RING E3 ligase. Biochem J *450*, 629-638.

154. Narlikar, G.J., Fan, H.Y., and Kingston, R.E. (2002). Cooperation between complexes that regulate chromatin structure and transcription. Cell *108*, 475-487.

155. Nathan, E., and Tzahor, E. (2009). sFRPs: a declaration of (Wnt) independence. Nat Cell Biol *11*, 13.

156. Neitzel, L.R., Spencer, Z.T., Nayak, A., Cselenyi, C.S., Benchabane, H., Youngblood, C.Q., Zouaoui, A., Ng, V., Stephens, L., Hann, T.*, et al.* (2019). Developmental regulation of Wnt signaling by Nagk and the UDP-GlcNAc salvage pathway. Mech Dev *156*, 20-31.

157. Nishisho, I., Nakamura, Y., Miyoshi, Y., Miki, Y., Ando, H., Horii, A., Koyama, K., Utsunomiya, J., Baba, S., and Hedge, P. (1991). Mutations of chromosome 5q21 genes in FAP and colorectal cancer patients. Science *253*, 665-669.

158. Noordermeer, J., Klingensmith, J., Perrimon, N., and Nusse, R. (1994). dishevelled and armadillo act in the wingless signalling pathway in Drosophila. Nature *367*, 80-83.

159. Nusse, R., Brown, A., Papkoff, J., Scambler, P., Shackleford, G., McMahon, A., Moon, R., and Varmus, H. (1991). A new nomenclature for int-1 and related genes: the Wnt gene family. Cell *64*, 231.

160. Nusse, R., and Varmus, H.E. (1982). Many tumors induced by the mouse mammary tumor virus contain a provirus integrated in the same region of the host genome. Cell *31*, 99-109.

161. Nusslein-Volhard, C., and Wieschaus, E. (1980). Mutations affecting segment number and polarity in Drosophila. Nature *287*, 795-801.

162. Oh, E., Akopian, D., and Rape, M. (2018). Principles of Ubiquitin-Dependent Signaling. Annual Review of Cell and Developmental Biology *34*, 137-162.

163. Oughtred, R., Rust, J., Chang, C., Breitkreutz, B.J., Stark, C., Willems, A., Boucher, L., Leung, G., Kolas, N., Zhang, F.*, et al.* (2021). The BioGRID database: A comprehensive biomedical resource of curated protein, genetic, and chemical interactions. Protein Sci *30*, 187-200.

164. Pan, W., Choi, S.C., Wang, H., Qin, Y., Volpicelli-Daley, L., Swan, L., Lucast, L., Khoo, C., Zhang, X., Li, L.*, et al.* (2008). Wnt3a-mediated formation of phosphatidylinositol 4,5-bisphosphate regulates LRP6 phosphorylation. Science *321*, 1350-1353.

165. Patterson, C. (2002). A new gun in town: the U box is a ubiquitin ligase domain. Sci STKE *2002*, pe4.

166. Peng, J. (1991). Appendix A: Solutions and Protocols. In Methods in Cell Biology (Elsevier BV), pp. 657-662.

167. Perrimon, N., and Mahowald, A.P. (1987). Multiple functions of segment polarity genes in Drosophila. Dev Biol *119*, 587-600.

168. Petroski, M.D., and Deshaies, R.J. (2005). Function and regulation of cullin-RING ubiquitin ligases. Nat Rev Mol Cell Biol *6*, 9-20.

169. Piao, S., Lee, S.H., Kim, H., Yum, S., Stamos, J.L., Xu, Y., Lee, S.J., Lee, J., Oh, S., Han, J.K.*, et al.* (2008). Direct inhibition of GSK3beta by the phosphorylated cytoplasmic domain of LRP6 in Wnt/beta-catenin signaling. PLoS One *3*, e4046.

170. Pinson, K.I., Brennan, J., Monkley, S., Avery, B.J., and Skarnes, W.C. (2000). An LDL-receptor-related protein mediates Wnt signalling in mice. Nature *407*, 535-538.

171. Port, F., and Basler, K. (2010). Wnt trafficking: new insights into Wnt maturation, secretion and spreading. Traffic *11*, 1265-1271.

172. Raiborg, C., and Stenmark, H. (2009). The ESCRT machinery in endosomal sorting of ubiquitylated membrane proteins. Nature *458*, 445-452.

173. Riggleman, B., Schedl, P., and Wieschaus, E. (1990). Spatial expression of the Drosophila segment polarity gene armadillo is posttranscriptionally regulated by wingless. Cell *63*, 549-560.

174. Riggleman, B., Wieschaus, E., and Schedl, P. (1989). Molecular analysis of the armadillo locus: uniformly distributed transcripts and a protein with novel internal repeats are associated with a Drosophila segment polarity gene. Genes Dev *3*, 96-113.

175. Rijsewijk, F., Schuermann, M., Wagenaar, E., Parren, P., Weigel, D., and Nusse, R. (1987). The Drosophila homolog of the mouse mammary oncogene int-1 is identical to the segment polarity gene wingless. Cell *50*, 649-657.

176. Ring, D.B., Johnson, K.W., Henriksen, E.J., Nuss, J.M., Goff, D., Kinnick, T.R., Ma, S.T., Reeder, J.W., Samuels, I., Slabiak, T.*, et al.* (2003). Selective glycogen synthase kinase 3 inhibitors potentiate insulin activation of glucose transport and utilization in vitro and in vivo. Diabetes *52*, 588-595.

177. Routledge, D., and Scholpp, S. (2019). Mechanisms of intercellular Wnt transport. Development *146*.

178. Saito-Diaz, K., Benchabane, H., Tiwari, A., Tian, A., Li, B., Thompson, J.J., Hyde, A.S., Sawyer, L.M., Jodoin, J.N., Santos, E.*, et al.* (2018). APC Inhibits Ligand-Independent Wnt Signaling by the Clathrin Endocytic Pathway. Dev Cell *44*, 566-581 e568.

179. Saito-Diaz, K., Chen, T.W., Wang, X., Thorne, C.A., Wallace, H.A., Page-McCaw, A., and Lee, E. (2013). The way Wnt works: components and mechanism. Growth Factors *31*, 1-31.

180. Salghetti, S.E., Kim, S.Y., and Tansey, W.P. (1999). Destruction of Myc by ubiquitin-mediated proteolysis: cancer-associated and transforming mutations stabilize Myc. EMBO J *18*, 717-726.

181. Sato, T., van Es, J.H., Snippert, H.J., Stange, D.E., Vries, R.G., van den Born, M., Barker, N., Shroyer, N.F., van de Wetering, M., and Clevers, H. (2011). Paneth cells constitute the niche for Lgr5 stem cells in intestinal crypts. Nature *469*, 415-418.

182. Sato, T., Vries, R.G., Snippert, H.J., van de Wetering, M., Barker, N., Stange, D.E., van Es, J.H., Abo, A., Kujala, P., Peters, P.J.*, et al.* (2009). Single Lgr5 stem cells build crypt-villus structures in vitro without a mesenchymal niche. Nature *459*, 262-265.

183. Schepers, A., and Clevers, H. (2012). Wnt signaling, stem cells, and cancer of the gastrointestinal tract. Cold Spring Harb Perspect Biol *4*, a007989.

184. Schilham, M.W., Wilson, A., Moerer, P., Benaissa-Trouw, B.J., Cumano, A., and Clevers, H.C. (1998). Critical involvement of Tcf-1 in expansion of thymocytes. J Immunol *161*, 3984-3991.

185. Schimmer, A.D., Dalili, S., Batey, R.A., and Riedl, S.J. (2006). Targeting XIAP for the treatment of malignancy. Cell Death Differ *13*, 179-188.

186. Schimmer, A.D., Welsh, K., Pinilla, C., Wang, Z., Krajewska, M., Bonneau, M.J., Pedersen, I.M., Kitada, S., Scott, F.L., Bailly-Maitre, B.*, et al.* (2004). Small-molecule antagonists of apoptosis suppressor XIAP exhibit broad antitumor activity. Cancer Cell *5*, 25-35.

187. Schulte, G., and Wright, S.C. (2018). Frizzleds as GPCRs - More Conventional Than We Thought! Trends Pharmacol Sci *39*, 828-842.

188. Semenov, M., Tamai, K., and He, X. (2005). SOST is a ligand for LRP5/LRP6 and a Wnt signaling inhibitor. J Biol Chem *280*, 26770-26775.

189. Semenov, M.V., Tamai, K., Brott, B.K., Kuhl, M., Sokol, S., and He, X. (2001). Head inducer Dickkopf-1 is a ligand for Wnt coreceptor LRP6. Curr Biol *11*, 951-961.

190. Seshagiri, S., Stawiski, E.W., Durinck, S., Modrusan, Z., Storm, E.E., Conboy, C.B., Chaudhuri, S., Guan, Y., Janakiraman, V., Jaiswal, B.S.*, et al.* (2012). Recurrent R-spondin fusions in colon cancer. Nature *488*, 660-664.

191. Sharma, K., D'Souza, R.C., Tyanova, S., Schaab, C., Wisniewski, J.R., Cox, J., and Mann, M. (2014). Ultradeep human phosphoproteome reveals a distinct regulatory nature of Tyr and Ser/Thr-based signaling. Cell reports *8*, 1583-1594.

192. Sharma, R.P., and Chopra, V.L. (1976). Effect of the Wingless (wg1) mutation on wing and haltere development in Drosophila melanogaster. Dev Biol *48*, 461-465.

193. Shi, J., Liu, Y., Xu, X., Zhang, W., Yu, T., Jia, J., and Liu, C. (2015). Deubiquitinase USP47/UBP64E Regulates beta-Catenin Ubiquitination and Degradation and Plays a Positive Role in Wnt Signaling. Mol Cell Biol *35*, 3301-3311.

194. Shivanna, S., Harrold, I., Shashar, M., Meyer, R., Kiang, C., Francis, J., Zhao, Q., Feng, H., Edelman, E.R., Rahimi, N.*, et al.* (2015). The c-Cbl ubiquitin ligase regulates nuclear beta-catenin and angiogenesis by its tyrosine phosphorylation mediated through the Wnt signaling pathway. J Biol Chem *290*, 12537-12546.

195. Siegfried, E., Chou, T.B., and Perrimon, N. (1992). wingless signaling acts through zeste-white 3, the Drosophila homolog of glycogen synthase kinase-3, to regulate engrailed and establish cell fate. Cell *71*, 1167-1179.

196. Smit, J.J., and Sixma, T.K. (2014). RBR E3-ligases at work. EMBO Rep *15*, 142-154.

197. Sokol, S., Christian, J.L., Moon, R.T., and Melton, D.A. (1991). Injected Wnt RNA induces a complete body axis in Xenopus embryos. Cell *67*, 741-752.

198. Spemann, H., and Mangold, H. (2001). Induction of embryonic primordia by implantation of organizers from a different species. 1923. Int J Dev Biol *45*, 13-38.

199. Su, L.K., Vogelstein, B., and Kinzler, K.W. (1993). Association of the APC tumor suppressor protein with catenins. Science *262*, 1734-1737.

200. Sun, M., Meares, G., Song, L., and Jope, R.S. (2009). XIAP associates with GSK3 and inhibits the promotion of intrinsic apoptotic signaling by GSK3. Cell Signal *21*, 1857-1865.

201. Suzuki, Y., Nakabayashi, Y., and Takahashi, R. (2001). Ubiquitin-protein ligase activity of X-linked inhibitor of apoptosis protein promotes proteasomal degradation of caspase-3 and enhances its anti-apoptotic effect in Fas-induced cell death. Proceedings of the National Academy of Sciences *98*, 8662-8667.

202. Swatek, K.N., and Komander, D. (2016). Ubiquitin modifications. Cell Res *26*, 399-422.

203. Takada, R., Satomi, Y., Kurata, T., Ueno, N., Norioka, S., Kondoh, H., Takao, T., and Takada, S. (2006). Monounsaturated fatty acid modification of Wnt protein: its role in Wnt secretion. Dev Cell *11*, 791-801.

204. Talis, A.L., Huibregtse, J.M., and Howley, P.M. (1998). The role of E6AP in the regulation of p53 protein levels in human papillomavirus (HPV)-positive and HPV-negative cells. J Biol Chem *273*, 6439-6445.

205. Tamai, K., Semenov, M., Kato, Y., Spokony, R., Liu, C., Katsuyama, Y., Hess, F., Saint-Jeannet, J.P., and He, X. (2000). LDL-receptor-related proteins in Wnt signal transduction. Nature *407*, 530-535.

206. Tang, Z., Li, C., Kang, B., Gao, G., Li, C., and Zhang, Z. (2017). GEPIA: a web server for cancer and normal gene expression profiling and interactive analyses. Nucleic Acids Research *45*, W98-W102.

207. Tauriello, D.V., Haegebarth, A., Kuper, I., Edelmann, M.J., Henraat, M., Canninga-van Dijk, M.R., Kessler, B.M., Clevers, H., and Maurice, M.M. (2010). Loss of the tumor suppressor CYLD enhances Wnt/beta-catenin signaling through K63-linked ubiquitination of Dvl. Mol Cell *37*, 607-619.

208. Tauriello, D.V., Jordens, I., Kirchner, K., Slootstra, J.W., Kruitwagen, T., Bouwman, B.A., Noutsou, M., Rudiger, S.G., Schwamborn, K., Schambony, A.*, et al.* (2012). Wnt/beta-catenin signaling requires interaction of the Dishevelled

DEP domain and C terminus with a discontinuous motif in Frizzled. Proc Natl Acad Sci U S A *109*, E812-820.

209. Thibault, B., Genre, L., Le Naour, A., Broca, C., Mery, E., Vuagniaux, G., Delord, J.P., Wiedemann, N., and Couderc, B. (2018). DEBIO 1143, an IAP inhibitor, reverses carboplatin resistance in ovarian cancer cells and triggers apoptotic or necroptotic cell death. Sci Rep *8*, 17862.

210. Thompson, B., Townsley, F., Rosin-Arbesfeld, R., Musisi, H., and Bienz, M. (2002). A new nuclear component of the Wnt signalling pathway. Nat Cell Biol *4*, 367-373.

211. Thorpe, C.J., and Moon, R.T. (2004). nemo-like kinase is an essential co-activator of Wnt signaling during early zebrafish development. Development *131*, 2899-2909.

212. Tran, H., Bustos, D., Yeh, R., Rubinfeld, B., Lam, C., Shriver, S., Zilberleyb, I., Lee, M.W., Phu, L., Sarkar, A.A.*, et al.* (2013). HectD1 E3 ligase modifies adenomatous polyposis coli (APC) with polyubiquitin to promote the APC-axin interaction. J Biol Chem *288*, 3753-3767.

213. Tran, H., Hamada, F., Schwarz-Romond, T., and Bienz, M. (2008). Trabid, a new positive regulator of Wnt-induced transcription with preference for binding and cleaving K63-linked ubiquitin chains. Genes Dev *22*, 528-542.

214. Turjanski, A.G., Vaque, J.P., and Gutkind, J.S. (2007). MAP kinases and the control of nuclear events. Oncogene *26*, 3240-3253.

215. van de Wetering, M., and Clevers, H. (1992). Sequence-specific interaction of the HMG box proteins TCF-1 and SRY occurs within the minor groove of a Watson-Crick double helix. EMBO J *11*, 3039-3044.

216. van Wijk, S.J., and Timmers, H.T. (2010). The family of ubiquitin-conjugating enzymes (E2s): deciding between life and death of proteins. FASEB J *24*, 981-993.

217. Veeman, M.T., Slusarski, D.C., Kaykas, A., Louie, S.H., and Moon, R.T. (2003). Zebrafish prickle, a modulator of noncanonical Wnt/Fz signaling, regulates gastrulation movements. Curr Biol *13*, 680-685.

218. Vijayakumar, S., Liu, G., Wen, H.C., Abu, Y., Chong, R., Nastri, H., Bornstein, G.G., Pan, Z.Q., and Aaronson, S.A. (2017). Extracellular LDLR repeats modulate Wnt signaling activity by promoting LRP6 receptor endocytosis mediated by the Itch E3 ubiquitin ligase. Genes Cancer *8*, 613-627.

219. Wehrli, M., Dougan, S.T., Caldwell, K., O'Keefe, L., Schwartz, S., Vaizel-Ohayon, D., Schejter, E., Tomlinson, A., and DiNardo, S. (2000). arrow encodes an LDL-receptor-related protein essential for Wingless signalling. Nature *407*, 527-530.

220. Wei, W., Li, M., Wang, J., Nie, F., and Li, L. (2012). The E3 ubiquitin ligase ITCH negatively regulates canonical Wnt signaling by targeting dishevelled protein. Mol Cell Biol *32*, 3903-3912.

221. Welters, H.J., and Kulkarni, R.N. (2008). Wnt signaling: relevance to beta-cell biology and diabetes. Trends Endocrinol Metab *19*, 349-355.

222. Wend, P., Holland, J.D., Ziebold, U., and Birchmeier, W. (2010). Wnt signaling in stem and cancer stem cells. Semin Cell Dev Biol *21*, 855-863.

223. Wiechens, N., and Fagotto, F. (2001). CRM1- and Ran-independent nuclear export of beta-catenin. Curr Biol *11*, 18-27.

224. Wieschaus, E., and Riggleman, R. (1987). Autonomous requirements for the segment polarity gene armadillo during Drosophila embryogenesis. Cell *49*, 177-184.

225. Willert, K., Brown, J.D., Danenberg, E., Duncan, A.W., Weissman, I.L., Reya, T., Yates, J.R., 3rd, and Nusse, R. (2003). Wnt proteins are lipid-modified and can act as stem cell growth factors. Nature *423*, 448-452.

226. Willert, K., and Nusse, R. (2012). Wnt proteins. Cold Spring Harb Perspect Biol *4*, a007864.

227. Wolf, D., Rodova, M., Miska, E.A., Calvet, J.P., and Kouzarides, T. (2002). Acetylation of beta-catenin by CREB-binding protein (CBP). J Biol Chem *277*, 25562-25567.

228. Wu, D., and Pan, W. (2010). GSK3: a multifaceted kinase in Wnt signaling. Trends Biochem Sci *35*, 161-168.

229. Wu, G., Huang, H., Garcia Abreu, J., and He, X. (2009). Inhibition of GSK3 phosphorylation of beta-catenin via phosphorylated PPPSPXS motifs of Wnt coreceptor LRP6. PLoS One *4*, e4926.

230. Wu, X., Tu, X., Joeng, K.S., Hilton, M.J., Williams, D.A., and Long, F. (2008). Rac1 activation controls nuclear localization of beta-catenin during canonical Wnt signaling. Cell *133*, 340-353.

231. Xu, Q., Wang, Y., Dabdoub, A., Smallwood, P.M., Williams, J., Woods, C., Kelley, M.W., Jiang, L., Tasman, W., Zhang, K.*, et al.* (2004). Vascular development in the retina and inner ear: control by Norrin and Frizzled-4, a high-affinity ligand-receptor pair. Cell *116*, 883-895.

232. Xue, J., Chen, Y., Wu, Y., Wang, Z., Zhou, A., Zhang, S., Lin, K., Aldape, K., Majumder, S., Lu, Z.*, et al.* (2015). Tumour suppressor TRIM33 targets nuclear beta-catenin degradation. Nat Commun *6*, 6156.

233. Yanagawa, S., van Leeuwen, F., Wodarz, A., Klingensmith, J., and Nusse, R. (1995). The dishevelled protein is modified by wingless signaling in Drosophila. Genes Dev *9*, 1087-1097.

234. Yin, J., Schoeffler, A.J., Wickliffe, K., Newton, K., Starovasnik, M.A., Dueber, E.C., and Harris, S.F. (2015). Structural Insights into WD-Repeat 48 Activation of Ubiquitin-Specific Protease 46. Structure *23*, 2043-2054.

235. Yokoya, F., Imamoto, N., Tachibana, T., and Yoneda, Y. (1999). beta-catenin can be transported into the nucleus in a Ran-unassisted manner. Mol Biol Cell *10*, 1119-1131.

236. Yoshida, Y., Saeki, Y., Murakami, A., Kawawaki, J., Tsuchiya, H., Yoshihara, H., Shindo, M., and Tanaka, K. (2015). A comprehensive method for detecting ubiquitinated substrates using TR-TUBE. Proc Natl Acad Sci U S A *112*, 4630-4635.

237. Zeng, X., Huang, H., Tamai, K., Zhang, X., Harada, Y., Yokota, C., Almeida, K., Wang, J., Doble, B., Woodgett, J.*, et al.* (2008). Initiation of Wnt signaling:

control of Wnt coreceptor Lrp6 phosphorylation/activation via frizzled, dishevelled and axin functions. Development *135*, 367-375.

238. Zeng, X., Tamai, K., Doble, B., Li, S., Huang, H., Habas, R., Okamura, H., Woodgett, J., and He, X. (2005). A dual-kinase mechanism for Wnt co-receptor phosphorylation and activation. Nature *438*, 873-877.

239. Zhai, L., Chaturvedi, D., and Cumberledge, S. (2004). Drosophila wnt-1 undergoes a hydrophobic modification and is targeted to lipid rafts, a process that requires porcupine. J Biol Chem *279*, 33220-33227.

240. Zhan, T., Rindtorff, N., and Boutros, M. (2017). Wnt signaling in cancer. Oncogene *36*, 1461-1473.

241. Zhang, Y. (2003). Transcriptional regulation by histone ubiquitination and deubiquitination. Genes Dev *17*, 2733-2740.

242. Zhang, Y., Liu, S., Mickanin, C., Feng, Y., Charlat, O., Michaud, G.A., Schirle, M., Shi, X., Hild, M., Bauer, A.*, et al.* (2011). RNF146 is a poly(ADP-ribose)-directed E3 ligase that regulates axin degradation and Wnt signalling. Nat Cell Biol *13*, 623-629.

243. Zhao, B., Schlesiger, C., Masucci, M.G., and Lindsten, K. (2009). The ubiquitin specific protease 4 (USP4) is a new player in the Wnt signalling pathway. J Cell Mol Med *13*, 1886-1895.

244. Zhu, H., Zhang, T., Wang, F., Yang, J., and Ding, J. (2019). Structural insights into the activation of USP46 by WDR48 and WDR20. Cell Discov *5*, 34.